Marmara University

Engineering Faculty

Department Of Mechanical Engineering

Thesis Project

Drive Train Design and Comparison of Diesel, Hybrid and Electrical Vehicles

2014

Thesis Supervisor= Assistant Professor Mustafa YILMAZ

Kıvanç ER

15041822

Acknowledgments

This thesis project is the direct result of the performed research, and experience built up from the past century to the modern world of electrical vehicles. The finalization of this thesis would not have been possible however without the support of many who have directly and indirectly contributed to this project.

First and foremost I have to express my gratitude to Associate Professor Mustafa Yılmaz and Dr. Hasan Köten at the mechanical engineering department of the Marmara University. They have always been my guide through the project and helped whenever I had faced a problem. I would like to thank them for giving me opportunity to study through AVL Cruise program and being understanding, patient and gentle. I also want to thank to Professor Abdulkerim Kar for teaching me the basic principles of system dynamics and control.

Finally I want to express my thanks to my parents who have always supported and helped me.

Kıvanç ER
January 2014

Content

List of Figures

List of Tables

Abstract

This thesis presents the modeling, Simulink and analysis of the electrical driven vehicles. Starting with the genesis of the first specific electric vehicle in the early 19th century, the evolutions of the history are followed up throughout the years, passing through the renewed interest in electric vehicles the last quarter of the century, up to the new developments like hybrids and fuel cells which are bringing the electric road vehicle into the 21st century.

Throughout the thesis, I have studied with AVL Cruise computer design program in order to design, simulate and analysis of the electrical vehicles. AVL CRUISE is used to perform simulation and analysis of the vehicle propulsion system. It is designed to develop and optimize low-emission engines, power trains and sophisticated engine control systems, cooling systems and transmissions. CRUISE allows modeling the entire optimization process for motor and vehicle in standard applications, such as fuel consumption reduction, acceleration tests, full load tests, traction diagrams and calculation of thermal, mechanical, electrical and control system parameters. In the paper are presented results obtained for a regular simulation of road vehicle behavior in working conditions.

Special attention has been devoted either the mathematical modelling and design or energy sources of the electrical cars. The importance of the electrical vehicles compered to diesel and gasoline engines are determined and the battery characteristics and the future of the electrical cars are also investigated. The mathematical and force model of the electrical vehicles are analyzed and all the internal and external forces exerted on the electrical vehicles are shown by figures.

1.Introduction to Electrical Cars

Electric vehicle concept have been dreamed and designed by the people for more than one hundred years now. Electrical vehicles has been always popular due to their energy efficiency, environmentally friendly design, performance benefits, reduce energy dependence, driving range, low battery cost and even Bulk & weight advantages. The modern concept cars are now mostly designed as having electrical motor due to those advantages.

Electric vehicles are becoming promising alternatives to be remedy for urban air pollution, greenhouse gases and depletion of the finite fossil fuel resources (the challenging triad) as they use centrally generated electricity as a power source. It is well known that power generation at centralized plants are much more efficient and their emissions can be controlled much easier than those emitted from internal combustion engines that scattered all over the world. Additionally, an electric vehicle can convert the vehicle's kinetic energy to electrical energy and store it during the braking and coasting. All the benefits of electrical vehicles are starting to justify, a century later, attention of industry, academia and policy makers again as promising alternatives for urban transport. Nowadays, industry and academia are striving to overcome the challenging barriers that block widespread use of electric vehicles. Lifetime, energy density, power density, weight and cost of battery packs are major barriers to overcome. However, modeling and optimization of other components of electric vehicles are also as important as they have strong impacts on the efficiency, drivability and safety of the vehicles. In this sense there is growing demand for knowledge to model and optimize the electrical vehicles **[1]**.

Environmental as well as economical issues provide a compelling impetus to develop clean, efficient and sustainable vehicles for urban transportation. Automobiles constitute an integral part of our everyday life, yet the exhaust emissions of conventional internal combustion (IC) engine vehicles are to blame for the major source of urban pollution that causes the greenhouse effect leading to global warming **[2]**. The dependence on oil as the sole source of energy for passenger vehicles has economical and political implications, and the crisis will inevitably become acute as the oil reserve of the World diminishes. The number of automobiles on our planet doubled to about a billion or so in the last 10 years. The increasing number of automobiles being introduced on the road every year is only adding to the pollution problem. There is also an economic factor inherent in the poor energy conversion efficiency of combustion engines

Although the number for alternative electric vehicles is not significantly higher when efficiency is evaluated on the basis of conversion from crude oil to traction effort at the wheels, it makes a difference. Emission due to power generation at localized plants is much easier to regulate than that emanating from IC engine vehicles (ICEV) that are individually maintained and scattered. People dwelling in cities are not exposed to power plant related emissions, because these are mostly located outside urban areas. Electric vehicles (EV) enabled by high-efficiency electric motors and controllers and powered by alternative energy sources provide the means for a clean, efficient, and environmentally friendly urban transportation system. Electric vehicles have no emission, having the potential to curb the pollution problem in an efficient way. Consequently, EVs are the only zero emission vehicles possible.

Electric vehicles paved their way into public use as early as the middle of the 19th century, even before the introduction of gasoline-powered vehicles **[3]**. In the year 1900, 4200 automobiles were sold, out of which 40% were steam powered, 38% were electric powered, and 22% were gasoline powered. However, the invention of the starter motor, improvements in mass production technology of gas powered vehicles, and inconvenience in battery charging led to the disappearance of the EV in the early 1900s. However, environmental issues and the unpleasant dependence on oil led to the resurgence of interest in EVs in the 1960s. Growth in the enabling technologies added to environmental and economic concerns over the next several decades, increasing the demand for investing in research and development for EVs. Interest and research in EVs soared in the 1990s, with the major automobile manufacturers embarking on plans for introducing their own electric or hybrid electric vehicles. The trend increases today, with EVs serving as zero-emission vehicles, and hybrid electric vehicles already filling in for ultralow-emission vehicles **[4]**.

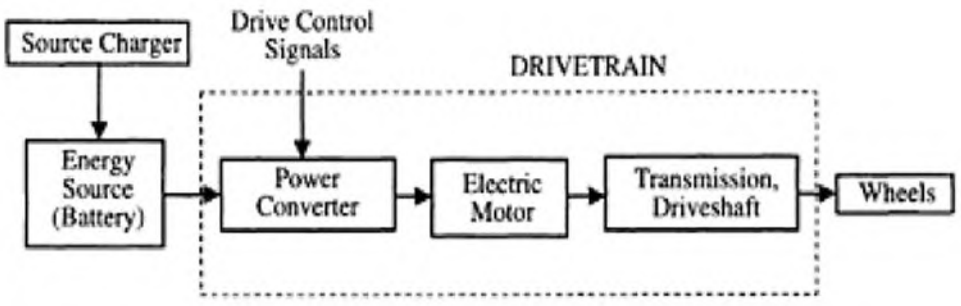

Figure 1.1 Top-level perspective of an EV system

Compared to conventional vehicles, there are more electrical components used in electric, hybrid, and fuel cell vehicles, such as electric machines, power electronics, electronic continuously variable transmissions (CVT), and embedded powertrain controllers **[5]** , **[6]**. Advanced energy storage devices and energy converters, such as Li-Ion batteries, ultracapacitors, and fuel cells, are introduced in the next generation powertrains. In addition to these electrification components or subsystems, conventional internal combustion engines (ICE) and mechanical and hydraulic systems may still be present. The dynamic interactions among various components and the multidisciplinary nature make it difficult to analyze a newly designed hybrid electric vehicle (HEV). Each of the design parameters must be carefully chosen for better fuel economy, enhanced safety, exceptional drivability, and a competitive dynamic performance at a price acceptable to the consumer market. Prototyping and testing each design combination is cumbersome, expensive, and time consuming. Modeling and simulation are indispensable for concept evaluation, prototyping, and analysis of electrical vehicles.

1.1 Electrical Vehicle System

An EV has the following two features:
1. The energy source is portable and chemical or electromechanical in nature.
2. Traction effort is supplied only by an electric motor.

Figure 1.1 shows an EV system driven by a portable energy source. The electromechanical energy conversion linkage system between the vehicle energy source and the wheels is the drivetrain of the vehicle. The drivetrain has electrical as well as mechanical components.

1.1.1 Components of an EV System

The primary components of an EV system are the motor, controller, power source, and transmission. The detailed structure of an EV system and the interaction among its various components are shown in **Figure 1.2**. Figure 1.2 also shows the choices available for each of the subsystem level components. Electrochemical batteries have been the traditional source of energy in EVs. Lead-acid batteries have been the primary choice, because of their well-developed technology and lower cost, although promising new battery technologies are being tested in many prototype vehicles. The batteries need a charger to restore the stored energy level once its available energy is near depletion due to usage. Alternative energy sources are also being developed for zero-emission vehicles.

The limited range problem of battery-driven EVs prompted the search for alternative energy sources, such as fuel cells and flywheels. Prototypes have been developed with fuel cells, while production vehicles will emerge in the near future. The majority of electric vehicles developed so far are based on DC machines, induction machines, or permanent magnet machines. The disadvantages of DC machines pushed EV developers to look into various types of AC machines. The maintenance-free, low-cost induction machines became an attractive alternative to many developers. However, high-speed operation of induction machines is only possible with a penalty in size and weight. Excellent performance together with high-power density features of permanent magnet machines makes them an attractive solution for EV applications, although the cost of permanent magnets can become prohibitive. High-power density and a potentially low production cost of switched reluctance machines make them ideally suited for EV applications. However, the acoustic noise problem has so far been a deterrent for the use of switched reluctance machines in EVs. The electric motor design includes not only electromagnetic aspects of the machine but also thermal and mechanical considerations. The motor design tasks of today are supported by finite element studies and various computer-aided design tools, making the design process highly efficient.

The electric motor is driven by a power-electronics-based power-processing unit that converts the fixed DC voltage available from the source into a variable voltage, variable frequency source controlled to maintain the desired operating point of the vehicle. The power electronics circuit comprised of power semiconductor devices saw tremendous development over the past 3 decades. The enabling technology of power electronics is a key driving force in developing efficient and high-performance power-train units for EVs. High-power devices in compact packaging are available today, enabling the development of lightweight and efficient power-processing units known as power electronic motor drives. Advances in power solid state devices and very large-scale integration (VLSI) technology are responsible for the development of efficient and compact power electronics circuits. The developments in high-speed digital signal processors or microprocessors enable complex control algorithm implementation with a high degree of accuracy. The controller includes algorithms for the motor drive in the inner loop as well as system-level control in the outer loop **[4]**.

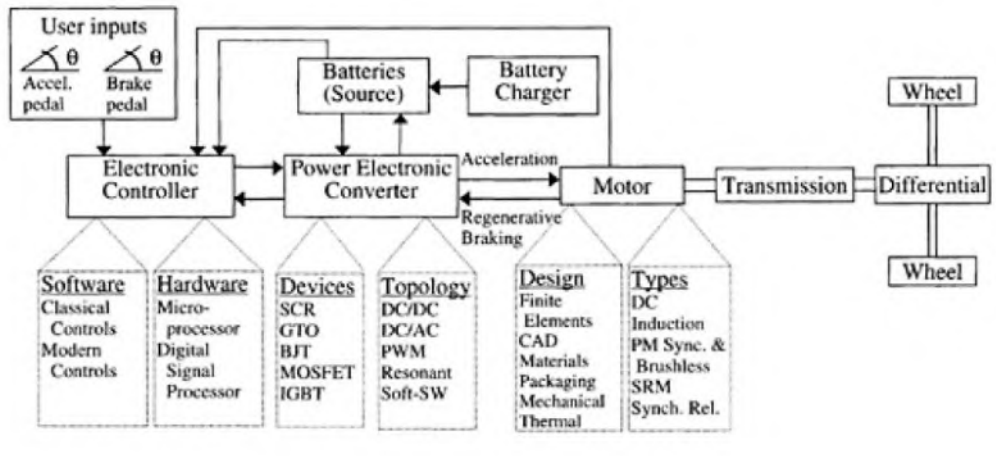

Figure 1.2 Major electrical components and choices for an EV system.

1.2 History of the Electrical Cars

The history of the electric vehicle began in the mid-19th century. An electrical vehicle held the vehicular land speed record until around 1900. The high cost, low top speed and short range of electric vehicles, compared to later internal combustion vehicles, led to a worldwide decline in their use. At the beginning of the 21st Century, interest in electrical and other alternative fuel vehicles has increased due to growing concern over the problems associated with hydrocarbon fueled vehicles, including damage to the environment caused by their emissions, and the sustainability of the current hydrocarbon-based transportation infrastructure.

1.2.1 Rise of the Electrical Vehicles in the World (Early Years)

Figure 1.3 German Elektrowagen 1888, known as the first electric car

The invention of the electric vehicle is attributed to various people. In 1828, Ányos Jedlik, a Hungarian who invented an early type of electric motor, created a tiny model car powered by his new motor. In 1834, Vermont blacksmith Thomas Davenport, the inventor of the first American electrical motor (DC), installed his motor in a small model car, which he operated on a short circular electrified track. In 1835, Professor Sibrandus Stratingh of Groningen, the Netherlands and his assistant Christopher Becker created a small-scale electrical car, powered by non-rechargeable primary cells. In 1838, Scotsman Robert Davidson built an electric locomotive that attained a speed of 4 mph (6.4 km/h). Between 1832 and 1839, Robert Anderson of Scotland invented a crude electrical carriage.

A patent for the use of rails as conductors of electric current was granted in England in 1840, and similar patents were issued to Lilley and Colten in the United States in 1847. Rechargeable batteries that provided a viable means for storing electricity on board a vehicle did not come into being until 1856 by French physicist Gaston Planté

The invention of improved battery technology, including efforts by Gaston Plante in France in 1865 **[7]** as well as his fellow countryman Camille Faure in 1881 **[8]**, paved the way for electric cars to flourish in Europe. An electric-powered two-wheel cycle was put on display at the 1867 World Exposition in Paris by the Austrian inventor Franz Kravogl **[9]**. France and Great Britain were the first nations to support the widespread development of electric vehicles **[10]**. The lack of natural fossil resources in Switzerland resulted in the tiny European nation's rapid electrification of its railway network to reduce its dependence on foreign energy. In November 1881, French inventor Gustave Trouvé demonstrated a working three-wheeled automobile at the International Exhibition of Electricity in Paris. English inventor Thomas Parker, who was responsible for innovations such as electrifying the London Underground, overhead tramways in Liverpool and Birmingham, and the smokeless fuel coalite, claimed to have perfected a working electric car as early as 1884. The first four-wheeled electric car was built by the German engineer Andreas Flocken in 1888.

Figure 1.4: German electric car, 1904,

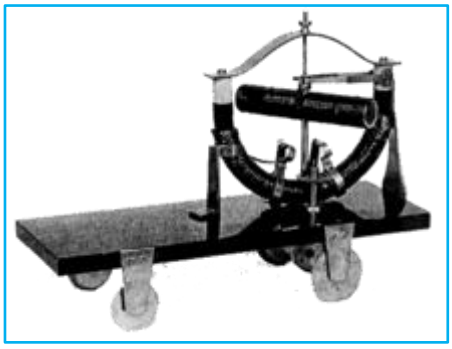

Figure 1.5: Electric vehicle by Ányos Jedlik (1828)

Electric trains were also used to transport coal out of mines, as their motors did not use up precious oxygen. Before the pre-eminence of internal combustion engines, electric automobiles also held many speed and distance records **[11]** . Among the most notable of these records was the breaking of the 100 km/h (62 mph) speed barrier, by Camille Jenatzy on 29 April 1899 in his 'rocket-shaped' vehicle Jamais Contente, which reached a top speed of 105.88 km/h (65.79 mph). Also notable was Ferdinand Porsche's design and construction of an all-wheel drive electric car, powered by a motor in each hub, which also set several records in the hands of its owner E.W. Hart. Electric trains were also used to transport coal out of mines, as their motors did not use up precious oxygen.

Prior to the 1830s, the means of transportation was only through steam power, because the laws of electromagnetic induction, and consequently, electric motors and generators, were yet to be discovered. Faraday demonstrated the principle of the electric motor as early as in 1820 through a wire rod carrying electric current and a magnet, but in 1831 he discovered the laws of electromagnetic induction that enabled the development and demonstration of the electric motors and generators essential for electric transportation **[4]**.

Before the pre-eminence of internal combustion engines, electric automobiles also held many speed and distance records. Among the most notable of these records was the breaking of the 100 km/h (62 mph) speed barrier, by Camille Jenatzy on 29 April 1899 in his 'rocket-shaped' vehicle Jamais Contente, which reached a top speed of 105.88 km/h (65.79 mph). Also notable was Ferdinand Porsche's design and construction of an all-wheel drive electric car, powered by a motor in each hub, which also set several records in the hands of its owner E.W. Hart.

Timeline of development of electrical motors history can be described as below;

• Pre-830-Steam-powered transportation
• 1831—Faraday's law, and shortly thereafter, invention of DC motor
• 1834—Non rechargeable battery-powered electric car used on a short track
• 1851—Non rechargeable 19 mph electric car
• 1859—Development of lead storage battery
• 1874—Battery-powered carriage
• Early 1870s-Electricity produced by dynamo-generators
• 1885—Gasoline-powered tricycle car
• 1900—4200 automobiles sold (40% steam powered, 38% electric powered, 22% gasoline powered)

The specifications of some of the early EVs are given below:
• 1897—French Krieger Co. EV: weight, 2230 lb; top speed, 15 mph; range, 50 mi/charge
• 1900—French B.G.S. Co. EV: top speed, 40 mph; range, 100 mi/charge
• 1912—34,000 EVs registered; EVs outnumber gas-powered vehicles 2-to-1
• 1915—Woods EV: top speed, 40 mph; range, 100 mi/charge
• 1915—Landsmen EV: weight, 2460 lb, top speed, 93 mi/charge, capacity, 1 ton payload
• 1920s—EVs disappear, and ICEVs become predominant **[12]**

1.2.2 1960s-1990s (Gasoline Dominates)

Figure 1.6: 1961 production electric car

Electric vehicles started to resurge in the 1960s, primarily due to environmental hazards being caused by the emissions of ICEVs. The major ICEV manufacturers, General Motors (GM) and Ford, became involved in EV research and development. General Motors started a $15 million program that culminated in the vehicles called Electrovair and Electrovan. The components and specifications of two Electrovair vehicles (Electrovair I (1964) and Electrovair II (1966) by GM) are given below.

Systems and characteristics:

Motor—three-phase induction motor, 115 hp, 13,000 rev/m
Battery—silver-zinc (Ag-Zn), 512 V, 680 lb
Motor drive—DC-to-AC inverter using a silicon-controlled rectifier (SCR)
Top speed—80 mi/h
Range—40 to 80 miles
Acceleration—0–60 mi/h in 15.6 s
Vehicle weight—3400 lb

The Electrovair utilized the Chevy Corvair body and chassis. Among the positive features was the acceleration performance that was comparable to the ICEV Corvair. The major disadvantage of the vehicle was the silver-zinc (Ag-Zn) battery pack that was too expensive and heavy, with a short cycle life and a long recharge time. An additional factor in the 1960s that provided the impetus for EV development included "The Great Electric Car Race" cross-country competition between an EV from Caltech and an EV from MIT in August 1968. The race generated great public interest in EVs and provided an extensive road test of the EV technology. However, technology of the 1960s was not mature enough to produce a commercially viable EV **[4]**.

In 1959, American Motors Corporation (AMC) and Sonotone Corporation announced a joint research effort to consider producing an electric car powered by a "self-charging" battery **[13]**. AMC had a reputation for innovation in economical cars while Sonotone had technology for making sintered plate nickel-cadmium batteries that could be recharged rapidly and weighed less than traditional lead-acid versions **[14]**. That same year, Nu-Way Industries showed an experimental electric car with a one-piece plastic body that was to begin production in early 1960 **[13]**.

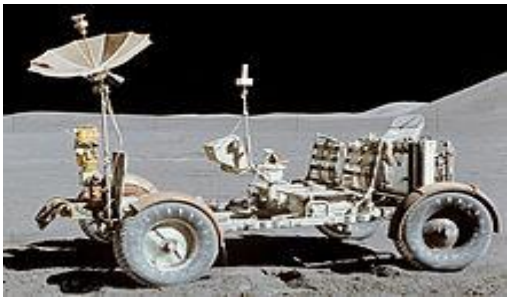

The U.S. and Canada Big Three automakers had their own electric car programs during the late1960s. In 1967, much smaller AMC partnered with Gulton Industries to develop a new battery based on lithium and a speed controller designed by Victor Wouk **[15]**.

Figure 1.7: The lunar rovers parked on the moon

A nickel-cadmium battery supplied power to an all-electric 1969 Rambler American station wagon **[15]**. Other "plug-in" experimental AMC vehicles developed with Gulton included the Amitron (1967) and the similar Electron (1977). More battery-electric concept cars appeared over the years, such as the Scottish Aviation Scamp (1965) **[16]**, the Enfield 8000 (1966) **[17]** and two electric versions of General Motors gasoline cars, such as the Electrovair (1966) and Electrovette (1976) **[18]**. None of them entered production.

On 31 July 1971, an electric car received the unique distinction of becoming the first manned vehicle to drive on the Moon; that car was the Lunar rover, which was first deployed during the *Apollo 15* mission. The "moon buggy" was developed by Boeing and Delco Electronics, and featured a DC drive motor in each wheel, and a pair of 36-volt silver-zinc potassium hydroxide non-rechargeable batteries.

The scenario turned in favor of EVs in the early 1970s, as gasoline prices increased dramatically due to an energy crisis. The Arab oil embargo of 1973 increased demands for alternate energy sources, which led to immense interest in EVs. It became highly desirable to be less dependent on foreign oil as a nation. In 1975, 352 electric vans were delivered to the U.S. Postal Service for testing. In 1976, Congress enacted Public Law 94–413, the Electric and Hybrid Vehicle Research, Development and Demonstration Act of 1976. This act authorized a federal program to promote electric and hybrid vehicle technologies and to demonstrate the commercial feasibility of EVs. The Department of Energy (DOE) standardized EV performance, which is summarized in **Table 1.1 [4].**

TABLE 1.1 EV Performance Standardization of 1976

Category	**Personal Use**	**Commercial Use**
Acceleration from 0 to 50 km/h	<15 s	<15 s
Gradability at 25 km/h	10%	10%
Gradability at 20 km/h	20%	20%
Forward speed for 5 min	80 km/h	70 km/h
Range:		
Electric	50 km, C cycle	50 km, B cycle
Hybrid	200 km, C cycle	200 km, B cycle
Recharge time from 80% discharge	<10 h	<10 h

Moreover, the case study that has done to express the system and characteristics of an 1970s electrical vehicle is on the fallowing part. The electrical vehicle is a modified Chevy Chevette chassis and body. This electrical vehicle was used mainly as a test bed for Ni-Zn batteries.

Over 35,500 miles of on-road testing proved that this EV was sufficiently road worthy.

System and characteristics**:**

Motor—separately excited DC, 34 hp, 2400 rev/m

Battery pack—Ni-Zn, 120 V, 735 lb

Auxiliary battery—Ni-Zn, 14 V

Motor drive—armature DC chopper using SCRs; field DC chopper using bipolar junction transistors (BJTs)

Top speed—60 mi/h

Range—60–80 miles

Acceleration—0–55 mi/h in 27 s **[4]**.

In 1980's the production of electrical vehicles and motors had a new trend. After years outside the limelight, the energy crises of the 1970s and 1980s brought about renewed interest in the perceived independence electric cars had from the fluctuations of the hydrocarbon energy market.

After years outside the limelight, the energy crises of the 1970s and 1980s brought about renewed interest in the perceived independence electric cars had from the fluctuations of the hydrocarbon energy market. At the 1990 Los Angeles Auto Show, General Motors President Roger Smith unveiled the GM Impact electric concept car, along with the announcement that GM would build electric cars for sale to the public.

The Honda EV Plus, one of the cars introduced as a result of the CARB ZEV mandate

Figure 1.8: The Honda EV Plus

In the early 1990s, the California Air Resources Board (CARB), the government of California's "clean air agency", began a push for more fuel-efficient, lower-emissions vehicles, with the ultimate goal being a move to zero-emissions vehicles such as electric vehicles**[19] [20]**. In response, automakers developed electric models, including the Chrysler TEVan, Ford Ranger EV pickup truck, GM EV1 and S10 EV pickup, Honda EV Plus hatchback, Nissan lithium-battery Altra EV mini wagon and Toyota RAV4 EV. The automakers were accused of pandering to the wishes of CARB in order to continue to be allowed to sell cars in the lucrative Californian market, while failing to adequately promote their electric vehicles in order to create the impression that the consumers were not interested in the cars, all the while joining oil

industry lobbyists in vigorously protesting CARB's mandate **[20]**. GM's program came under particular scrutiny; in an unusual move, consumers were not allowed to purchase EV1s, but were instead asked to sign closed-end leases, meaning that the cars had to be returned to GM at the end of the lease period, with no option to purchase, despite lessor interest in continuing to own the cars **[20]**. Chrysler, Toyota, and a group of GM dealers sued CARB in Federal court, leading to the eventual neutering of CARB's ZEV (Zero Emission Vehicle) Mandate.

The trends in EV developments in recent years can be attributed to the following:

- High level of activity exists at the major automotive manufacturers.
- New independent manufacturers bring vigor.
- New prototypes are even better.
- High levels of activity overseas exist.
- There are high levels of hybrid vehicle activity.
- A boom in individual ICEV to EV conversions is ongoing.
- The fuel cell shows great promise in solving the battery range problem.

The case studies of two GM EVs of the 1990s are given below **[21] [22]**;

Gm Impact 3

Saturn EV1

Motor	137 hp, 12,000 rev/m	one three phase induction motor
Battery Pack	lead acid(26), 312V, 869 Lb	Lead acid batteries
Motor Drive	DC-to-AC inverter using bipolar transistors	Dc to Ac inverter using IGBTs
Top Speed	75 mph	75 mph
Range	90 miles on highway	95 miles highway, 70 miles in city
Acceleration	0 to 60 miles in 8.5s	0 to 60 miles in 8.5
Vehicle Weight	2900 lb	2700lb

Throughout the 1990s, interest in fuel-efficient or environmentally friendly cars declined among Americans, who instead favored sport utility vehicles, which were affordable to operate despite their poor fuel efficiency thanks to lower gasoline prices. American automakers chose to focus their product lines around the truck-based vehicles, which enjoyed larger profit margins than the smaller cars which were preferred in places like Europe or

Japan. In 1999, the Honda Insight hybrid car became the first hybrid to be sold in North America since the little-known Woods hybrid of 1917.

Figure 1.9: The 1st generation Toyota Prius 1997

Hybrid electric vehicles, which featured a combined gasoline and electric powertrain, were seen as a balance, offering an environmentally friendly image and improved fuel economy, without being hindered by the low range of electric vehicles, albeit at an increased price over comparable gasoline cars. Sales were poor, the lack of interest attributed to the car's small size and the lack of necessity for a fuel-efficient car at the time.

The 2000s energy crisis brought renewed interest in hybrid and electric cars. In America, sales of the Toyota Prius (which had been on sale since 1999 in some markets) jumped, and a variety of automakers followed suit, releasing hybrid models of their own. Several began to produce new electric car prototypes, as consumers called for cars that would free them from the fluctuations of oil prices. In response to a lack of large-automaker participation in the electric car industry, a number of small companies cropped up in their place, designing and marketing electric cars for the public.

Most electric vehicles in the world roads are low-speed, low-range neighborhood electric vehicles (NEVs). Pike Research estimated there were almost 479,000 NEVs on the world roads in 2011 **[23]**. The top selling NEV is the Global Electric Motorcars (GEM) vehicles, with more than 46,000 units sold worldwide by April 2013 **[24]**. As of July 2006, there were between 60,000 and 76,000 low-speed battery-powered vehicles in use in the United States, up from about 56,000 in 2004 **[25]**. The two largest NEV markets in 2011 were the United States, with 14,737 units sold, and France, with 2,231 units **[26]**. Other micro electric cars sold in Europe were the Kewet, since 1991, and replaced by the Buddy, launched in 2008 **[27]**.

1.2.3 Recent EVs and HEVs (Modern Electrical Cars)

All of the major automotive manufacturers have production EVs, many of which are available for sale or lease to the general public. The status of these vehicle programs changes rapidly, with manufacturers suspending production frequently due to the small existing market demand of such vehicles. Examples of production EVs which are or until recently have been available are GM EVl, BMW i8, i3, Ford Think City, Toyota RAV4, Nissan Hyper mini, and Peugeot 106 Electric. There are also many prototype and

experimental EVs being developed by the major automotive manufacturers. Most of these vehicles use AC induction motors or PM synchronous motors. Also, interestingly, almost all of these vehicles use battery technology other than the lead-acid battery pack. The list of EVs in production and under development is extensive, and readers are referred to the literature **[4]** for the details of many of these vehicles.

Figure 1.10: BMW i8 spider concept (2012)

The manufacturers of EVs in the 1990s realized that their significant research and development efforts on ZEV technologies were hindered by unsuitable battery technologies. A number of auto industries started developing hybrid electric vehicles (HEVs) to overcome the battery and range problem of pure electric vehicles. The Japanese auto industries lead this trend with Toyota, Honda, and Nissan already marketing their Prius, Insight, and Tino model hybrids. The hybrid vehicles use an electric motor and an internal combustion engine and, thus, do not solve the pollution problem, although it does mitigate it. It is perceived by many that the hybrids, with their multiple propulsion units and control complexities, aren't economically viable in the long run, although currently a number of commercial, prototype, and experimental hybrid vehicle models are available from almost all of the major automotive industries around the world **[4]**. BMW, Toyota, Honda, and Nissan are marketing the hybrid vehicles well below the production cost, with significant subsidy and incentive from the government. However, the cost of

HEVs and EVs are expected to be high until production volume increases significantly. Fuel cell electric vehicles (FCEV) can be a viable alternative to battery electric vehicles, serving as zero-emission vehicles without the range problem. Toyota is leading the way with FCEV, announcing the availability of its FCEV in 2003. The Toyota FCEV is based on the Toyota RAV4 model.

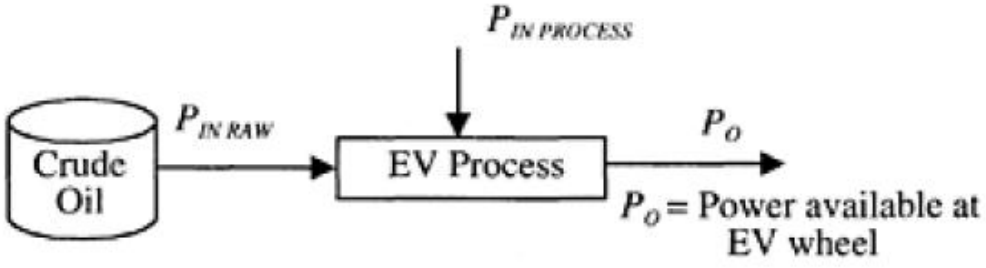

Figure 1.11: EV process from crude oil to power at the wheels.

The global economic recession in the late 2000s led to increased calls for automakers to abandon fuel-inefficient SUVs, which were seen as a symbol of the excess that caused the recession, in favor of small cars, hybrid cars, and electric cars. California electric car maker Tesla Motors began development in 2004 on the Tesla Roadster, which was first delivered to customers in 2008 **[28]**. The Roadster was the first highway-capable all-electric vehicle in serial production available in the world. Since 2008 Tesla has sold more than 2,100 Roadsters in 31 countries through December 2011. **[29]** The Roadster was also the first production automobile to use lithium-ion battery cells and the first production all-electric car to travel more than 200 miles (320 km) per charge **[30]**. Tesla expects to sell the Roadster until early 2012, when its supply of Lotus Elise gliders is expected to run out, as its contract with Lotus Cars for 2,500 gliders expired at the end of 2011 **[31][32]**. Tesla stopped taking orders for the Roadster in the U.S. market in August 2011, **[33] [34]** and the 2012 Tesla Roadster will be sold in limited numbers only in Europe, Asia and Australia. **[29] [35]** The next generation is expected to be introduced in 2014 **[36]**.

The Mitsubishi i-MiEV was launched in Japan for fleet customers in July 2009, and for individual customers in April 2010, **[37] [38] [39]** followed by sales to the public in Hong Kong in May 2010, and Australia in July 2010 via leasing **[40] [41]**. The i-MiEV was launched in Europe in December 2010, including a rebadged version sold in Europe as Peugeot i-On and Citroën C-Zero **[42] [43]** . The market launch in the Americas began in Costa Rica in February 2011, followed by Chile in May 2011**[44] [45]**. Fleet and retail

customer deliveries in the U.S. and Canada began in December 2011 **[46] [47] [48]**. Accounting for all vehicles of the iMiEV brand, Mitsubishi reports around 27,200 units sold or exported since 2009 through December 2012, including the minicab MiEVs sold in Japan, and the units rebadged and sold as Peugeot i-On and Citroën C-Zero in the European market. **[49]**

Figure 1.12: Chrysler-Dodge Zeo (2008)

The most immediate result of this was the announcement of the Chrysler-Dodge Zeo in 2008 and then 2010 release of the Chevrolet Volt, a plug-in hybrid car that represents the evolution of technologies pioneered by the GM EV1 of the 1990s. The Volt can travel for up to 40 miles (64 km) on battery power alone before activating its gasoline-powered engine to run generator which re-charges its batteries. Deliveries of the Volt began in the United States in December 2010, and by late 2011 were released in Canada and Europe. Deliveries of its sibling, the Opel Ampera, began in Europe February 2012.

The Tesla Model S ranked as the top selling plug-in electric car in North America during the first quarter of 2013 with 4,900 cars sold, ahead of the Chevrolet Volt (4,421) and the Nissan Leaf (3,695) **[50]**. Since its introduction, cumulative sales reached around 9,650 units through April 2013, with most units delivered in the U.S **[51] [50] [52]**.

As of July 2013, the Renault–Nissan Alliance is the world's leading plug-in electric vehicle manufacturer with global sales of 100,000 all-electric units delivered since December 2010 **[53]**.

TABLE 1.2 List of the some EV's Throughout the History

Automobile	Production Years	Top Speed
Baker Electric	1899–1915	23 km/h
Detroit Electric	1907–1939	32 km/h
Henney Kilowatt	1958–1960	97 km/h
Skoda Favorit	1992–1994	80 km/h
General Motor EV1	1996–2003	129 km/h
Chevrolet S10 EV	1997–1998	118 km/h
Honda EV Plus	1997–1999	130+ km/h
Toyota RAV4 EV	1997–2002	125 km/h
Ford Ranger EV	1998–2002	120 km/h
Think City	1999–2002	90 km/h
Reva	2001–	72 km/h
ZAP Xebra	2006–2009	65 km/h
Tesla Roadster	2008–2012	210 km/h
Mitsubishi i-MiEV	2009–	130 km/h
Nissan Leaf	2010–	150 km/h
Tesla Model	2012–	210 km/h

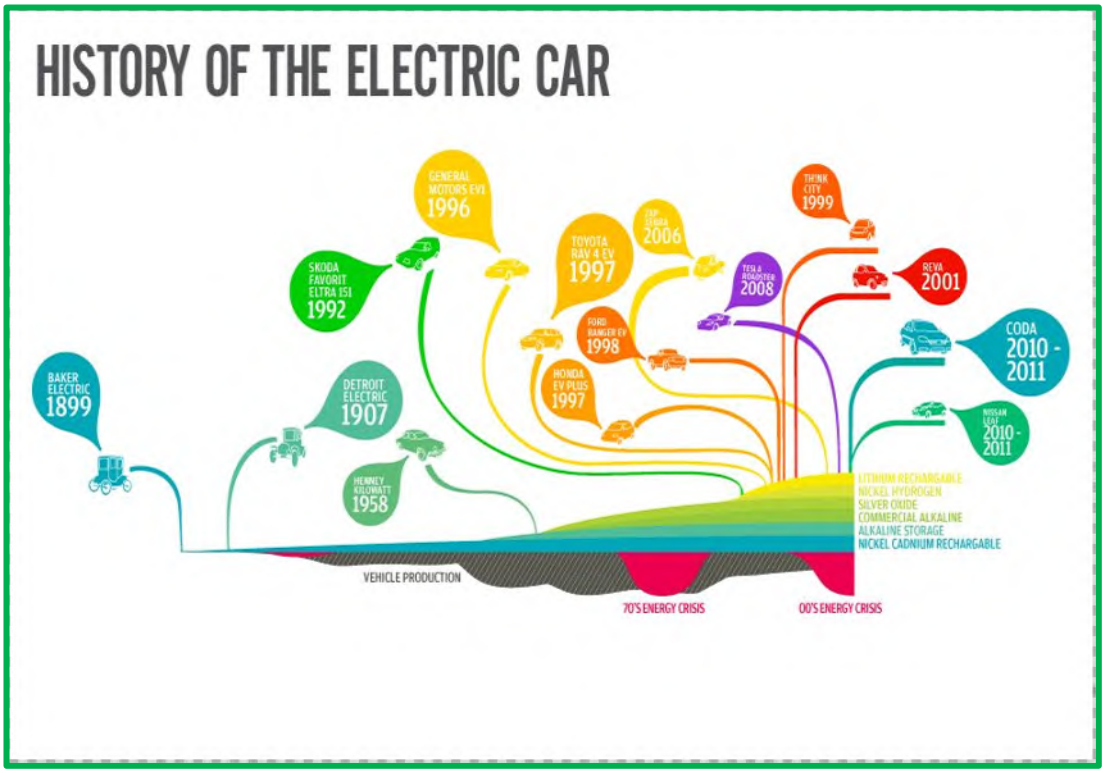

Figure 1.13: Timeline of the Electrical cars

1.3 Advantages of Electric Vehicles

The relative advantages and disadvantages of an electrical vehicle over an internal combustion engine vehicle can be better appreciated from a comparison of the two on the bases of efficiency, pollution, cost, and dependence on oil. The comparison must be executed with care, ensuring fairness to both systems.

1.3.1 Efficiency Comparison

To evaluate the efficiencies of EV (Electrical Vehicles) and ICEV (Internal Combustion Engine Vehicles) on level ground, the complete process in both systems starting from crude oil to power available at the wheels must be considered. The EV process starts not at the vehicles, but at the source of raw power whose conversion efficiency must be considered to calculate the overall efficiency of electric vehicles. The power input *PIN* to the EV comes from two sources—the stored power source and the applied power source. Stored power is available during the process from an energy storage device. The power delivered by a battery through electrochemical reaction on demand or the power extracted from a piece of coal by burning it are examples of stored power. Applied power is obtained indirectly from raw materials. Electricity generated from crude oil and delivered to an electric car for battery charging is an example of applied power. Applied power is labeled as *PIN RAW* while stored power is designated as *PIN PROCESS* in **Figure 1.11** [4]. Therefore, we have the following: $P_{in} = P_{in\ Process} + P_{in\ Raw}$

The complete EV process can be broken down into its constituent stages involving a chain of events responsible for power generation, transmission, and usage, as shown in **Figure 1.4** [4]. Raw power from the applied source is fed to the system only at the first stage, although stored power can be added in each stage. Each stage has its efficiency based on total input to that stage and output delivered to the following stage. For example, the efficiency of the first stage based on the input and output shown in **Figure 1.4** is;

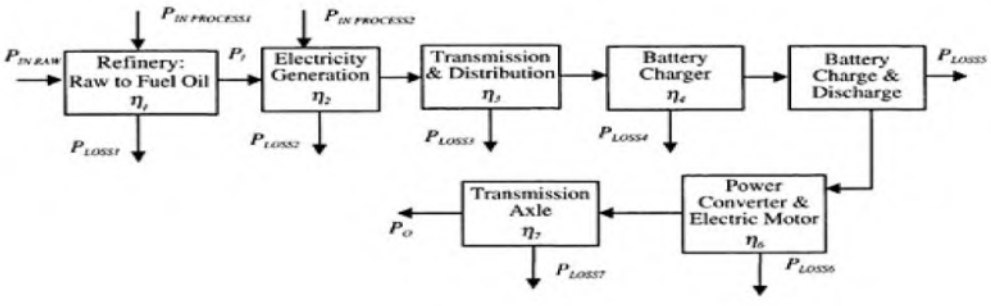

Figure 1.14: The complete EV process broken into stages.

1.3.2 Pollution Comparison

Transportation accounts for one third of all energy usage, making it the leading cause of environmental pollution through carbon emissions. The DOE projected that if 10% of automobiles nationwide were zero-emission vehicles, regulated air pollutants would be cut by 1,000,000 tons per year, and 60,000,000 tons of green-house carbon dioxide gas would be eliminated. With 100% electrification, i.e., every ICEV replaced by an EV, the following was claimed:

- Carbon dioxide in air, which is linked to global warming, can be cut in half.
- Nitrogen oxides (a greenhouse gas causing global warming) would be cut slightly, depending on government-regulated utility emission standards.
- Sulfur dioxide, which is linked to acid rain, would increase slightly.
- Waste oil dumping would decrease, because EVs don't need crankcase oil.
- EVs reduce noise pollution, because they are quieter than ICEVs.
- Thermal pollution by big power plants increase with increased EV usage.

EVs will considerably reduce the major causes of smog, substantially eliminate ozone depletion, and reduce greenhouse gases. With stricter SO2 power plant emission standards, EVs would have little impact on SO2 levels. Pollution reduction is the driving force behind EV usage **[4]**.

1.3.3 Capital and Operating Cost Comparison

The initial EV capital costs are higher than ICEV capital costs primarily due to the lack of mass production opportunities. However, EV capital costs are expected to decrease as volume increases. Capital costs of EVs easily exceed capital costs of ICEVs due to the cost of the battery. The power electronics stages are also expensive, although not at the same level as batteries. Total life cycle cost of an EV is projected to be less than that of a comparable ICEV. EVs are more reliable and will require less maintenance, giving a favorable bias over ICEV as far as operating cost is concerned.

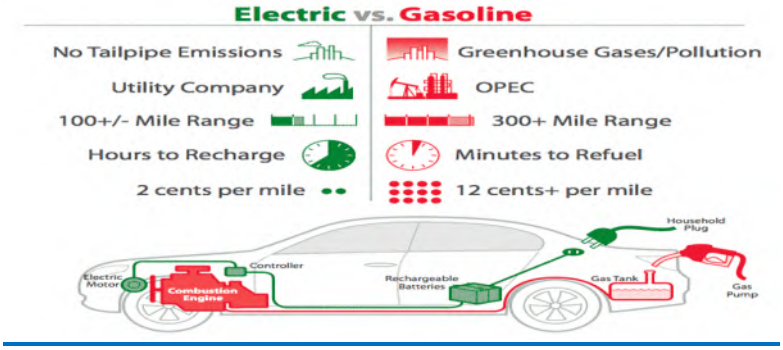

Figure 1.15: The complete EV process broken into stages.

2. Electric Vehicle Design and Modeling

Electric vehicles are by many seen as the cars of the future as they are high efficient, produces no local pollution, are silent, and can be used for power regulation by the grid operator. However, electric vehicles still have critical issues which need to be solved. The three main challenges are limited driving range, long charging time, and high cost. The three main challenges are all related to the battery package of the car. The battery package should both contain enough energy in order to have a certain driving range and it should also have a sufficient power capability for the accelerations and decelerations. In order to be able to estimate the energy consumption of an electric vehicles it is very important to have a proper model of the vehicle (Gao et al., 2007; Mapelli et al., 2010; Schaltz, 2010) **[54]**.

The model of an electric vehicle is very complex as it contains many different components, e.g., transmission, electric machine, power electronics, and battery. Each component needs to be modeled properly in order prevent wrong conclusions. The design or rating of each component is a difficult task as the parameters of one component affect the power level of another one.

There is therefore a risk that one component is rated inappropriate which might make the vehicle unnecessary expensive or inefficient. In this chapter a method for designing the power system of an electric vehicle is presented. The method insures that the requirements due to driving distance and acceleration is fulfilled.

The focus in this chapter will be on the modeling and design of the power system of a battery electric vehicle. Less attention will therefore be put on the selection of each component (electric machines, power electronics, batteries, etc.) of the power system as this is a very big task in itself. This chapter will therefore concentrate on the methodology of the modeling and design process. However, the method presented here is also suitable for other architectures and choice of components.

The chapter is organized as follows: After the introduction Section 2 describes the modeling of the electric vehicle, Section 3 presents the proposed design method, Section 4 provides a case study in order to demonstrate the proposed method, and Section 5 gives the conclusion remarks **[54]**.

2.1. Vehicle Modeling

2.1.1 Architecture

Many different architectures of an electric vehicle exist (Chan et al., 2010) as there are many possibilities, e.g., 1 to 4 electric machines, DC or AC machines, gearbox/no gearbox, high or low battery voltage, one or three phase charging, etc. However, in this chapter the architecture in **Fig2.1** is chosen.

The purpose of the different components in Fig. 1 will here shortly be explained: The traction power of the wheels is delivered by the three phase electric machine. The torque of the left and right wheels are provided by a differential with also has a gear ratio in order to fit the high speed of the electric machine shaft to the lower speed of the wheels. The torque and speed of the machine are controlled by the inverter which inverts the battery DC voltage to a three phase AC voltage suitable for the electric machine. When analyzing the energy consumption of an electric vehicle it is important also to include the losses due to the components which not are a part of the power chain from the grid to the wheels. These losses are denoted as auxiliary loss and include the lighting system, comfort system, safety systems, etc. During the regenerative braking it is important that the maximum voltage of the battery is not exceeded. For this reason a braking resistor is introduced. The rectifier rectifies the three phase voltages and currents of the grid to DC levels and the boost converter makes it possible to transfer power from the low voltage side of the rectifier to the high voltage side of the battery **[54]**.

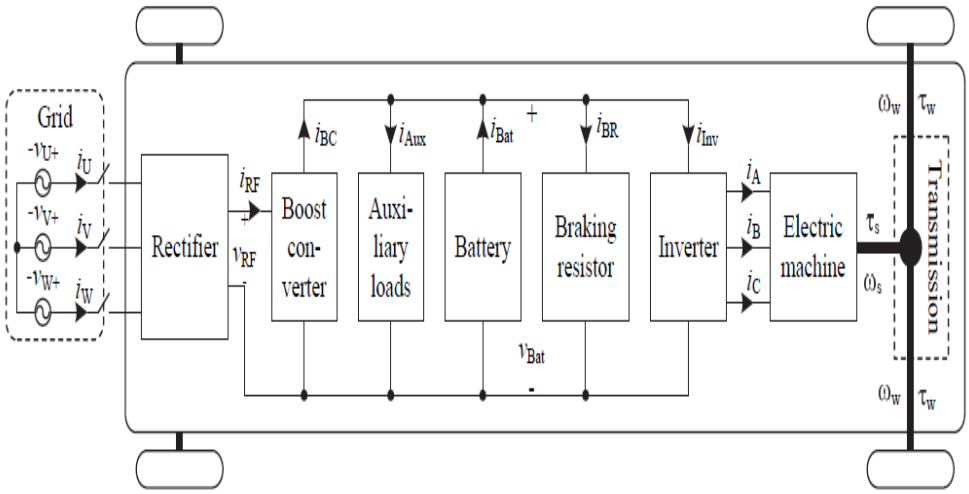

Figure 2.1: Architecture of the battery electrical vehicle

2.1.2 Force Model

The forces which the electric machine of the vehicle must overcome are the forces due to gravity, wind, rolling resistance, and inertial effect. These forces can also be seen in **Fig. 2.2a**[55] where the forces acting on the vehicle are shown.

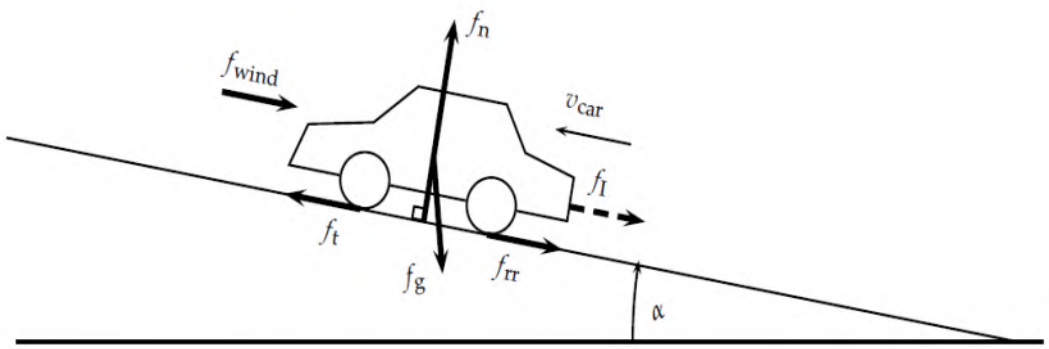

Figure 2.2(a): Free Body diagram of the forces acting on a car

The traction force of a vehicle can be described by the two equations;

$$\boldsymbol{ft} = \underbrace{Mcar.\dot{v}car}_{fl} + \underbrace{Mcar.g}_{fg}.\sin(\alpha) + sign(vcar)\overbrace{\underbrace{Mcar.g.\cos(\alpha)}_{frr}.Crr}^{fn} + sign(vcar + vwind)\underbrace{\frac{1}{2}\rho airCdragAfront(vcar + vvind)^2}_{fwind}$$

$$\boldsymbol{Crr} = 0.01(1 + \frac{3.6}{100}vcar$$

where,

f_t [N] Traction force of the vehicle
f_l [N] Inertial force of the vehicle
f_{rr} [N] Rolling resistance force of the wheels
f_g [N] Gravitational force of the vehicle
f_n [N] Normal force of the vehicle
f_{wind} [N] Force due to wind resistance
α [rad] Angle of the driving surface
M_{car} [kg] Mass of the vehicle
v_{car} [m/s] Velocity of the vehicle
$\dot{v}_{car}$ [m/s$^{2]}$ Acceleration of the vehicle
g = 9.81 m/s^2 Free fall acceleration
ρ_{air} = 1.2041 kg/m^3 Air density of dry air at 20 ◦C
c_{rr} [−] Tire rolling resistance coefficient
C_{drag} [−] Aerodynamic drag coefficient
A_{front} [m^2] Front area
v_{wind} [m/s] Headwind speed

2.1.3 Mathematical Model

To determine how a commute would look if an electric car was driven instead of a gasoline car, a mathematical model for the car's motion is necessary. This allows us to take altitude and position data and translate it into power, allowing us to calculate the theoretical electric car's demands for the trip**[56]**.

The model we use takes into account several forces and assumptions:

- $F_{motor} = ma$, where m is the mass of the car and a is the acceleration experienced as a result of the force exerted by the motors.
- $F_g = mgsin\Theta$, where m is the mass of the car, g is the acceleration due to gravity (9.81 m/s^2) and Θ represents the angle with horizontal created by the change in altitude.
- $F_{rr} = C_{rr}mg$, where C_{rr} is a constant of rolling resistance, m is the mass of the car, and g is the acceleration due to gravity.
- $F_{ar} = \frac{1}{2}pv^2C_dA$ where v is the velocity of the car, C_d is the coefficient of the drag of the car, A is the frontal area of the car, p is the density of air which is calculated by;

$$p = p_o.(1 - \frac{L.h}{T_o})^{\frac{Q.m}{R.L}}$$

$$p = \frac{p.M}{R.T}$$

Where,
p_o = 101325 Pa, Sea level standard atmospheric pressure
T_o = 288.15K, Sea level standard temperature
g = 9.81 m/s^2, Earth-surface gravitational acceleration
L = 0.0065 K/m Temperature lapse rate
R = 8.31447 J/(Mol.K) Universal gas constant
M = 0.0289644 kg/mol Molar mass of dry air

These forces are all calculated, then converted to power using the formula $P = F_{total}, v$, where F_{total} is the sum of the forces and v is the velocity of the car.

We also keep track of changes in internal resistance as temperature of the battery changes, in order to accurately account for heat waste. To find the heat loss, we use:

- $Q_{cooling} = h.A.(T - T_A)$, where Q is the heat flow out of the car due to air cooling, h=10.45-v-10$\sqrt{v}$, A is the exposed surface area of the battery, T is the battery temperature and TA is the air temperature.
- $P = I^2R$, where P is the power lost to heat, I is the current and R is the resistance
- $Q_{tot} = mc\Delta t$, where Q_{tot} is the net increase in heat energy in the battery over the time step, m is the mass of the battery, c is the specific heat of the battery and Δt is the change in temperature.
- $R(T) = T^{-0.02573644} - 0.8555693034$, where R(T) is the internal resistance and T is the temperature.

The model assumes:

- There is a -0.35 kW constant discharge due to car accessories.
- If there is regenerative braking (covered in F_{motor}), the car takes in a constant proportion of .35 of the possible recoverable energy. All braking is considered regenerative.
- We assume a constant discharge efficiency of .80 due to drivetrain inefficiencies.
- If the car is stopped, it uses only the constant discharge.
- Since the GPS data is not continuous and has discrete time steps, we assume that the power output is constant between steps. **[56]**

When the model is implemented, it compares somewhat closely to measured, actual data. There are several sources of error in the assumptions and in satellite error, accounting for the imperfections of the model. In **figure 2.2b**, the model compared against a real trip with power measurements:

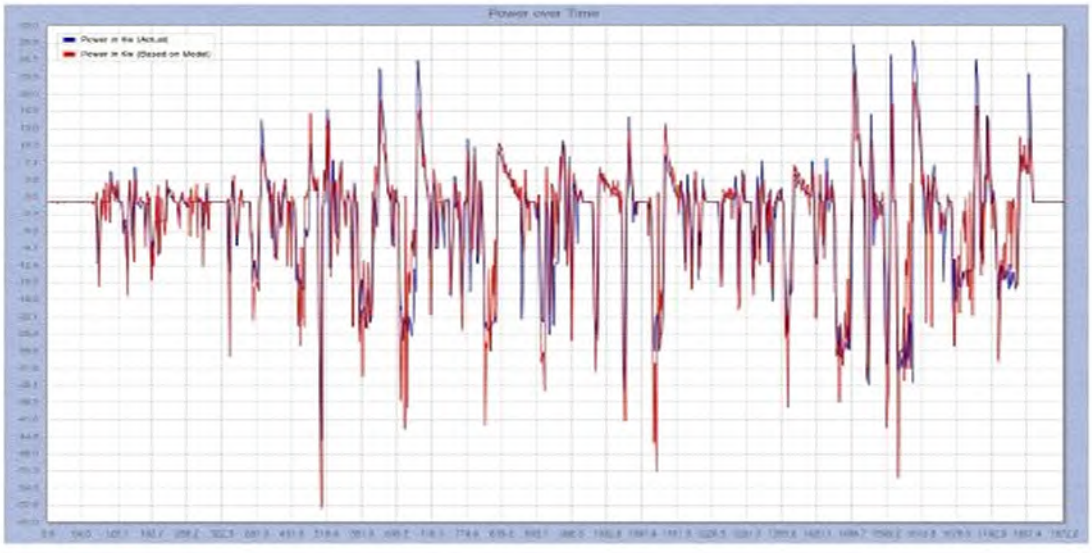

Figure 2.2(b): A model compared against a real trip with power measurements

2.1.4 Auxiliary Loads

The main purpose of the battery is to provide power for the wheels. However, a modern car has also other loads which the battery should supply. These loads are either due to safety, e.g., light, wipers, horn, etc. and/or comfort, e.g., radio, heating, air conditioning, etc. These loads are not constant, e.g., the power consumption of the climate system strongly depends on the surrounding temperature. Even though some average values are suggested which can be seen in **Table 2.1**. From the table it may be understood that the total average power consumption is p_{Aux} = 857 W. **[54]**

Radio	**52W**
Heating Ventilation Air Condition (HVAC)	**489W**
Lights	**316W**
Total p_{aux}	**857W**

Table 2.1: Average power level of the auxiliary loads of the vehicle.

2.1.5 Transmission

From Figure 2.1 it can be understood that the torque, angular velocity, and power of the transmission system are given by the following 4 equations:

$$\tau t = ftrw \quad \textbf{(1)}$$

$$\tau w = \frac{\tau t}{2} \quad \textbf{(2)}$$

$$\omega w = \frac{vcar}{rw} \quad \textbf{(3)}$$

$$\rho t = ftvcar \quad \textbf{(4)}$$

Where,

τ_t [Nm] Traction torque
τ_w [Nm] Torque of each driving wheel
r_w [m] Wheel radius
ω_w [rad/s] Angular velocity of the wheels
p_t [W] Traction power

It is assumed that the power from the shaft of the electric machine to the two driving wheels has a constant efficiency of η_{TS} = 0.95 (Ehsani et al., 2005) **[54]**. The shaft torque, angular velocity, and power of the electric machine are therefore;

$$\tau s = \begin{cases} \eta ts \dfrac{\tau t}{G}, \rho t < 0 \\ \dfrac{\tau t}{\eta T ts G}, \rho t \geq 0 \end{cases}$$

$$\omega s = G \omega w$$

$$\rho s = \tau s \omega s,$$

Where,

τs [Nm] Shaft torque of electric machine
ωs [rad/s] Shaft angular velocity of electric machine
ρs [W] Shaft power of electric machine
G [−] Gear ratio of differential

2.1.6 Electric Machine

For propulsion usually the induction machine (IM), permanent magnet synchronous machine (PMSM), and switched reluctance machine (SRM) are considered. The "best" choice is like many other components a tradeoff between, cost, mass, volume, efficiency, reliability, maintenance, etc. However, due to its high power density and high efficiency the PMSM is selected. The electric machine is divided into an electric part and mechanic part **[57]**. The electric part of the PMSM is modeled in the DQ-frame, i.e.,

$$Vd = R_s i_d + Ld \frac{di_d}{dt} - \omega e L q i q$$

$$V_q = R_s i_q + L_q \frac{di_q}{d_t} + \omega_e L_d i_d + \omega_e \lambda_{pm}$$

$$\rho_{EM} = \frac{3}{2}(V_d i_d + V_q i_q)$$

Where,

v_d [V] D-axis voltage
v_q [V] Q-axis voltage
i_d [A] D-axis current
i_q [A] Q-axis current
R_s [Ω] Stator phase resistance
L_d [H] D-axis inductance
L_q [H] Q-axis inductance
λ_{pm} [Wb] Permanent magnet flux linkage

ω_e [rad/s] Angular frequency of the stator
λ_{pm} [Wb] Permanent magnet flux linkage
p_{EM} [W] Electric input power

The mechanical part of the PMSM can be modeled as follows:

$$\tau_e = J_s \frac{d\omega_s}{d_t} + B_v \omega_s + \tau_c + \tau_s$$

$$\rho_s = \tau_s \omega_s$$

Where,

J_s [kgm^2] Shaft moment of inertia
τ_e [Nm] Electromechanical torque
τ_c [Nm] Coulomb torque
B_v [Nms/rad] Viscous friction coefficient

The coupling between the electric and mechanic part is given by,

$$\tau_e = \frac{3}{2}\frac{P}{2}(\lambda_{pm} i_q + (L_d - L_q) i_d i_q)$$

$$\omega_e = \frac{P}{2}\omega_S$$

2.1.7 Inverter

A circuit diagram of the inverter can be seen in **Figure 2.3**. The inverter transmits power between the electric machine (with phase voltages vA, vB, and vC) and the battery by turning on and off the switches QA+, QA-, QB+, QB-, QC+, and QC-. The switches have an on-resistance RQ, Inv. The diodes in parallel of each switch are creating a path for the motor currents during the dead time, i.e., the time where both switches in one branch are non-conducting in order to avoid a shoot-through.

The average power losses of one switch $p_{Q,}$ Inv and diode $p_{D,}$ Inv in Figure 2.3 during one fundamental period are (Casanellas, 1994):

$$\rho_{Q,Inv} = \left(\frac{1}{8} + \frac{m_i}{3\pi}\right) R_{Q,Inv} \dot{I}p^2 + \left(\frac{1}{2\pi} + \frac{mi}{8}\cos(\phi_{EM})\right) V_{Q,th,Inv} \dot{I}_P$$

$$\rho_{D,Inv} = \left(\frac{1}{8} - \frac{m_i}{3\pi}\right) R_{D,Inv} \dot{I}p^2 + \left(\frac{1}{2\pi} - \frac{mi}{8}\cos(\phi_{EM})\right) V_{D,th,Inv} \dot{I}_P$$

$$m_i = \frac{2V_P}{V_{Bat}}$$

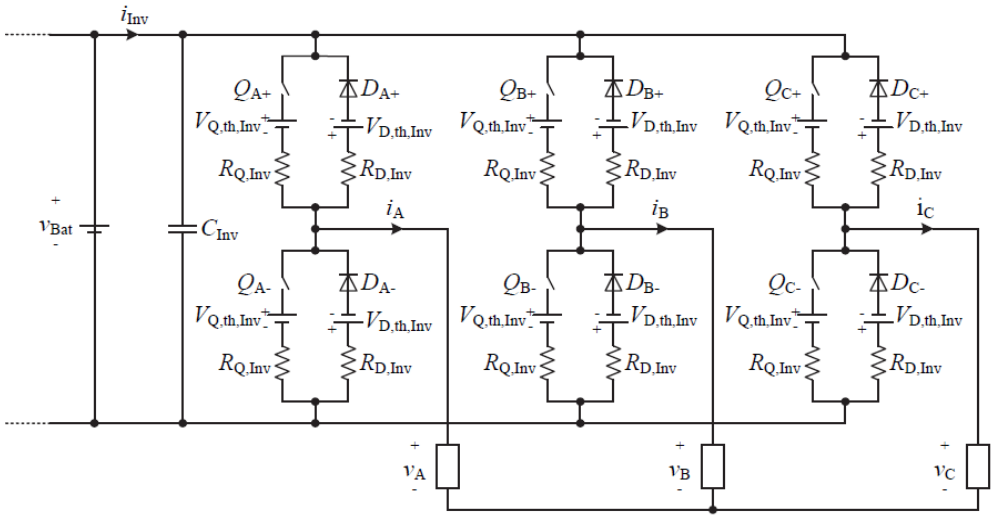

Figure 2.3: Circuit diagram of inverter.

Where,
$p_{Q,Inv}$ [W] Power loss of one switch
$p_{D,Inv}$ [W] Power loss of one diode
φ_{EM} [rad] Power factor angle
I_p [A] Peak phase current
V_p [V] Peak phase voltage
m_i [−] Modulation index
V_{Bat} [V] Battery voltage
$R_{Q,Inv}$ [Ω] Inverter switch resistance
$R_{D,Inv}$ [Ω] Inverter diode resistance
$V_{Q,th,Inv}$ [V] Inverter switch threshold voltage
$V_{D,th,Inv}$ [V] Inverter diode threshold voltage

If it is assumed that the threshold voltage drop of the switches and diodes are equal, i.e., $V_{th,Inv} = V_{Q,th,Inv} = V_{D,th,Inv}$, and that the resistances of the switches and diodes also are equal, i.e., $R_{Inv} = R_{Q,Inv} = R_{D,Inv}$, the total power loss of the inverter is given by **[57]**,

$$P_{Inv,loss} = 6\left(P_{Q,Inv} + P_{D,Inv}\right) = \frac{3}{2}R_{Inv}\dot{I}p^2 + \frac{6}{\pi}V_{th,Inv}\dot{I}_P$$

The output power of the inverter is the motor input power p_{EM}. The inverter input power and efficiency are therefore,

$$\rho_{Inv} = v_{Bat}i_{Inv} = \rho_{EM} + \rho_{Inv,loss}$$

$$\eta_{Inv} = \begin{cases} \frac{\rho_{EM}}{\rho_{Inv}}, \rho_{EM} \geq 0 \\ \frac{\rho_{Inv}}{\rho_{EM}}, \rho_{EM} < 0 \end{cases}$$

2.1.8 Battery

The battery pack is the heart of an electric vehicle. Many different battery types exist, e.g., lead-acid, nickel-metal hydride, lithium ion, etc. However, today the lithium ion is the preferred choice due to its relatively high specific energy and power. In this chapter the battery model will be based on a Saft VL 37570 lithium ion cell. It's specifications can be seen in **Table 2.2 [54].**

Maximum Voltage	$V_{Bat,max,cell}$	4.2V
Nominal Voltage	$V_{Bat,nom,cell}$	3.7V
Minimum Voltage	$V_{Bat,min,cell}$	2.5V
1h Capacity	$Q_{1,cell}$	7Ah
Nominal 1h discharge current	$I_{Bat,1,cell}$	7A
Maximum pulse discharge current	$I_{Bat,max,cell}$	28A

Table 2.2: Data sheet specifications of Saft VL 37570 Lion battery

2.1.8.1 Electric Model

The battery will only be modeled in steady-state, i.e., the dynamic behavior is not considered. The electric equivalent circuit diagram can be seen in **Figure 2.4**. The battery model consists of an internal voltage source and two inner resistances used for charging and discharging. The two diodes are ideal and have only symbolic meaning, i.e., to be able to shift between the charging and discharging resistances. Discharging currents are treated as positive currents, i.e., charging currents are then negative.

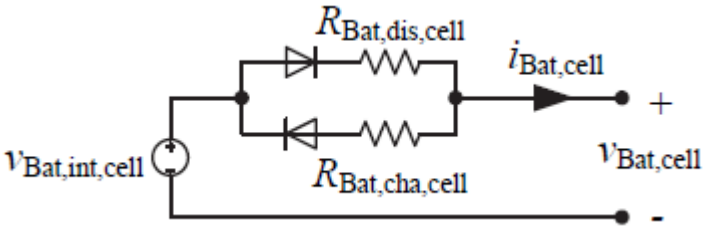

Figure 2.4: Electric equivalent circuit diagram of a battery cell.

From Figure 2.4 the cell voltage is therefore given by,

$$v_{Bat,cell} = \begin{cases} v_{Bat,int,cell} - R_{Bat,cell,diss} i_{Bat,cell}, & i_{Bat,cell} \geq 0 \\ v_{Bat,int,cell} - R_{Bat,cell,cha} i_{Bat,cell}, & i_{Bat,cell} < 0 \end{cases}$$

In the equation,
$V_{Bat,cell}$ [V] Battery cell voltage
$V_{Bat,int,cell}$ [V] Internal battery cell voltage
$I_{Bat,cell}$ [A] Battery cell current
$R_{Bat,cell,dis}$ [Ω] Inner battery cell resistance during discharge mode
$R_{Bat,cell,cha}$ [Ω] Inner battery cell resistance during charge mode

The inner voltage source and the two resistances in Fig. 4 depend on the depth-of-discharge of the battery. The battery cell has been modeled by the curves given in the data sheet of the battery. It turns out that the voltage source and the resistances can be described as 10th order polynomials, for example **[58]**,

$$R_{Bat,cell,dis} = a_{10}DoD_{Bat}^{10} + a_9DoD_{Bat}^{9} + a_8DoD_{Bat}^{8} + a_7DoD_{Bat}^{7} + a_6DoD_{Bat}^{6} + a_5DoD_{Bat}^{5} + a_4DoD_{Bat}^{4} + a_3DoD_{Bat}^{3} + a_2DoD_{Bat}^{2} + a_1DoD_{Bat}^{1} + a_0$$

$$V_{Bat,int,cell} = b_{10}DoD_{Bat}^{10} + b_9DoD_{Bat}^{9} + b_8DoD_{Bat}^{8} + b_7DoD_{Bat}^{7} + b_6DoD_{Bat}^{6} + b_5DoD_{Bat}^{5} + b_4DoD_{Bat}^{4} + b_3DoD_{Bat}^{3} + b_2DoD_{Bat}^{2} + b_1DoD_{Bat}^{1} + b_0$$

$$R_{Bat,cell,cha} = c_{10}DoD_{Bat}^{10} + c_9DoD_{Bat}^{9} + c_8DoD_{Bat}^{8} + c_7DoD_{Bat}^{7} + c_6DoD_{Bat}^{6} + c_5DoD_{Bat}^{5} + c_4DoD_{Bat}^{4} + c_3DoD_{Bat}^{3} + c_2DoD_{Bat}^{2} + c_1DoD_{Bat}^{1} + c_0$$

Where,

a10 = -634, a9 = 2942,1, a8 = -5790,6, a7 = 6297,4, a6 = -4132,1, a5 = 1677,7
a4 = -416,4, a3 = 60,5, a2 = -4,8, a1 = 0,2, a0 = 0
b10 = -8848, b9 = 40727, b8 = -79586, b7 = 86018, b6 = -56135, b5 = -5565
b4 = 784, b3 = -25, b2 = 55, b1 = 0, b0 = 4
c10 = 2056, c9 = -9176, c8 = 17147, c7 = -17330, c6 = 10168, c5 = -3415
c4 = 578, c3 = 25, c2 = 3, c1 = 0, c0 = 0

2.1.8.2 Capacity Model

The inner voltage source, charging resistance, and discharge resistance all depend on the depth-of-discharge. The state-of-charge and depth-of-discharge depend on the integral of the current drawn or delivered to the battery, for instance,

$$D_oD_{Bat} = D_oD_{Bat,ini} + \int \frac{i_{Bat,eq,cell}}{Q_{Bat,1,cell}} dt$$

$$S_OC_{Bat} = 1 - D_oD_{Bat}$$

In the equation,
D_oD_{Bat} [−] Depth-of-discharge
$D_oD_{Bat,ini}$ [−] Initial depth-of-discharge
S_oC_{Bat} [−] Battery state-of-charge
$i_{Bat,eq,cell}$ [A] Equivalent battery cell current

The equivalent battery cell current depends on the sign and amplitude of the current (Schaltz, 2010). Therefore,

$$i_{Bat,eq,cell} = \begin{cases} I_{Bat,1,cell}\left(\frac{i_{Bat,cell}}{I_{Bat,1,cell}}\right)^k, i_{Bat,cell} \geq 0 \\ \eta_{Bat,cha} i_{Bat,cell} \quad , i_{Bat,cell} < 0 \end{cases}$$

$$k = \begin{cases} 1 \quad , \ i_{Bat,cell} \leq I_{Bat,1,cell} \\ 1.125, i_{Bat,cell} > I_{Bat,1,cell,} \end{cases}$$

In the equation,
k [−] Peukert number
$\eta_{Bat,cha}$ = 0.95 [−] Charging efficiency **[58]**

It is seen that the peukert number has two different values depending on the amplitude of the discharge current. For currents higher than the nominal 1 hour discharge current $I_{Bat,1,cell}$ the capacity is therefore reduced significant.

2.1.8.3 Simulation Results

In order to verify the methods used to calculate the state-of-charge, internal voltage source, and charging resistance calculations are compared to the data sheet values. The results can be seen in **Figure 2.5** where the battery cell voltage is shown for different C-values (1 C is the nominal discharge current of $I_{Bat,1,cell}$ = 7A, which means that C/2 is equal to 3.5 A). In the fallowing figure (**Figure 2.5**) **[59]**data sets of C/5, C/2, 1C, 2C has been calculated according to data sheet values (Saft, 2010) and calculations of the battery voltage during constant discharge currents. It is also seen that the calculated voltages almost are identical to the data sheet values. It is also noticed that the voltage is strongly depending on the current level and the delivered Ah, and that the voltage drops significant when the battery is almost completely discharged.

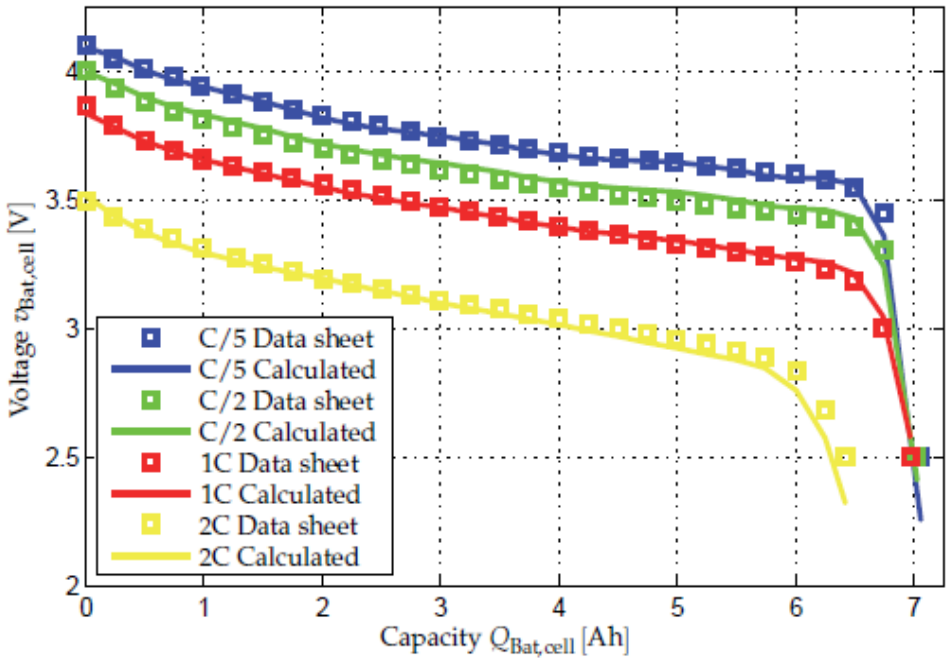

Figure 2.5: Data sheet calculations of battery voltage during constant discharge currents.

2.1.9. Boost Converter

The circuit diagram of the boost converter can be seen in **Figure 2.6**. The losses of the boost converter are due to the switch resistance RQ,BC and threshold voltage $V_{Q,th,BC}$ and the diodes resistance $R_{D,BC}$ and threshold voltage $V_{D,th,BC}$. In order to simplify it is assumed that the resistances and threshold voltages of the switch QBC and diode DBC are equal, for instance, $R_{BC} = R_{Q,BC} = R_{D,RF}$ and $V_{th,BC} = V_{Q,th,BC} = V_{D,th,BC}$. The power equations of the boost converter are therefore given by **[57]**

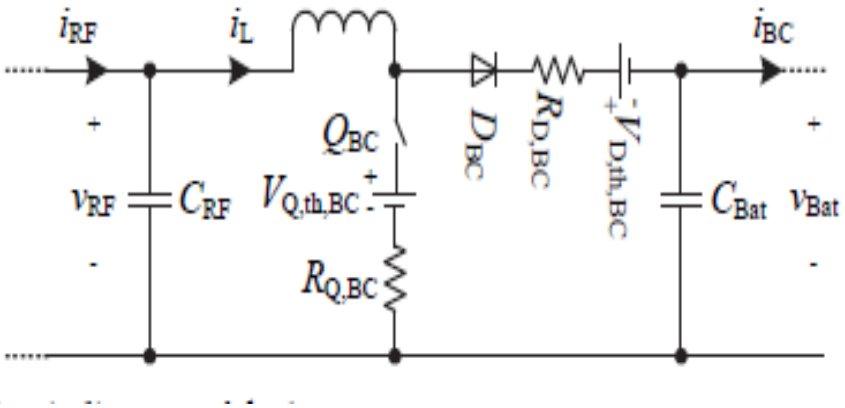

Figure 2.6: Electric circuit diagram of the boost converter.

$$P_{RF} = V_{RF}i_{RF} = P_{BC} + P_{Loss,\ BC}$$
$$P_{BC} = V_{Bat}i_{BC}$$
$$P_{Loss,\ BC} = R_{BC}i^2_{RF} + V_{th,BC}i_{RF},$$

In the equation,

P_{RF} [W] Input power of boost converter
P_{BC} [W] Output power of boost converter
$P_{Loss,BC}$ [W] Power loss of boost converter
V_{RF} [V] Input voltage of boost converter
$V_{th,BC}$ [V] Threshold voltage of switch and diode
R_{BC} [Ω] Resistance of switch and diode
i_{RF} [A] Input current of boost converter
i_{BC} [A] Output current of boost converter

2.1.10. Rectifier

In order to utilize the three phase voltages of the grid V_U, V_V, and V_W they are rectified by a rectifier as seen in **Figure 2.7**[60]. In the rectifier the loss is due to the resistance R_D, R_F and threshold voltage $V_{D,th,RF}$.

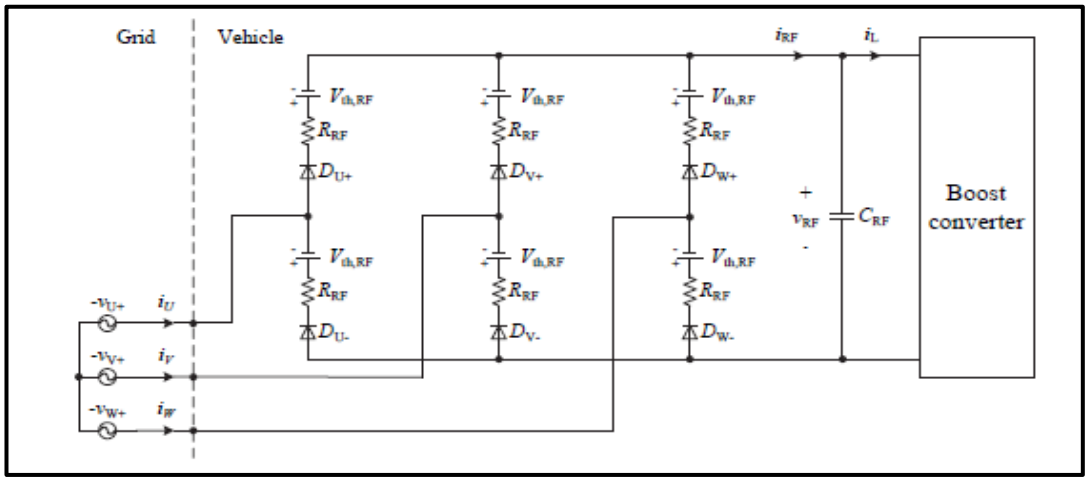

Figure 2.7: Electric circuit diagram of the rectifier.

The average rectified current, voltage, and power are given by,

$$i_{RF} = I_{Grid}\sqrt{\frac{3}{2}} \qquad P_{Grid} = \frac{3\sqrt{2}}{\pi}V_{LL}I_{RF}$$

$$V_{RF} = \frac{3\sqrt{2}}{\pi}V_{LL} - 2R_{RF}\dot{I}_{RF} - 2V_{th,RF} \qquad P_{RF,loss} = 2R_{RF}i^2_{RF} + 2V_{th,RF}i_{RF},$$

$$P_{RF} = V_{RF}i_{RF} = P_{Grid} - P_{RF,loss}$$

In the equations,

I_{Grid} [A] Grid RMS-current
P_{Grid} [W] Power of three phase grid
$Pl_{oss,RF}$ [W] Total loss of the rectifier
R_{RF} [Ω] Resistance of switch and diode
$V_{th,RF}$ [V] Threshold voltage of switch and diode

2.1.11. Simulation Model

The models of each component of the power system in the electric vehicle have now been explained. When combining all the sub models a model of the battery electric vehicle is obtained. In **Figure 2.8** the implementation in a Matlab/Simulink environment can be seen. The overall vehicle model includes the model of the forces acting on the vehicle (wind, gravity, rolling resistance, etc.), and the individual components of the power train, i.e., transmission, electric machine, inverter, battery, boost converter, rectifier. The wind speed V_{wind} and road angle α has been set to zero for simplicity. The input to the simulation model is a driving cycle and the output of the model is all the currents, voltages, powers and torques inside the vehicle **[54]**.

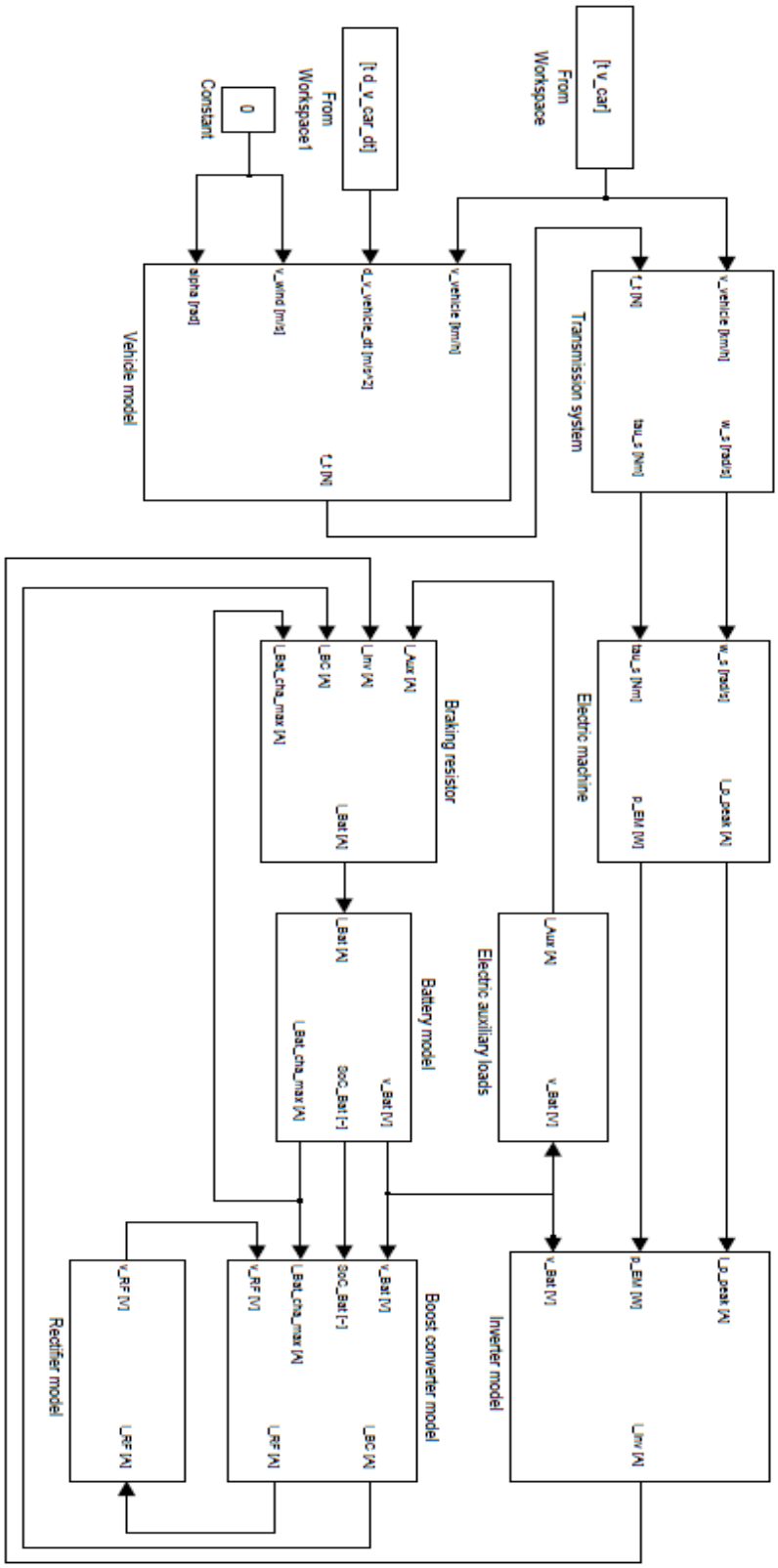

Figure 2.8: Matlab/Simulink implementation of the battery electric vehicle.

2.2. Design Method

2.2.1. Parameter Determination

The parameter determination of the components in the vehicle is an iterative process. The parameters are calculated by using the models given in Section 2 and the outputs of the Matlab/Simulink model shown in **Figure 2.8.** **[61]**

2.2.1.1. Battery

The maximum rectified voltage can be calculated from in no-load mode, for instance,

$$V_{RF,max} = \frac{3\sqrt{2}}{\pi} V_{LL} = \frac{3\sqrt{2}}{\pi} 400V = 540V$$

In order to insure boost operation during charging the rectified voltage of the rectifier should always be greater than this value. The required number of series connected cells is therefore

$$N_{Bat,s} = \frac{V_{RF,max}}{V_{Bat,cell,min}} = \frac{540V}{2.5V} = 216\ cells.$$

The number of series connected cells $N_{Bat,s}$ is due to the voltage requirement of the battery pack. However, in order to insure that the battery pack contains sufficient power and energy it is probably not enough with only one string of series connected cells. The battery pack will therefore consist of $N_{Bat,s}$ series connected cells and $N_{Bat,p}$ parallel strings. The number of parallel strings $N_{Bat,p}$ are calculated in an iterative process. The flow chart of the sizing procedure of the battery electric vehicle can be seen in Fig. 9. In the "Initialization"-process the base parameters are defined, e.g., wheel radius and nominal bus voltage, initial power ratings of each component of the vehicle are given, and the base driving cycle is loaded into the workspace of Matlab. In the "Is the minimum number of parallel string obtained?"-decision block it is verified if the minimum number of parallel strings that fulfills both the energy and power requirements of the battery have been reached. If not a "Simulation routine"-process is executed. This process is executed several times during the sizing procedure and its flow chart is therefore shown separately in **Figure 2.9** **[54]**. This process consists of three sub-processes. The first sub-process is "Design components". In this process the parameters of each component of the battery electric vehicle are determined, e.g., motor and power electronic parameters. The next sub-process is the "Vehicle simulation"-process. In this process the Simulink-model of the vehicle is executed due to the parameters specified in the previous sub-process.

In the third and last sub-process, i.e., the "Calculate the power and energy of each component"-process, the energy and power of each component of the vehicle are calculated. The three sub-processes in the "Simulation routine"-process are executed three times in order to make sure that parameters converge to the same values for the same input. After the "Simulation routine"-process is finishes the "Calculate number of parallel strings"-process is applied. In this process the number of parallel strings NBat,p is either increased or decreased. When the minimum possible number of parallel strings that fulfills both the energy and power requirements of the battery has been found the "Simulation routine"-process is executed in order to calculate the grid energy due to the final number of parallel strings.

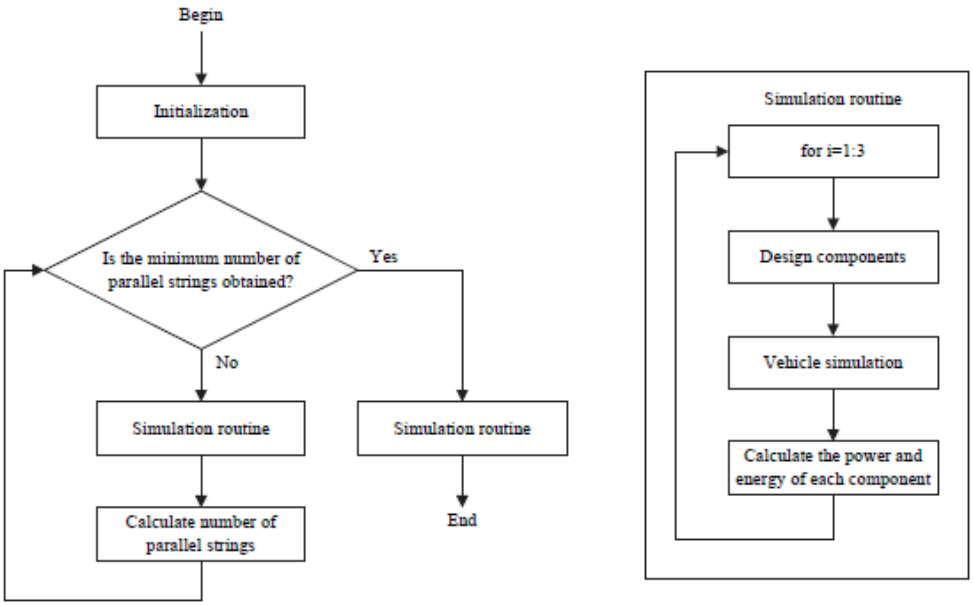

Figure 2.9: Sizing procedure of the battery electric vehicle.

In principle all the energy of a battery could be used for the traction. However, in order to prolong the lifetime of the battery it is usually recommended not to charge it to more than 90% of its rated capacity and not to discharge it below $SoC_{Bat,min}$ = 20%, i.e., only 70% of the available energy is therefore utilized. In Figure 2.10, it can be seen how the "Calculate number of parallel strings"-process finds the minimum number of parallel strings NBat,p that fulfills both the energy and power requirements. This process is a part of the sizing procedure shown in Figure 2.9. In Figure 2.10(a) the minimum state-of-charge min(SoC_{Bat}) is shown and in Figure 2.10(b) the maximum battery cell discharge current max($i_{Bat,cell}$) is shown. From the figure it is understood that the first iteration is for NBat,p = 10. However, both the minimum state-of-charge and maximum discharge current are satisfying their limits, i.e., $SoC_{Bat,min}$ = 0.2 and $I_{Bat,max,cell}$ = 28 A, respectively. Therefore the number of parallel strings is reduced to $N_{Bat,p}$ = 3 for iteration number

two. However, now the state-of-charge limit is exceeded and therefore the number of parallel strings is increased to $N_{Bat,p}$ = 8 for iteration three. This process continuous until iteration number six where the number of parallel strings settles to $N_{Bat,p}$ = 6, as this is the minimum number of parallel strings which ensures that both the state-of-charge and maximum current requirements are fulfilled **[62]**.

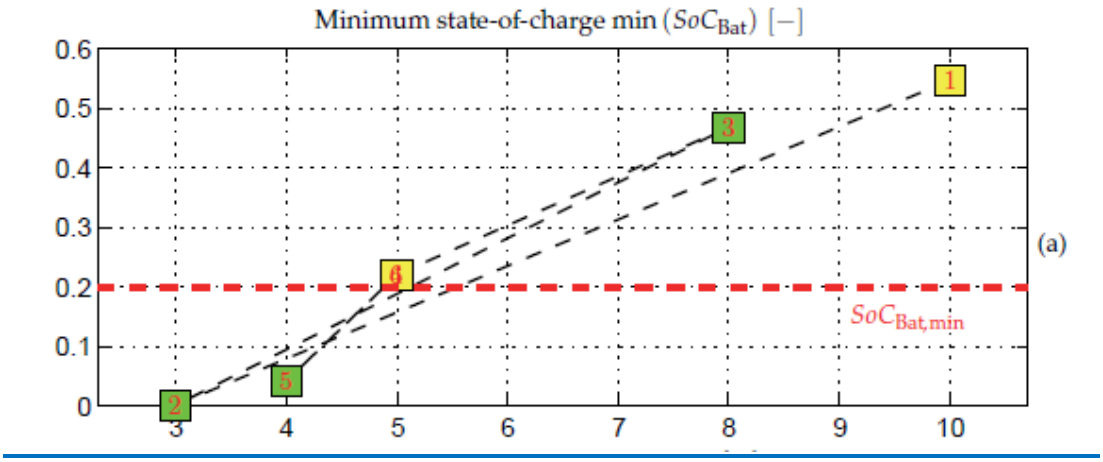

Figure 2.10(a): Number of parallel strings $N_{Bat,p}$ [–]

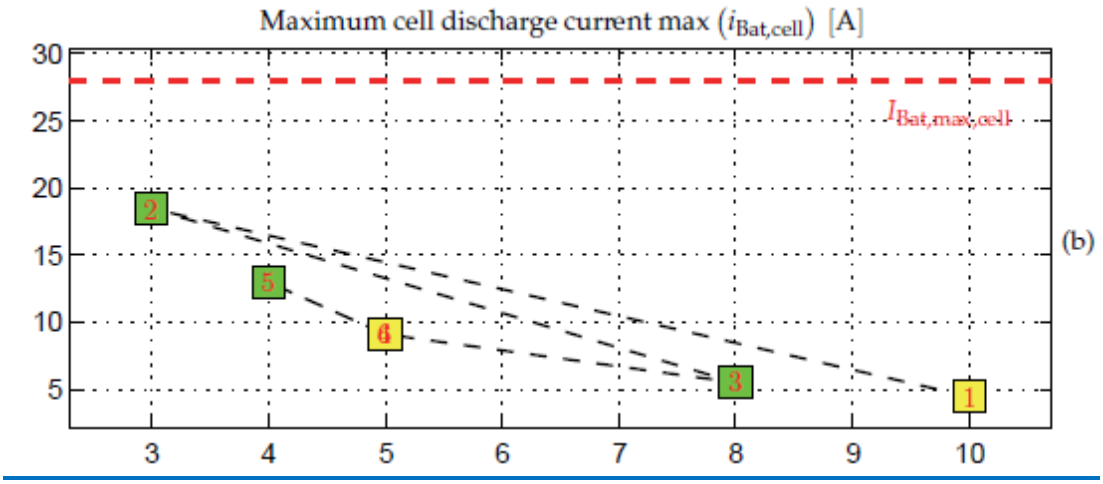

Figure 2.10(b): Number of parallel strings $N_{Bat,p}$ [–]

Number of parallel strings $N_{Bat,p}$ due to the "Calculate number of parallel strings"-process in Figure 2.9. The numbers in the green and yellow boxes indicate the iteration number of the design procedure. The yellow boxes are the first and last iteration number. (a) Minimum state-of-charge $SoC_{Bat,min}$. The red dashed horizontal lines indicate the minimum allowed state-of-charge. (b) Maximum cell discharge current max ($i_{Bat,cell}$). The dashed red horizontal line indicates the maximum allowed discharge current. **[63]**

2.2.1.2. Electric Machine

In order to design the machine design constraints from UQM Technologies (UQM, 2010) are applied. The machine from UQMTechnologies is a brushless permanent magnet synchronous machine with the specifications in Table 2.3.

The phase angle between the voltage and current is not specified, but is assumed to be $\varphi_{EM,nom}$ = 0.55 rad, which corresponds to a power factor of $\cos(\varphi_{EM,nom})$ = 0.85. The shaft angular velocity at (maximum power, maximum torque), (maximum power, continuous torque), and maximum speed are therefore,

$$\omega_{s,corner} = \frac{\eta_{s,corner}}{60s/min} 2\pi = 314.2\, rad/s$$

$$\omega_{s,nom} = \frac{P_{s,max,UQM}}{\tau_{s,cont,UQM}} = 500\, rad/s$$

$$\omega_{s,max} = \frac{\pi_{s,max}}{60s/min} 2\pi = 837.8\, rad/s$$

The relationship between the maximum and continuous shaft torque can be defined as,

$$a_{EM} = \frac{\tau_{s,cont,UQM}}{\tau_{s,max,UQM}} = 1.6$$

It is only possible to have the maximum shaft torque of a PMSM as long as the product of the shaft torque and angular velocity is below the maximum shaft power due to the voltage induced by the permanent magnet. For a PMSM with a given shaft peak torque $\tau_{s,max}$ the speed-torque contour can be written as,

$$P_{s,max} = \tau_{s,max}\omega_{s,corner}$$

$$\tau_{s,limit} = \begin{cases} \tau_{s,max}, \omega s \leq \omega_{s,corner} \\ \frac{P_{s,max}}{\omega s}, \omega s > \omega_{s,corner} \end{cases}$$

The peak shaft torque $\tau_{s,max}$ is selected in such a way that the (τ_s,ω_s)-output from the Matlab/Simulink simulation is below the shaft torque contour $\tau_{s,limit}$ calculated by the above equation

By trial-and-error-method it turns out that if the coulomb torque and viscous friction are responsible for 2% and 6 %, respectively, of the power loss at maximum speed and power, the maximum efficiency is located around the nominal point of operation **[54]**. Therefore,

$$\tau_c = \frac{0.02}{\omega_s} \frac{P_{s,max}}{\eta_{EM,b}}$$

$$B_v = \frac{0.06}{\omega_s^2} \frac{P_{s,max}}{\eta_{EM,b}}$$

The nominal electro mechanical torque is:

$$\tau_{s,cont} = \frac{\tau_{s,max}}{\alpha_{EM}}$$
$$\tau_{e,cont} = \tau_c + B_v\omega_{s,nom} + \tau_{s,cont}$$

The machine will be designed at nominal speed $\omega_{s,nom}$, maximum power $P_{s,max}$, and minimum bus voltage $V_{Bus,min}$. The speed is approximately proportional to the terminal voltage. At the minimum bus voltage the machine should be able run at maximum speed with a modulation index mi = 1. Because the machine is designed at nominal speed, but at the minimum battery voltage, the modulation index is

$$m_{i,nom} = \frac{\omega_{s,nom}}{\omega_{s,max}} = 0.3581$$

The voltages of the machine are therefore:

$$\hat{V}_{p,nom} = m_{i,nom}\frac{V_{Bat,min}}{2}$$
$$V_{d,nom} = -\hat{V}_{p,nom}\sin(\phi_{EM,nom})$$
$$V_{q,nom} = \hat{V}_{p,nom}\cos(\phi_{EM,nom})$$

Several control properties of the PMSM can be applied. Due to its simple implementation the I_d = 0 property is selected even though the reluctance then cannot be utilized. Therefore, when using I_d = 0 control the machine parameters can be calculated as follows:

$$P_{EM,max} = \frac{P_{s,max}}{\eta_{EM,a}}$$
$$I_{q,cont} = \frac{2}{3}\frac{P_{EM,max}}{V_{q,nom}}$$
$$\lambda_{pm} = \frac{2}{3}\frac{2}{P}\frac{\tau_{e,cont}}{I_{q,cont}}$$
$$\omega_{e,nom} = \omega_{s,nom}\frac{P}{2} = 4500\ rad/s$$
$$L_q = -\frac{V_{d,nom}}{\omega_{e,nom}I_{q,cont}}$$
$$R_s = \frac{V_{q,nom} - \omega_{e,nom}\lambda_{pm}}{I_{q,cont}}$$

The efficiency of the machine for different torque-speed characteristics can be seen in **Figure 2.11**[54]. It is seen that the efficiency is highest at continuous torque $\tau_{s,cont}$ and nominal speed $n_{s,nom}$. A common mistake in electric vehicle modeling is to assume a fixed efficiency of the components and it can be understood from Figure 2.11 that wrong conclusions therefore can be made if the electric machines not is operating in a sufficient point of operation. The corner speed $n_{s,corner}$, nominal speed $n_{s,nom}$, maximum speed $n_{s,max}$, continuous torque $\tau_{s,cont}$, peak torque $\tau_{s,max}$, and the torque contour $\tau_{s,limit}$ are also shown in the figure.

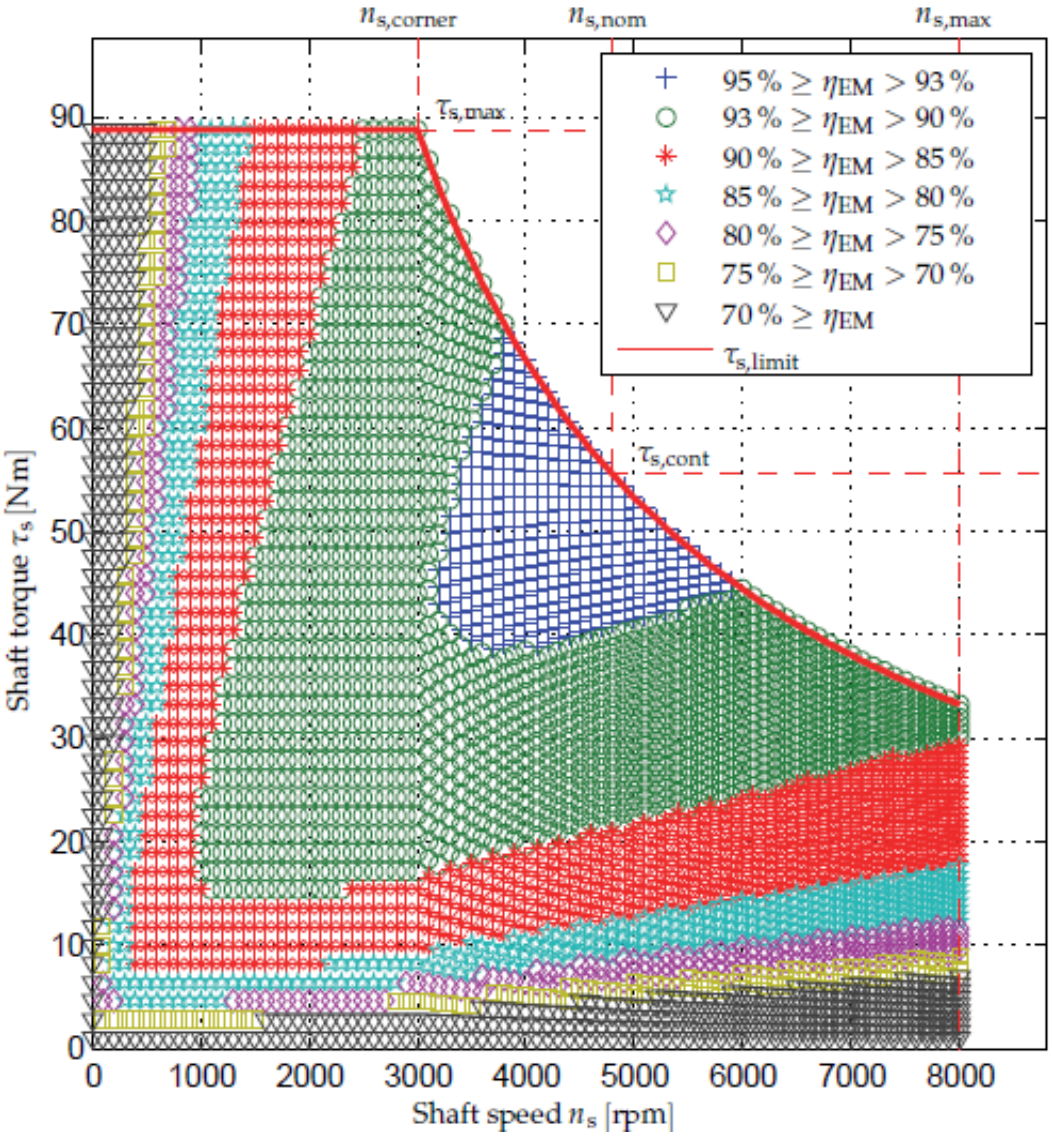

Figure 2.11: Efficiency map of the electric machine.

2.2.1.3. Transmission

The maximum speed of the electric machine is $n_{s,max}$ = 8000 rpm. The required gear ratio of the differential is therefore,

$$G = \frac{\eta_{S,max}}{V_{car,max}} \frac{2\pi}{60} \frac{rw}{1.1}$$

From the above equation, it is seen that the differential is designed with a 10%buffer of the maximum speed of the car **[57]**.

2.2.1.4. Rectifier

It is expected that most of the charging of the vehicle will take place at private homes, where the maximum RMS-current is $I_{Grid,max}$ = 16A. The maximum grid power and rectifier current are therefore,

$$P_{Grid,max} = \frac{3\sqrt{3}}{\pi} V_{LL} I_{Grid,max} = 10.6kW$$

$$I_{RF,max} = \sqrt{\frac{3}{2}} I_{Grid,max} = 19.6A$$

It is assumed that the rectifier has an efficiency of $\eta_{RF,nom}$ = 0.98 at maximum grid power.

$$P_{RF,max} = \eta_{RF,nom} P_{Grid,max} = P_{Grid,max} - (2R_{RF} I_{RF,max}^2 + 2V_{th,RF} I_{RF,max})$$

$$R_{RF} = \frac{P_{Grid,max}(1 - \eta_{RF,nom}) - 2V_{th,RF} I_{RF,max}}{2I_{RF,max}^2} = 199m\Omega$$

2.2.1.5. Boost Converter

It is assumed that the boost converter has efficiency $\eta_{BC,nom}$ = 0.98 at maximum power. The maximum power of the boost converter is therefore,

$$P_{BC,max} = P_{RF,max} \eta_{BC,nom}$$

The threshold voltage is $V_{th,BC}$ = 1.5V. From the resistance of the boost converter is therefore from $P_{RF} = V_{RF} i_{RF} = P_{BC} + P_{Loss,\ BC}$

$$P_{RF,max} = \eta_{BC,nom} P_{RF,max} + R_{BC} I_{RF,max}^2 + V_{th,BC} I_{RF,max}$$

$$R_{BC} = \frac{P_{RF,max}(1 - \eta_{BC,rat}) - V_{th,BC} I_{RF,max}}{I_{RF,max}^2} = 475\ \Omega$$

It might be noticed that the values of the resistances of the rectifier and boost converter are higher than one would expect. However, this is because it is assumed that all the loss is due to the threshold voltage and resistance of the switches and diodes **[60]**.

2.2.1.6. Inverter

The inverter is also designed at the maximum power of the electric machine and at minimum battery voltage. However, the inverter is designed at the peak shaft torque instead of at the maximum speed. The inverter is assumed to have an efficiency of $\eta_{Inv,nom}$ = 0.98 at this point of operation. The loss $P_{Inv,loss,max}$ and resistance R_{Inv} of the inverter are therefore,

$$P_{Inv,loss,max} = \frac{1-\eta_{Inv,nom}}{\eta_{Inv,nom}} P_{EM,max}$$

$$\tau_{e,max} = \tau_c + B_v \omega_{s,corner} + \tau_{s,max}$$

$$I_{q,max} = \frac{2}{3}\frac{2}{P}\frac{\tau_{e,max}}{\lambda_{pm}}$$

$$R_{Inv} = \frac{P_{Inv,loss,max} - \frac{6}{\pi} V_{th,Inv} I_{q,max}}{\frac{3}{2} I_{q,max}^2}$$

The threshold voltage is assumed to be $V_{th,Inv}$ = 1V.

2.2.2. Battery Charging Control

During the charging of the battery, i.e., both due to the regenerative braking and the grid, it is very important that the maximum battery charging current and voltage not are exceeded. The maximum allowed cell charging current can be calculated from the inner and outer voltage of the battery cell, for example,

$$i_{Bat,cell,cha,max} = \begin{cases} \frac{V_{Bat,max,cell} - V_{Bat,int,cell}}{R_{Bat,cell,cha}}, & \frac{V_{Bat,max,cell} - V_{Bat,int,cell}}{R_{Bat,cell,cha}} \leq I_{Bat,1,cell} \\ I_{Bat,1,cell}, & \frac{V_{Bat,max,cell} - V_{Bat,int,cell}}{R_{Bat,cell,cha}} > I_{Bat,1,cell} \end{cases}$$

In above equation, it is insured that neither the maximum allowed voltage or current are exceeded. The battery pack consist of $N_{Bat,s}$ series connected cells and $N_{Bat,p}$ parallel connected strings. The total voltage and current of the battery pack can therefore be calculated as,

$$V_{Bat} = N_{Bat,s} V_{Bat,cell}$$

$$i_{Bat} = N_{Bat,p} i_{Bat,cell}$$

$$i_{Bat,cha,max} = N_{Bat,p} i_{Bat,cell,cha,max}$$

During the charging of the battery the battery cell voltage $v_{Bat,cell}$ should not exceed $V_{Bat,max,cell}$ = 4.2V and the maximum cell charging current should not be higher than $I_{Bat,1,cell}$ = 7A (Saft, 2010). In order to charge the battery as fast as possible either the maximum voltage or maximum current should be applied to the battery. The requested battery charging current, i.e., the output current of the boost converter i_{BC}, is therefore,

$$i_{BC}^{*} = i_{Bat,cha,max}$$

This means that the requested output power of the boost converter is

$$p_{BC}^{*} = V_{Bat} i_{BC}^{*}$$

The requested charging current insures that neither the maximum allowed voltage or current are exceeded. However, for a big battery pack the required charging power might be so high that a special charging station is necessary. The requested input current of the boost converter, i.e., the rectifier current i_{RF}, can be calculated by the fallowing equation **[54]**,

$$i_{RF}^{*} = \frac{-(V_{th,BC} - v_{RF}) - \sqrt{(V_{th,BC} - V_{RF})^2 - 4R_{BC}p_{BC}^{*}}}{2R_{BC}}$$

The grid RMS-current can therefore from above equations be calculated as

$$I_{Grid} = \begin{cases} \sqrt{\frac{2}{3}} i_{RF}^{*}, \sqrt{\frac{2}{3}} i_{RF}^{*} < I_{Grid,max} \\ I_{Grid,max}, \sqrt{\frac{2}{3}} i_{RF}^{*} \geq I_{Grid,max} \end{cases}$$

Nomenclature	**Symbol**	**Value**
Glider Mass	M_{glider}	670 kg
Wheel Radius	r_w	0.2785 m
Front Area	A_{front}	1.68 m^2
Aerodynamic Drag Coefficient	C_{drag}	0.3

Table 2.3: Parameters of the vehicle used for the case study.

Thereby it is ensured that the maximum RMS grid current is not exceeded. The actual values can therefore be obtained by calculating backwards, for instance[54],

$$i_{RF} = \sqrt{\frac{3}{2}} I_{Grid}$$

$$p_{RF} = v_{RF} i_{RF}$$

$$p_{BC} = p_{RF} - R_{BC} i_{RF}^2 - V_{th,BC} i_{RF}$$

$$i_{BC} = \frac{p_{BC}}{v_{Bat}}$$

2.2.3 Case Study

2.2.3.1 Driving Cycle

When different cars are compared in terms of energy consumption a standard driving cycle is used. An often used driving cycle is the New European Driving Cycle (NEDC) as this driving cycle contains both city driving with several start-and-stops and motorway driving, i.e., it is a good representation of a realistic driving environment. The NEDC has a maximum speed of 120 km/h, an average speed of 33.2 km/h, a duration of 1184 s, and a length of 10.9 km. The NEDC profile can be seen in **Figure 2.12**[54]. The input to the simulation will be the NEDC repeated 14 times as this should provide a driving distance of 153 km which is assumed to be an acceptable driving distance.

2.2.3.2 Vehicle Parameters

The energy consumption of a given vehicle depends on the physical dimensions and total mass of the vehicle. For this case study the parameters in Table 4 are used. The glider mass is the mass of the vehicle without motor, battery, power electronics, etc. It might be understood from the parameters in **Table 2.3** that it is a rather small vehicle, i.e., similar to a Citroen C1.

2.2.3.3 Results

In Figure 2.13 the battery state-of-charge, current, voltage, and the power of the grid and battery can be seen. It is understood from Figure 2. 13(a) that the battery is designed due to its energy requirement rather than the power requirement as the state-of-charge reaches the minimum allowed value of $SoC_{Bat,min}$ = 0.2. In Figure 2.13(b) and (c) the battery current and voltage are shown, respectively. It is seen that when the current becomes

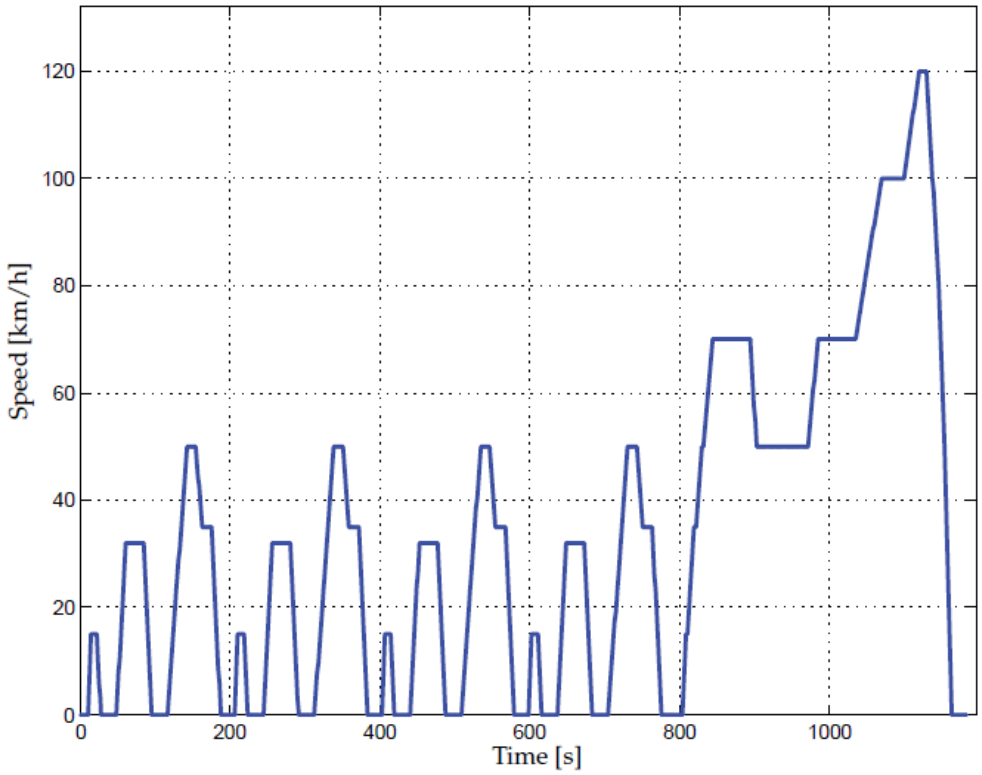

Figure 2.12: New European Driving Cycle (NEDC)

higher the voltage becomes lower as the power should be the same. In Figure 2.13(d) the battery and grid power are shown. It is seen that the charging of the battery is limited by the maximum allowed grid power $P_{Grid,max}$. After approximately two hours the battery reaches the maximum voltage, and it is therefore seen that the battery then is charged under constant-voltage approach, which means that the battery current and power and grid power slowly are decreased until the battery reaches its initial state-of-charge value. Due to the minimum battery pack voltage requirement $N_{Bat,s}$ = 216 series connected battery cells are required. The chosen vehicle is designed to be able to handle 14 repetitions of the NEDC. From Figure 2.10 it is understood that $N_{Bat,p}$ = 5 parallel strings are demanded in order to fulfill this requirement. This means that the battery pack has a capacity of

$$E_{Bat} = \frac{V_{Bat,nom,cell} N_{Bat,s} Q_{Bat,1,cell} N_{Bat,s}}{1000\ Wh/kWh} = 28.0\ kWh$$

The energy distribution of the vehicle can be seen in **Fig. 2.14**[63]. During the 14 NEDC repetitions E_t = 11.2 kWh is delivered to the surface between the driving wheels and the road, but E_{Grid} = 22.7 kWh charging energy is taken from the grid. This means that only 49% of the charging energy from

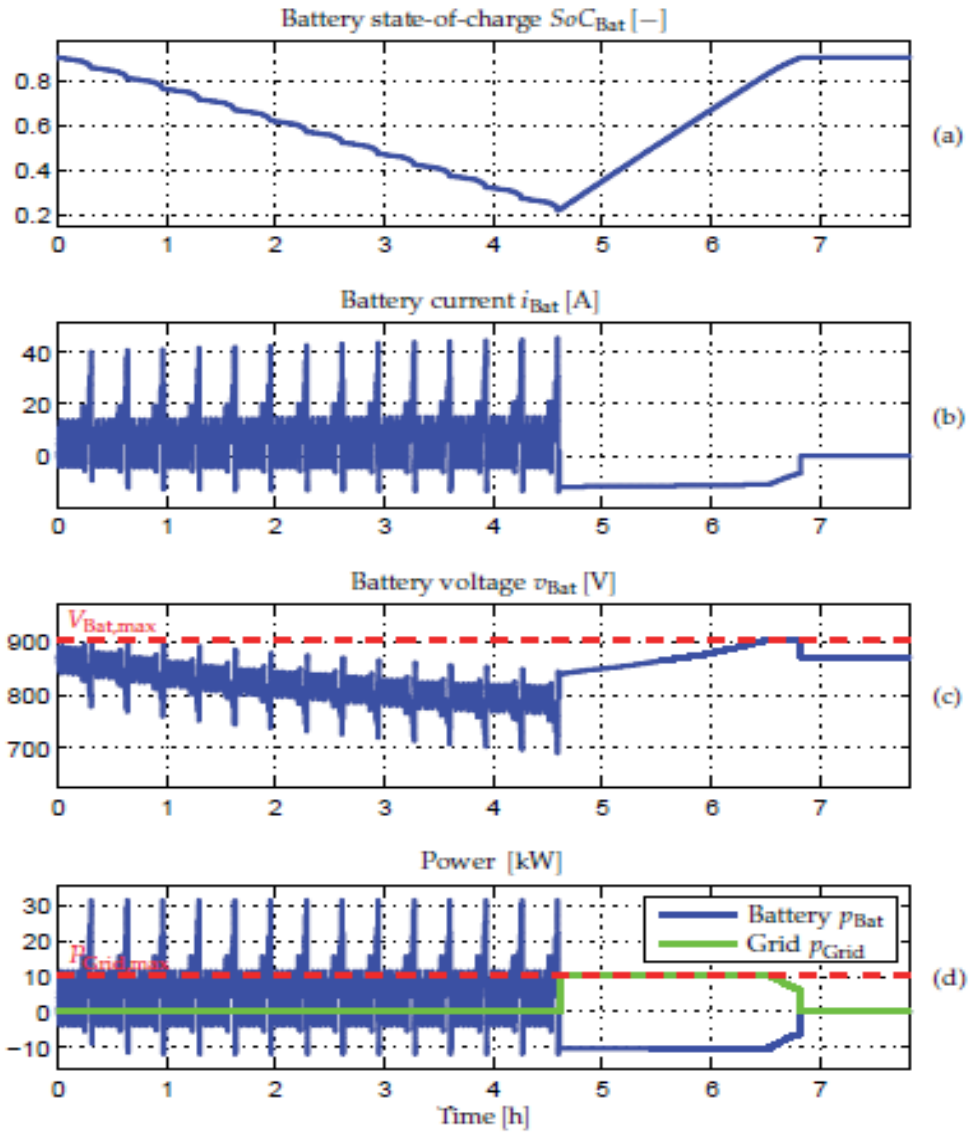

Figure 2.13: Simulation results of the vehicle with 14 repeated NEDC cycles as input. **(a)** Battery state-of-charge. **(b)** Battery current. **(c)** Battery voltage. **(d)** Power of the battery and grid.

the grid is used for the traction and that the grid energy consumption is 148.3Wh/km. The rest of the energy is lost in the path between the wheels and the grid. The auxiliary loads are responsible for the biggest energy loss at 17 %. However, it is believed that this can be reduced significant by using diodes for the light instead of bulbs, and to use heat pumps for the heating instead of pure resistive heating **[65]**. The battery is responsible for the second largest energy waist as 14% of the grid energy is lost in the battery. The battery was only designed to be able to handle the energy and power requirements. However, in order to reduce the loss of the battery it might be beneficial to oversize the battery as the battery peak currents then will become closer to its nominal current which will reduce the negative influence

of the peukert phenomena. However, a heavier battery will also increase the traction power, so the gained reduction in battery loss should be higher than the increased traction power. A bigger battery will of course also make the vehicle more expensive, but these issues are left for future work.

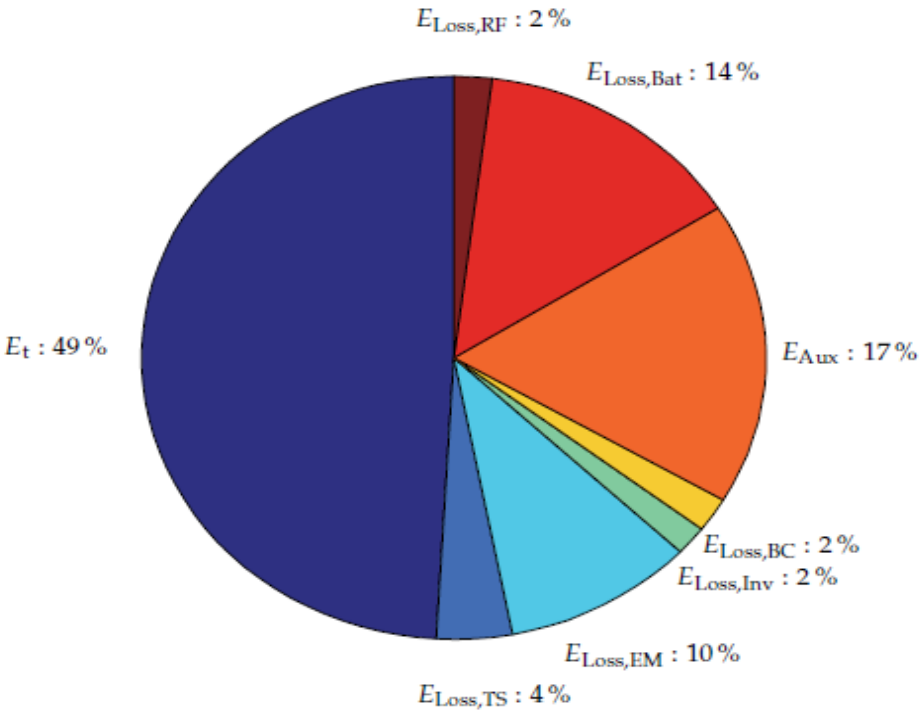

Figure 2.14: Energy distribution in the vehicle relative to the grid energy.

In this chapter a battery electric vehicle have been modeled and designed. The battery of the electric vehicle is designed in such a way that both the power and energy requirements are fulfilled for a given driving cycle. The design procedure is an iterative process as the power flow inside the vehicle depends on the parameters of each component of the power system between the grid and driving wheels. The loss of each component in the vehicle depends on the internal states of the vehicle, i.e., the voltages, currents, speed, torques, and state-of-charge. These states have been included in the modeling in order to obtain a realistic energy calculation of the vehicle. A case study with a small vehicle undergoing 14 driving cycles of type NEDC resulted in a grid energy consumption of 148.3Wh/km with an efficiency of 49% from the grid to the driving wheels. However, a relatively big part of the energy loss is due to the auxiliary loads, e.g., light, safety systems, comfort systems, etc., and the battery. For this work the only design constraint of the battery was the voltage limit, and the energy and power requirements. For future work it is recommended also to include the cost and overall efficiency as design parameters. It is also suggested to investigate how the loss due to the auxiliary loads can be reduced.

3. Energy Source: Battery

A basic requirement for electric vehicles (EVs) is a portable source of electrical energy, which is converted to mechanical energy in the electric motor for vehicle propulsion. Electrical energy is typically obtained through conversion of chemical energy stored in devices such as batteries and fuel cells. A flywheel is an alternative portable source in which energy is stored in mechanical form to be converted into electrical energy on demand for vehicle propulsion. The portable electrical energy source presents the biggest obstacle in commercialization of EVs. A near-term solution for minimizing the environmental pollution problem due to the absence of a suitable, high-energy-density energy source for EVs is perceived in the hybrid electric vehicles (HEVs) that combine propulsion efforts from gasoline engines and electric motors.

A comparison of the specific energy of the available energy sources is given in Table 3.1. The specific energy is the energy per unit mass of the energy source. The specific energies are shown without taking containment into consideration. The specific energy of hydrogen and natural gas would be significantly lower than that of gasoline when containment is considered.

Among the available choices of portable energy sources, batteries have been the most popular choice of energy source for EVs since the beginning of research and development programs in these vehicles. The EVs and HEVs commercially available today use batteries as the electrical energy source. The various batteries are usually compared in terms of descriptors, such as specific energy, specific power, operating life, etc. Similar to specific energy, *specific power* is the power available per unit mass from the source. The *operating life* of a battery is the number of deep discharge cycles obtainable in its lifetime or the number of service years expected in a certain application. The desirable features of batteries for EV and HEV applications are high specific power, high specific energy, high charge acceptance rate for recharging and regenerative braking, and long calendar and cycle life. Additional technical issues include methods and designs to balance the battery segments or packs electrically and thermally, accurate techniques to determine a battery's state of charge, and recycling facilities of battery components. And above all, the cost of batteries must be reasonable for EVs and HEVs to be commercially viable.

Battery technology has been undergoing extensive research and development efforts over the past 30 years, yet there is currently no battery that can deliver an acceptable combination of power, energy, and life cycle for high-volume production vehicles. The small number of EVs and HEVs that were introduced in the market used batteries that were too expensive and

have short calendar life, making the batteries the biggest impediment in commercializing EVs and HEVs **[4]**.

TABLE 3.1 Nominal Energy Density of Sources

Energy Source	Nominal Specific Energy (Wh/kg)
Gasoline	12,500
Natural gas	9350
Methanol	6050
Hydrogen	33,000
Coal (bituminous)	8200
Lead-acid battery	35
Lithium-polymer battery	200
Flywheel (carbon-fiber)	200

Table 3.1: Nominal Energy Density of Sources

3.1 Battery Basics

The batteries are made of unit cells containing the chemical energy that is convertible to electrical energy. One or more of these electrolytic cells are connected in series to form one battery. The grouped cells are enclosed in a casing to form a battery module. A battery pack is a collection of these individual battery modules connected in a series and parallel combination to deliver the desired voltage and energy to the power electronic drive system.

The energy stored in a battery is the difference in free energy between chemical components in the charged and discharged states. This available chemical energy in a cell is converted into electrical energy only on demand, using the basic components of a unit cell, which are the positive and negative electrodes, the separators, and the electrolytes. The electrochemically active ingredient of the positive or negative electrode is called the active material. Chemical oxidation and reduction processes take place at the two electrodes, thereby bonding and releasing electrons, respectively. The electrodes must be electronically conducting and are located at different sites, separated by a separator, as shown in **Figure 3.1**[4]. During battery operation, chemical reactions at each of the electrodes cause electrons to flow from one electrode to another; however, the flow of electrons in the cell is sustainable only if electrons generated in the chemical reaction are able to flow through an external electrical circuit that connects the two electrodes. The connection points between the electrodes and the external circuit are called the battery terminals. The external circuit ensures that most of the stored chemical energy is released only on demand and is utilized as electrical energy. It must

be mentioned that only in an ideal battery does current flow only when the circuit between the electrodes is completed externally. Unfortunately, many batteries do allow a slow discharge, due to diffusion effects, which is why they are not particularly good for long-term energy storage. This slow discharge with open-circuit terminals are known as self-discharge, which is also used as a descriptor of battery quality.

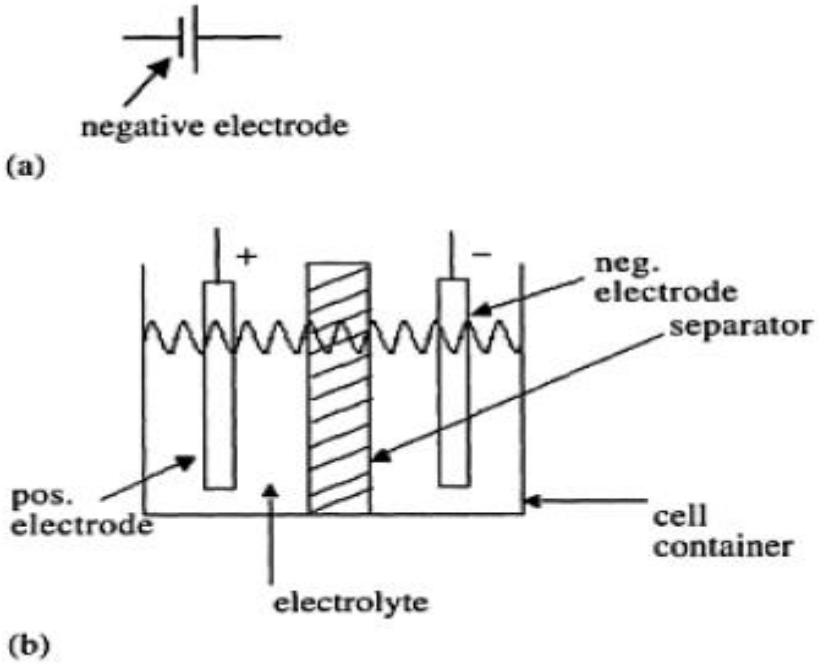

Figure 3.1: Components of a battery cell. (a) Cell circuit symbol; (b) cell cross-section.

The components of the battery cell are described as follows **[66]**:

1. Positive electrode: The positive electrode is an oxide or sulfide or some other compound that is capable of being reduced during cell discharge. This electrode consumes electrons from the external circuit during cell discharge. Examples of positive electrodes are lead oxide (PbO2) and nickel oxyhydroxide (NiOOH). The electrode materials are in the solid state.
2. Negative electrode: The negative electrode is a metal or an alloy that is capable of being oxidized during cell discharge. This electrode generates electrons in the external circuit during cell discharge. Examples of negative electrodes are lead (Pb) and cadmium (Cd). Negative electrode materials are also in the solid state within the battery cell.
3. Electrolyte: The electrolyte is the medium that permits ionic conduction between positive and negative electrodes of a cell. The electrolyte must have high and selective conductivity for the ions that take part in electrode reactions, but it must be a nonconductor for electrons in order to avoid

self-discharge of batteries. The electrolyte may be liquid, gel, or solid material. Also, the electrolyte can be acidic or alkaline, depending on the type of battery. Traditional batteries such as lead-acid and nickel-cadmium use liquid electrolytes. In lead-acid batteries, the electrolyte is the aqueous solution of sulfuric acid [H2SO4(aq)]. Advanced batteries currently under development for EVs, such as sealed lead-acid, nickel-metal-hydride (NiMH), and lithium-ion batteries use an electrolyte that is gel, paste, or resin. Lithium-polymer batteries use a solid electrolyte.

4. Separator: The separator is the electrically insulating layer of material that physically separates electrodes of opposite polarity. Separators must be permeable to the ions of the electrolyte and may also have the function of storing or immobilizing the electrolyte. Present day separators are made from synthetic polymers.

There are two basic types of batteries: primary batteries and secondary batteries. Batteries that cannot be recharged and are designed for a single discharge are known as primary batteries. Examples of these are the lithium batteries used in watches, calculators, cameras, etc., and the manganese dioxide batteries used to power toys, radios, torches, etc. Batteries that can be recharged by flowing current in the direction opposite to that during discharge are known as secondary batteries. The chemical reaction process during cell charge operation when electrical energy is converted into chemical energy is the reverse of that during discharge. The batteries needed and used for EVs and HEVs are all secondary batteries, because they are recharged during regeneration cycles of vehicle operation or during the battery recharging cycle in the stopped condition using a charger. All the batteries that will be discussed in the following are examples of secondary batteries.

The major types of rechargeable batteries considered for EV and HEV applications are:

- Lead-acid (Pb-acid)
- Nickel-cadmium (NiCd)
- Nickel-metal-hydride (NiMH)
- Lithium-ion (Li-ion)
- Lithium-polymer (Li-poly)
- Sodium-sulfur (NaS)
- Zinc-air (Zn-Air)

The lead-acid type of battery has the longest development history of all battery technology, particularly for their need and heavy use in industrial EVs, such as for golf carts in sports, passenger cars in airports, and forklifts in storage facilities and supermarkets. Research and development for batteries picked up momentum following the resurgence of interest in EVs and HEVs in the late 1960s and early 1970s. Sodium-sulfur batteries showed great promise in the 1980s, with high energy and power densities, but safety and manufacturing difficulties led to the abandonment of the technology. The development of battery technology for low-power applications, such as cell phones and calculators, opened the possibilities of scaling the energy and power of nickel-cadmium- and lithium-ion-type batteries for EV and HEV applications **[66]**.

The development of batteries is directed toward overcoming significant practical and manufacturing difficulties. Theoretical predictions are difficult to match in manufactured products due to practical limitations. Theoretical and practical specific energies of several batteries are given in **Table 3.2** for comparison.

The characteristics of some of the more important battery technologies mentioned above are given in the following. The theoretical aspects of the lead-acid battery will be discussed in detail first, followed by shorter descriptions of the other promising technologies.

TABLE 3.2 Specific Energy of Batteries

	Specific Energy (Wh/kg)	
Battery	Theoretical	Practical
Lead-acid	108	50
Nickel-cadmium		20–30
Nickel-zinc		90
Nickel-iron		60
Zinc-chlorine		90
Silver-zinc	500	100
Sodium-sulfur	770	150–300
Aluminum-air		300

Table 3.2: Specific Energy of Batteries

3.2 Lead-Acid Battery

Lead-acid batteries have been the most popular choice of batteries for EVs. Lead-acid batteries can be designed to be high powered and are inexpensive, safe, and reliable. A recycling infrastructure is in place for them. However, low specific energy, poor cold temperature performance, and short calendar and cycle life are among the obstacles to their use in EVs and HEVs. The lead-acid battery has a history that dates to the middle of the 19th century, and it is currently a mature technology. The first lead-acid battery was produced as early as in 1859. In the early 1980s, over 100,000,000 lead-acid batteries were produced per year. The long existence of the lead-acid battery is due to the following:

- Relatively low cost
- Easy availability of raw materials (lead, sulfur)
- Ease of manufacture
- Favorable electromechanical characteristics

The battery cell operation consists of a cell discharge operation, when the energy is supplied from the battery to the electric motor to develop propulsion power, and a cell charge operation, when energy is supplied from an external source to store energy in the battery **[4]**.

3.2.1 Lead-Acid Battery

In the cell discharge operation (**Figure 3.2**), electrons are consumed at the positive electrode, the supply of which comes from the negative electrode. The current flow is, therefore, out of the positive electrode into the motor-load, with the battery acting as the source.

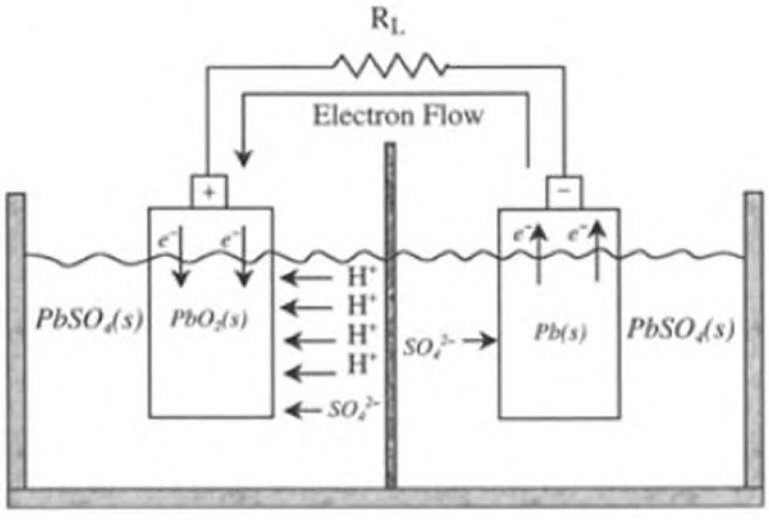

Figure 3.2: Lead-acid battery: cell discharge operation

The positive electrode equation is given by:

$$PbO_2(s) + 4H^+(aq) + SO_4^{-2}(aq) + 2e \rightarrow PbSO_4 + 2H_2O(l)$$

A highly porous structure is used for the positive electrode to increase the PbO2(s)/electrolyte contact area, which is about 50 to 150 m2 per Ah of battery capacity. This results in higher current densities, as PbO2 is converted to PbSO4(s). As discharge proceeds, the internal resistance of the cell rises due to PbSO4 formation and decreases the electrolyte conductivity as H2SO4 is consumed. PbSO4(s) deposited on either electrode in a dense, fine-grain form can lead to sulfatation. The discharge reaction is largely inhibited by the buildup of PbSO4, which reduces cell capacity significantly from the theoretical capacity.

The negative electrode equation during cell discharge is:

$$Pb(s) + SO_4^{-2}(aq) \rightarrow PbSO_4 + 2e$$

The electrons are released at the negative electrode during discharge operation. The production of PbSO4(s) can degrade battery performance by making the negative electrode more passive **[4]**.

3.2.2 Cell Charge Operation

The cell charge operation **Figure 3.3** **[67]** is the reverse of the cell discharge operation. During cell charging, lead sulfate is converted back to the reactant states of lead and lead oxide. The electrons are consumed from the external source at the negative electrode, while the positive electrode releases the electrons. The current flows into the positive electrode from the external source, thereby delivering electrical energy into the cell, where it gets converted into chemical energy. The chemical reaction at the positive electrode during cell charging is:

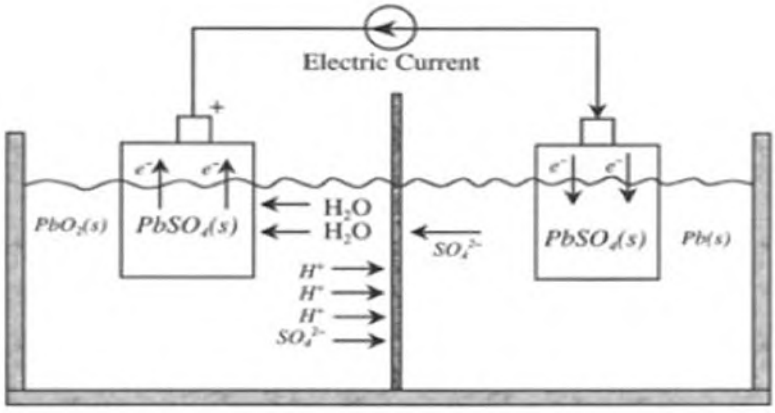

Figure 3.3: Lead-acid battery: cell charge operation.

$$PbSO_4(s) + 2H_2O(l) \rightarrow PbO_2(s) + 4H^+(aq) + SO_4^{-2}(aq) + 2e$$

The chemical reaction at the negative electrode during cell charging is:

$$PbSO_4(s) + 2e \rightarrow Pb(s) + SO_4^{-2}(aq)$$

The overall chemical reaction during cell charging is:

$$2PbSO_4(s) + 2H_2O(l) \rightarrow Pb(s) + PbO_2(s) + 2H_2SO_4(aq)$$

Conventionally, lead-acid batteries are of flooded-electrolyte cells, where free acid covers all the plates. This imposes the constraint of maintaining an upright position for the battery, which is difficult in certain portable situations. Efforts in developing hermetically sealed batteries faced the problem of buildup of an explosive mixture of hydrogen and oxygen on approaching the top-of-charge or overcharge condition during cell recharging. The problem is addressed in the valve-regulated-lead-acid (VRLA) batteries by providing a path for the oxygen, liberated at the positive electrode, to reach the negative electrode, where it recombines to form lead-sulfate. There are two mechanisms for making sealed VRLA batteries, the gel battery, and the AGM (absorptive glass microfiber) battery. These types are based on immobilizing the sulfuric acid electrolyte in the separator and the active materials, leaving sufficient porosity for the oxygen to diffuse through the separator to the negative plate **[67]**.

3.2.3Construction

Construction of a typical battery consists of positive and negative electrode groups (elements) interleaved to form a cell. The through partition connection in the battery is illustrated in **Figure 3.4**. The positive plate is made of stiff paste of the active material on a lattice type grid, which is shown in **Figure 3.5**. The grid, made of a suitably selected lead alloy, is the framework of a portable battery to hold the active material. The positive plates can be configured in flat pasted or tubular fashion. The negative plates are always manufactured as pasted types.

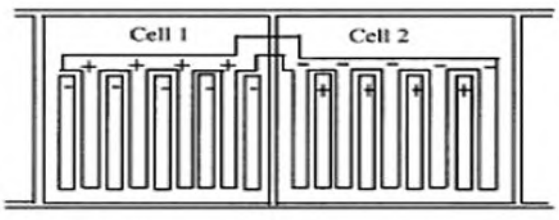

Figure 3.4: Schematic diagram of a lead-acid battery through-partition connection.

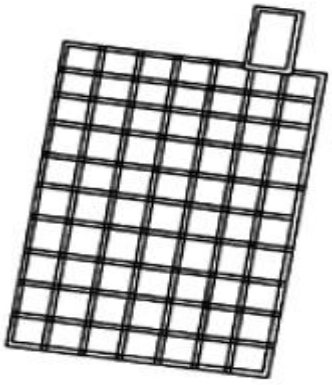

Figure 3.5: A lead-acid battery grid.

3.3 Alternative Batteries

3.3.1 Nickel-Cadmium Battery

Nickel-cadmium (NiCd) and nickel-metal-hydride (NiMH) batteries are examples of alkaline batteries with which electrical energy is derived from the chemical reaction of a metal with oxygen in an alkaline electrolyte medium. The specific energy of alkaline batteries is lowered due to the addition of weight of the carrier metal. The NiCd battery employs a nickel oxide positive electrode and a metallic cadmium negative electrode. The net reaction occurring in the potassium hydroxide (KOH) electrolyte is:

$$Cd + 2NiOOH + 2H_20 \xrightarrow[Discharge]{} 2Ni(OH)_2 + Cd(OH)_2(1.299\ volts)$$

The practical cell voltage is 1.2 to 1.3 V, and the atomic mass of cadmium is 112. The specific energy of NiCd batteries is 30 to 50 Wh/kg, which is similar to that of lead-acid batteries. The advantages of NiCd batteries are superior low-temperature performance compared to lead-acid batteries, flat discharge voltage, long life, and excellent reliability. The maintenance requirements of the batteries are also low. The biggest drawbacks of NiCd batteries are the high cost and the toxicity contained in cadmium. Environmental concerns may be overcome in the long run through efficient recycling, but the insufficient power delivered by the NiCd batteries is another important reason for not considering these batteries for EV and HEV applications. The drawbacks of the NiCd batteries led to the rapid development of NiMH batteries, which are deemed more suitable for EV and HEV applications **[67]**.

3.3.2 Nickel-Metal-Hybride (NiMH) Battery

The nickel-metal-hydride battery is a successor to the nickel-hydrogen battery and is already in use in production HEVs. In NiMH batteries, the positive electrode is a nickel oxide similar to that used in a NiCd battery, while the negative electrode is a metal hydride where hydrogen is stored. The concept of NiMH batteries is based on the fact that fine particles of certain metallic alloys, when exposed to hydrogen at certain pressures and temperatures, absorb large quantities of the gas to form the metalhydride compounds. Furthermore, the metal hydrides are able to absorb and release hydrogen many times without deterioration. The two electrode chemical reactions in a NiMH battery are:
At the positive electrode,

$$NiOOH + H_2o + e^- \xrightarrow[Discharge]{} Ni(OH)_2 + OH^-$$

At the negative electrode,

$$MH_x + OH^- \xrightarrow[Discharge]{} MH_{x-1} + H_2O + e^-$$

M stands for metallic alloy, which takes up hydrogen at ambient temperature to form the metal hydride MHX. The negative electrode consists of a compressed mass of fine metal particles. The proprietary alloy formulations used in NiMH are known as AB5 and AB2 alloys. In the AB5 alloy, A is the mixture of rare earth elements, and B is partially substituted nickel. In the AB2 alloy, A is titanium or zirconium, and B is again partially substituted nickel. The AB2 alloy has a higher capacity for hydrogen storage and is less costly. The operating voltage of NiMH is almost the same as that of NiCd, with flat discharge characteristics. The capacity of the NiMH is significantly higher than that of NiCd, with specific energy ranging from 60 to 80 Wh/kg. The specific power of NiMH batteries can be as high as 250 W/kg. The NiMH batteries have penetrated the market in recent years at an exceptional rate. The Chrysler electric minivan "Epic" uses a NiMH battery pack, which gives a range of 150 km. In Japan, NiMH battery packs produced by Panasonic EV Energy are being used in Toyota EV RAV-EV and Toyota HEV Prius. The components of NiMH are recyclable, but a recycling structure is not yet in place. NiMH batteries have a much longer life cycle than lead-acid batteries and are safe and abuse tolerant. The disadvantages of NiMH batteries are the relatively high cost, higher self-discharge rate compared to NiCd, poor charge acceptance capability at elevated temperatures, and low cell efficiency **[4]**.

3.3.3 Li-ion Battery

Lithium metal has high electrochemical reduction potential (3.045 V) and the lowest atomic mass (6.94), which shows promise for a battery of 3 V cell potential when combined with a suitable positive electrode. The interest in secondary lithium cells soared soon after the advent of lithium primary cells in the 1970s, but the major difficulty was the highly reactive nature of the lithium metal with moisture, restricting the use of liquid electrolytes. Discovery in the late 1970s by researchers at Oxford University that lithium can be intercalated (absorbed) into the crystal lattice of cobalt or nickel to form LiCoO2 or LiNiO2 paved the way toward the development of Li-ion batteries. [3] The use of metallic-lithium is bypassed in Li-ion batteries by using lithium intercalated (absorbed) carbons (LixC) in the form of graphite or coke as the negative electrode, along with the lithium metallic oxides as the positive electrode. The graphite is capable of hosting lithium up to a composition of LiC6. The majority of the Li-ion batteries uses positive electrodes of cobalt oxide, which is expensive but proven to be the most satisfactory. The alternative positive electrode is based on nickel oxide LiNiO2, which is structurally more complex but costs less. Performance is similar to that of cobalt oxide electrodes. Manganeseoxide- based positive electrodes (LiMn2O4 or LiMnO2) are also under research, because manganese is cheaper, widely available, and less toxic. The cell discharge operation in a lithium ion cell using LiCoO2 is illustrated in fallowing equation. During cell discharge, lithium ions (Li+) are released from the negative electrode that travels through an organic electrolyte toward the positive electrode. In the positive electrode, the lithium ions are quickly incorporated into the lithium compound material. The process is completely reversible. The chemical reactions at the electrodes are as follows:
At the positive electrode,

$$xLi^{+} + xe^{-} + Li_{(1-x)}CoO_2 \xrightarrow[Discharge]{} LiCoO_2$$

During cell charge operation, lithium ions move in the opposite direction from the positive electrode to the negative electrode. The nominal cell voltage for a Li-ion battery is 3.6 V, which is equivalent to three NiMH or NiCd battery cells.

Lithium-ion batteries have high specific energy, high specific power, high energy efficiency, good high-temperature performance, and low self-discharge. The components of Li-ion batteries are also recyclable. These characteristics make Li-ion batteries highly suitable for EV and HEV and other applications of rechargeable batteries **[4]**.

3.3.4 Li-Polymer Battery

Lithium-polymer evolved out of the development of solid state electrolytes, i.e., solids capable of conducting ions but that are electron insulators. The solid state electrolytes resulted from research in the 1970s on ionic conduction in polymers. These batteries are considered solid state batteries, because their electrolytes are solids. The most common polymer electrolyte is polyethylene oxide compounded with an appropriate electrolyte salt.

The most promising positive electrode material for Li-poly batteries is vanadium oxide V6O13.1 This oxide interlaces up to eight lithium atoms per oxide molecule with the following positive electrode reaction:

$$Li_x + V_6O_{13} + xe^- \xrightarrow[Discharge]{} Li_xV_6O_{13} \text{ where } 0<x<8$$

Li-poly batteries have the potential for the highest specific energy and power. The solid polymers, replacing the more flammable liquid electrolytes in other type of batteries, can conduct ions at temperatures above 60°C. The use of solid polymers also has a great safety advantage in case of EV and HEV accidents. Because the lithium is intercalated into carbon electrodes, the lithium is in ionic form and is less reactive than pure lithium metal. The thin Li-poly cell gives the added advantage of forming a battery of any size or shape to suit the available space within the EV or HEV chassis. The main disadvantage of the Li-poly battery is the need to operate the battery cell in the temperature range of 80 to 120°C. Li-poly batteries with high specific energy, initially developed for EV applications, also have the potential to provide high specific power for HEV applications. The other key characteristics of the Li-poly are good cycle and calendar life **[4]**.

3.3.5 Zinc-Air Battery

Zinc-air batteries have a gaseous positive electrode of oxygen and a sacrificial negative electrode of metallic zinc. The practical zinc-air battery is only mechanically rechargeable by replacing the discharged product, zinc hydroxide, with fresh zinc electrodes. The discharged electrode and the potassium hydroxide electrolyte are sent to a recycling facility. In a way, the zinc-air battery is analogous to a fuel cell, with the fuel being the zinc metal. A module of zinc air batteries tested in German Mercedes Benz postal vans had a specific energy of 200 Wh/kg, but only a modest specific power of 100 W/kg at 80% depth-of-discharge. With present-day technology, the range of zinc-air batteries can be between 300 to 600 km recharges.

Other metal-air systems have been investigated, but the work has been discontinued due to severe drawbacks in the technologies. These batteries include iron-air and aluminum-air batteries, in which iron and aluminum are, respectively, used as the mechanically recyclable negative electrode.

The practical metal-air batteries have two attractive features: the positive electrode can be optimized for discharge characteristics, because the battery is recharged outside of the battery; and the recharging time is rapid, with a suitable infrastructure **[66]**.

3.3.6 Sodium-Sulfur Battery

Sodium, similar to lithium, has a high electrochemical reduction potential (2.71 V) and low atomic mass (23.0), making it an attractive negative electrode element for batteries. Moreover, sodium is abundant in nature and available at a low cost. Sulfur, which is a possible choice for the positive electrode, is also a readily available and low-cost material. The use of aqueous electrolytes is not possible due to the highly reactive nature of sodium, and because the natures of solid polymers like those used for lithium batteries are not known. The solution of electrolyte came from the discovery of beta-alumina by scientists at Ford Motor Company in 1966. Beta-alumina is a sodium aluminum oxide with a complex crystal structure.

Despite several attractive features of NaS batteries, there are several practical limitations. The cell operating temperature in NaS batteries is around 300°C, which requires adequate insulation as well as a thermal control unit. This requirement forces a certain minimum size of the battery, limiting the development of the battery for only EVs, a market that is not yet established. Another disadvantage of NaS batteries is the absence of an overcharge mechanism. At the top-of-charge, one or more cells can develop a high resistance, which pulls down the entire voltage of the series connected battery cells. Yet another major concern is safety, because the chemical reaction between molten sodium and sulfur can cause excessive heat or explosion in the case of an accident. Safety issues were addressed through efficient design, and manufactured NaS batteries have been shown to be safe.

Practical limitations and manufacturing difficulties of NaS batteries have led to the discontinuation of its development programs, especially when the simpler concept of sodium-metal-chloride batteries was developed.

3.3.7 Sodium-Metal-Chloride Battery

The sodium-metal-chloride battery is a derivative of the sodium-sulfur battery with intrinsic provisions of overcharge and overdischarge. The construction is similar to that of the NaS battery, but the positive sulfur electrode is replaced by nickel chloride ($NiCl_2$) or a mixture of nickel chloride and ferrous chloride ($FeCl_2$). The negative electrode and the electrolyte are the same as in a NaS battery. The schematic diagram of a $NaNiCl_2$ cell is shown in Figure 3.7. In order to provide good ionic contact between the positive electrode and the electrolyte, both of which are solids, a second electrolyte of sodium chloraluminate ($NaAlCl_4$) is introduced in a layer between $NiCl_2$ and beta-alumina. The $NaAlCl_4$ electrolyte is a vital component of the battery, although it reduces the specific energy of the battery by about 10%.[3] The operating temperature is again high, similar to that of the NaS battery. The basic cell reactions for the nickel chloride and ferrous chloride positive electrodes are as follows:

$$NiCl_2 + 2Na \xrightarrow[Discharge]{} Ni + 2NaCl\ (2.58V)$$

$$FeCl_2 + 2Na \xrightarrow[Discharge]{} Fe + 2NaCl\ (2.35V)$$

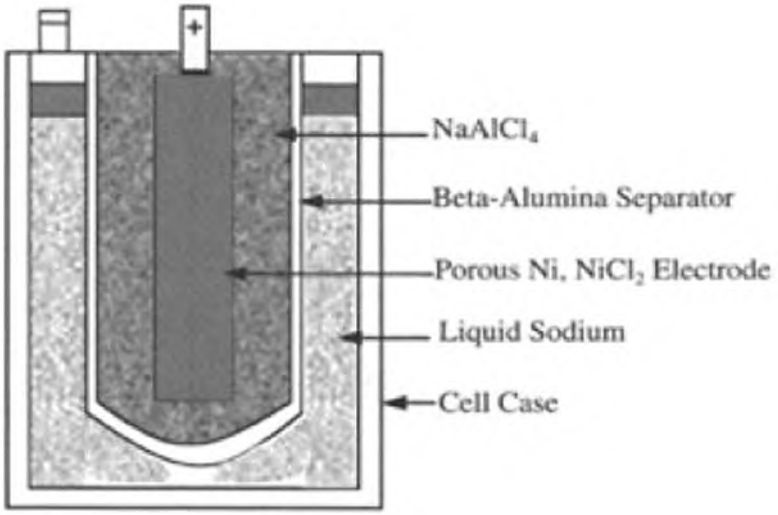

Figure 3.6: Lithium-ion cell

The cells in a sodium metal chloride battery are assembled in a discharged state. The positive electrode is prefabricated from a mixture of Ni or Fe powder and NaCl (common salt). On charging after assembly, the positive electrode compartment is formed of the respective metal, and the negative electrode compartment is formed of sodium. This procedure has

two significant advantages: pure sodium is manufactured in situ through diffusion in beta-alumina, and the raw materials for the battery (common salt and metal powder) are inexpensive. Although iron is cheaper than nickel, the latter is more attractive as the metallic component because of fewer complications and a wider operating temperature range.

Sodium chloride batteries are commonly known as ZEBRA batteries, which originally resulted from a research collaboration between scientists from the United Kingdom and South Africa in the early 1980s. ZEBRA batteries have been shown to be safe under all conditions of use. They have high potential for being used as batteries for EVs and HEVs. There are several test programs utilizing the ZEBRA batteries **[67]**.

3.4 Battery Parameters

3.4.1 Battery Capacity

The amount of free charge generated by the active material at the negative electrode and consumed by the positive electrode is called the *battery capacity*. The capacity is measured in Ah (1 Ah=3600 C, or coulomb, where 1 C is the charge transferred in 1 s by 1 A current in the MKS unit of charge).

3.4.2 Discharge Rate

The *discharge rate* is the current at which a battery is discharged. The rate is expressed as *Q/h* rate, where *Q* is rated battery capacity, and *h* is discharge time in hours. For a battery that has a capacity of *QT* Ah and that is discharged over t, the discharge rate is *QT/ t*.

For example, let the capacity of a battery be 1 Q=100 Ah. (1 Q usually denotes the rated capacity of the battery.) Therefore,

$$Q/5\text{rate is } \frac{100\ Ahr}{5\ hr} = 20\ A$$

3.4.3 State of Charge

The *state of charge* (SoC) is the present capacity of the battery. It is the amount of capacity that remains after discharge from a top-of-charge condition. The battery *SoC* measurement circuit is shown in **Figure 3.7**. The current is the rate of change of charge given by

$$i(t) = \frac{dq}{dt}$$

where *q* is the charge moving through the circuit. The instantaneous theoretical state of charge *SoCT(t)* is the amount of equivalent positive charge on the positive electrode. If the state of charge is *QT* at the initial time *t0,* then *SOCT(t0)= QT*. For a time interval *dt,*

Integrating from the initial time *t0* to the final time *t,* the expression for instantaneous state of charge is obtained as follows **[68]**:

$$SoC_t(t) = Q_T - \int_0^1 i(\tau)d\tau$$

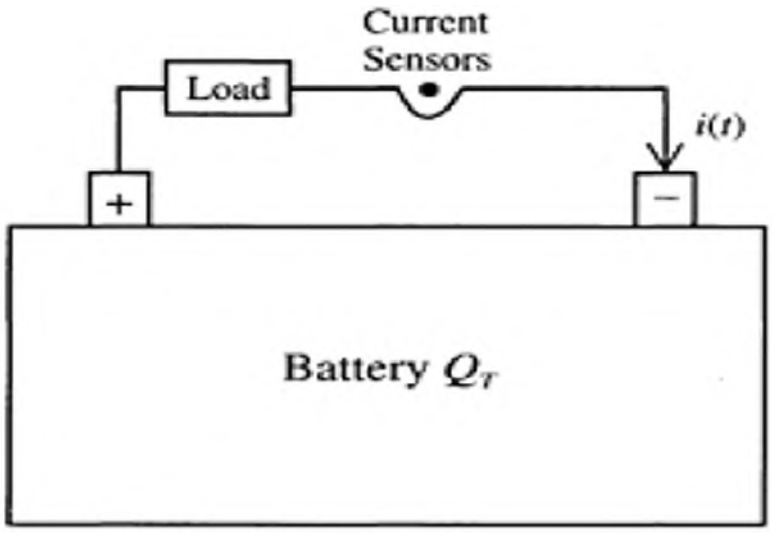

Figure 3.7: Battery *SoC* measurement.

3.4.4 State of Discharge

The *state of discharge (SoD)* is a measure of the charge that has been drawn from a battery. Mathematically, state of discharge is given as follows:

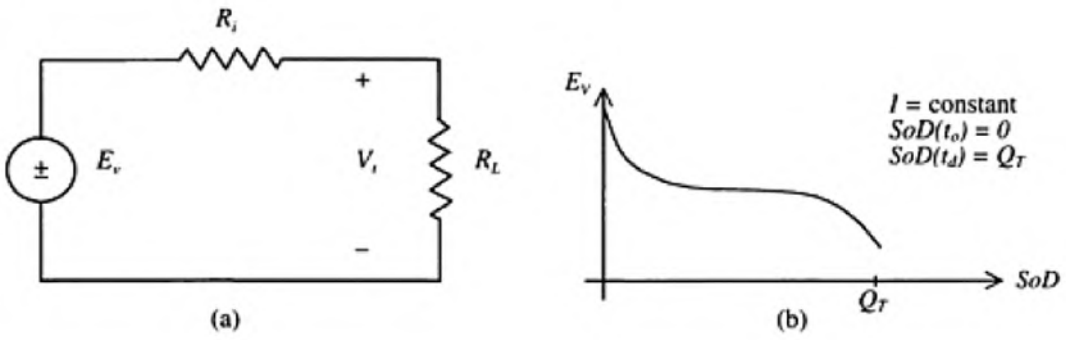

Figure 3.8: (a) Steady-state battery circuit. (b) Battery open circuit voltage characteristics

3.4.5 Depth of Discharge

The *depth of discharge (DoD)* is the percentage of battery capacity (rated capacity) to which a battery is discharged. The depth of discharge is given by

$$DoD_{(t)} = \frac{Q_T - S_o C_t(t)}{Q_T} x100\%$$

$$= \frac{\int_0^1 i(\tau)d\tau}{Q_t} x100\%$$

The withdrawal of at least 80% of battery (rated) capacity is referred to as deep discharge.

3.5 Technical Characteristics

The battery in its simplest form can be represented by an internal voltage *Ev* and a series resistance *Ri,* as shown in **Figure 3.8a**. The internal voltage appears at the battery terminals as open circuit voltage when there is no load connected to the battery. The internal voltage or the open circuit voltage depends on the state of charge of the battery, temperature, and past discharge/charge history (memory effects), among other factors. The open circuit voltage characteristics are shown in **Figure 3.8b**. As the battery is gradually discharged, the internal voltage decreases, while the internal resistance increases. The open circuit voltage characteristics have a fairly extended plateau of linear characteristics, with a slope close to zero. The open circuit voltage is a good indicator of the state of discharge. Once the battery reaches 100% *DoD,* the open circuit voltage decreases sharply with more discharge.

The battery terminal voltage (**Figure 3.9**) is the voltage available at the terminals when a load is connected to the battery. The terminal voltage is at its full charge voltage *VFC* when the battery *DoD* is 0%. In the case of a lead-acid battery, it means that there is no more PbSO4 available to react with H2O to produce active material. V_{cut} is the battery cut-off voltage, where discharge of battery must be terminated **[68]**.

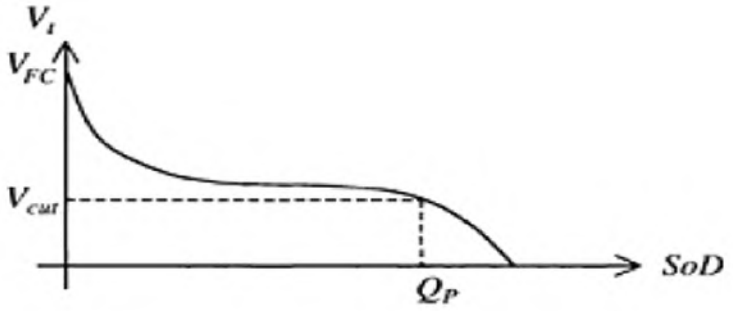

Figure 3.9: Battery terminal voltage.

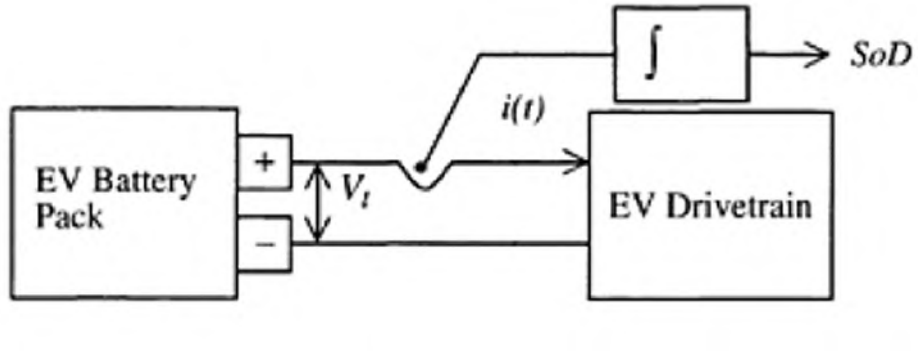

Figure 3.10: Battery *SoD* measurement.

3.6 Target and properties of Batteries

The push for zero-emission vehicles led to numerous research and development initiatives in the United States, Europe, and Japan. The California legislative mandates in the early 1990s led to the formation of the U.S. Advanced Battery Consortium (USABC) to oversee the development of power sources for EVs. The USABC established objectives focusing on battery development for mid-term (1995 to 1998) and long-term criteria. The purpose of the mid-term criteria was to develop batteries with a reasonable goal, while the long-term criteria were set to develop batteries for EVs, which would be directly competitive with IC engine vehicles (ICEVs). At the advent of the 21st century and following the developments in the 1990s, intermediate commercialization criteria were developed. The major objectives for the three criteria are summarized in **Table 3.3.**

The two most developed battery technologies of today are lead-acid and nickel-cadmium batteries. However, these batteries will not be suitable for EVs, because the former store too little energy, while the latter have cost and toxicity problems. The future of the other batteries is difficult to predict, because these are mostly prototypes, where system design and performance data are not always available. The status of the promising batteries described in the previous section is summarized in **Table 3.4** from information obtained from recent literature **[4]**.

Parameter	Mid-Term	Commercialization	Long-Term
Specific energy (Wh/kg) (C/3 discharge rate)	80–100	150	200
Energy density (Wh/liter) (C/3 discharge rate)	135	230	300
Specific power (W/kg) (80% *DoD* per 30 s)	150–200	300	400
Specific power (W/kg), Regen. (20% *DoD* per 10 s)	75	150	200
Power density (W/liter)	250	460	600
Recharge time, h (20% 100% *SoC)*	<6	4–6	3–6
Fast recharge time, min	<15	<30	<15
Calendar life, years	5	10	10
Life, cycles	600 @ 80% *DoD*	1000 @ 80% *DoD* 1600 @ 50% *DoD* 2670 @ 30% *DoD*	1000 @ 80% *DoD*
Lifetime urban range, miles	100,000	100,000	100,000
Operating environment, °C	-30 to+65	-40 to+50	-40 to+85
Cost, US$/kWh	<150	<150	<100
Efficiency, %	75	80	80

Table 3.3: USABC Objectives for EV Battery Packs

Battery Type	Specific Energy, Wh/kg	Specific Power, W/kg	Energy Efficiency, %	Cycle Life	Estimated Cost, US$/KWh
Lead-acid	35–50	150–400	80	500–1000	100–150
Nickel-cadmium	30–50	100–150	75	1000–2000	250–350
Nickel-metal-hydride	60–80	200–300	70	1000–2000	200–350
Aluminum-air	200–300	100	<50	Not available	Not available
Zinc-air	100–220	30–80	60	500	90–120
Sodium-sulfur	150–240	230	85	1000	200–350
Sodium-nickel-chloride	90–120	130–160	80	1000	250–350
Lithium-polymer	150–200	350	Not available	1000	150
Lithium-ion	80–130	200–300	>95	1000	200

Table 3.4: Properties of EV and HEV Batteries

4. AVL Cruise Software

AVL CRUISE is the simulation package that supports everyday tasks in vehicle system and driveline analysis throughout all development phases, from concept planning, through to launch and beyond. Its application envelope covers all conventional vehicle powertrains through to highly-advanced HEV systems.

An object-orientated physical model approach makes CRUISE powertrain topologies reflect their real life counterparts. The program offers the flexibility to build up a single system model, which can then be used to meet the requirements of diverse applications in the powertrain and driveline development. Starting with only a few inputs in the early phases, the model matures during the development process according to the continuously increasing simulation needs.

CRUISE offers a streamlined workflow for all kinds of parameter optimization, component matching - guiding the user through to practical and attainable solutions. Due to its structured interfaces and advanced data management, AVL CRUISE has established itself as a data communication and integration tool for different teams **[69]**.

4.1 AVL Cruise Application Areas

AVL CRUISE is typically used in powertrain and engine development to optimize the vehicle system including cars, busses, trucks and hybrid vehicles, its components and control strategies with regard to:

• Fuel consumption and emissions for any driving cycle or profile.

• Driving performance for acceleration, hill climbing, traction forces, braking.

AVL CRUISE is also used for tasks like:

• Evaluation of new vehicle concepts such as hybrid powertrain systems.

• Analysis of standard and new gear box layouts like DCT and AMT.

• Analysis of torsional vibrations of elastic drivelines (under dynamic load).

• Drive quality assessment of transient events such as gear shifting and launching.

• Vehicle thermal management.

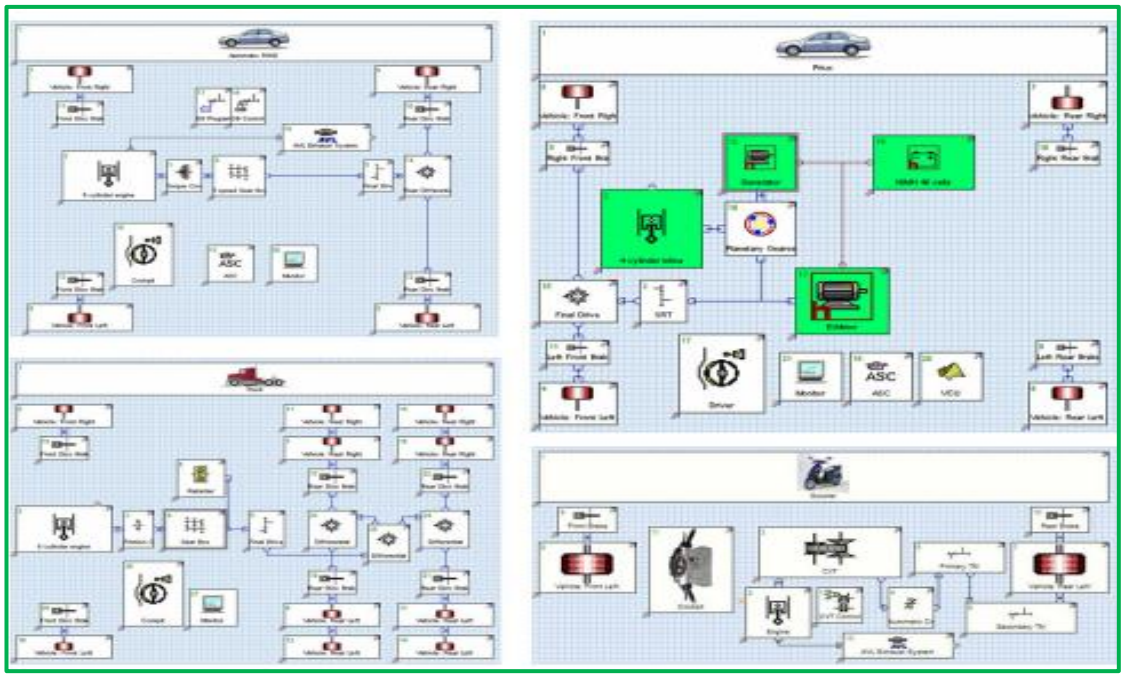

Figure 4.1: AVL Software Layout

The workflows in CRUISE are developed for all kinds of parameter optimization, component matching, in order to efficiently find the best balance between fuel economy, performance and drivability **[70]**:

• Multi-parameter sensitivity analysis of any scalar, characteristic or value within a characteristic or map.
• Overall component variation analysis for finding the right combination of various powertrain components quickly.
• DOE plans can be imported and exported.
• Advanced results representation (variation cubes, trade-off diagrams).
• Significant reduction in manual work for doing driveline studies and the risk of making mistakes.
• Achievement of the best compromise between performance, fuel economy, emissions and drivability in one integrated simulation loop.

4.2 Data Management

Oracle database, with data version control, access rights administration, search and filter options for any CRUISE related data – designed to complement existing company databases.

• File-based data management of projects and its versions, vehicle models, components, maps, etc., including unique search functionality for CRUISE data stored anywhere on a local disk or in the network**[69]**.

• Efficient data handling features like import, export and copy-and-paste for all input parameters and results.

• Traceability of data and decisions through the development process.

The simulation model is modular, which guarantees fast and flexible modelling. The modules are connected through physical properties and data links. This modelling method is advantageous, because some of the programs in their unique modular design (40% software are based on Matlab/Simulink and 90% are able to generate Simulink functions). Processes can be parallelized and every sub-calculation can be optimized.

The modelling software enables us to reverse the direction of the simulation. In that way, velocity, acceleration values, and losses can be calculated backwards from the wheels to the motor. This process is fast, but gives inaccurate results because the electric motor can operate in a work point which is not realistic within the given time period. Instead of that solution, the model chain is the reverse: the kinetic energy generated by the drive unit is reduced through mechanical connections (taking losses into account). This is the natural model of the physical system. For example, if an undersized engine or electric motor is given for the model, then the vehicle will not be able to reach or keep prescribed speed profile**[69]**.

The following calculation is valid for the simulation model:

1. Between the modules of the vehicle model – where connection is interpreted between two modules – the following non-linear differential equation is applied:

$$\dot{y} = f(t, y)$$
$$y(0) = y_0$$

2. This ordinary differential equation is converted into the following integral equation:

$$y = y_0 + \int_0^t f(\tau, y)d\tau \,.$$

3. The trapezoidal rule discretization leads to the following equation:

$$y_{n+1} - \frac{t_{n+1} - t_n}{2} f(t_{n+1}, y_{n+1}) = y_n + \frac{t_{n+1} - t_n}{2} f(t_n, y_n). \quad (3)$$

4. This non-linear system of equations is solved by the software in each cycle.

The software performs the prior interpolation of parameters (efficiency, torque, losses, fields, etc.). The program is using local bilinear interpolation.

CAD drawings of drive-train were used in the modelling process and the technical documentation. During validation, the unknown parameters were determined by characteristic values (from technical literature) and measurements, which were performed. Since the two drive modes (electric and diesel) are available separately, during the development of the model, we had to stick to the principle, which says the diesel engine does not operate together with the electric motors and vice versa. Fortunately, the software provides the opportunity to handle drives separately as subsystems. This modelling method is practical because major physical parameters of the vehicles examined are the same, while the power-train may vary widely. Just think of the same model in different passenger cars with different internal combustion engines **[69]**.

4.3 Vehicle Model

In CRUISE, a vehicle model is comprised of different components as it is in reality. This enables the user to model different vehicles, such as motorcycles, passenger cars, trucks, and buses. Additionally, all kinds of drivetrain configurations can be modeled, such as hybrids, twin-engine concepts and sophisticated transmission systems, like DCT and AMT.

The available components in CRUISE cover the whole range of vehicle parts, such as:

• Vehicle and trailers

• Combustion engine, exhaust gas after treatment system

• Clutches (friction clutch, hydraulic torque converter, viscous coupling, automatic clutch)

• Transmission elements (multiple step gear box, single ratio transmission, differential gear, planetary gear, double pinion gear, CVT, double clutch transmission)

• Control elements (transmission control, gearbox program, clutch control, clutch program, engine shut-off, cylinder deactivation, start stop automatic, brake control, AMT control – automated manual transmission control, DCT

control – double clutch transmission control, CVT control, ASC – anti slip control, PID control)

• Shafts (rigid or torsion-elastic)

• Wheel/tire (including slip and advanced rolling resistance models)

• Electrical components (electric motor, generator, battery, electrical supply)

• Hybrid components (electric machine, super capacitor, DC/DC converter)

• Brakes, Retarder

• Auxiliaries (for applications like: oil pump, air conditioning, power steering)

• Driver

• Environment (wind, road surface,…)

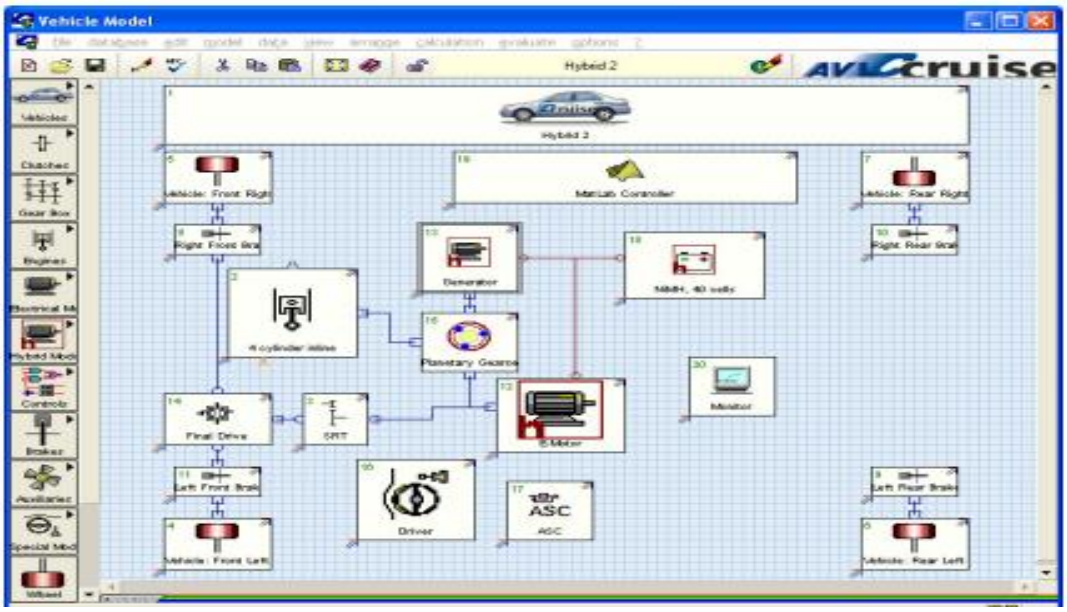

Figure 4.2: A Vehicle Model

Depending on the calculation task and the desired accuracy of the results, the complexity (modeling depth) of the vehicle models can be increased from simple to complex continuously in a very efficient way.

The data to be defined is in general the data needed for a dynamic calculation as masses or mass moments of inertia. In addition, data such as dimensions of the parts, transmission ratios, and losses in the different parts can be defined. For the engine different characteristics are needed such as full load characteristic, motoring curve, consumption maps, emission maps, etc. **[69]**.

It is possible to use different model depths for the single components. These model depths mean that different amounts of input data are needed for the calculation. As an example, this means for the Engine: For pure performance calculations, there is no need to input fuel consumption or emission maps. For the calculation of fuel consumption, fuel consumption maps are needed. In this case, steady state measured or calculated fuel consumption map are used.
Additional effects such as acceleration enrichment, warm-up enrichment, and turbo charger response can also be activated. Another example is the definition of the gearbox losses via efficiencies or transmission losses maps, speed, load or even temperature dependent **[69]**.

4.4 Calculation Task and Application

All standard tasks are provided for the different applications, which were designed especially for use in vehicle analyses. These tasks are:

• **Cycle Run:** The main goal of this task is the calculation of fuel consumption and emissions on time-based driving cycles. All common driving cycles, time and distance dependent, are predefined (e.g. ECER15, EUDC, NEDC, US-city (FTP75), US-highway, Japan10-15 mode, Artemis). Additional cycles needed for special applications may be defined. E.g., this can be done directly in a table, imported from other sources, or by using the graphical profile editor.

• **Climbing Performance:** This task is designed for the calculation of the maximum ascending gradients the vehicle can surmount.

• **Constant Drive:** This task mainly serves for the determination of fuel consumption and emissions at constant velocities. An additional task is the calculation of the current and the theoretical top speed.

• **Full and Partial Load Acceleration:** This task comprises three sub-tasks:

• **Maximum Accelerations in all Gears:** Maximum accelerations of the vehicle are computed for the whole engine speed range in all gears.

• **Acceleration from Standstill:** Vehicle is accelerated from rest to top speed with shifting gears.

• **Elasticity:** Starting with a definable velocity and a definable gear, the vehicle is accelerated to the defined upper velocity border, with or without shifting gears.

• **Maximum Traction Force:** This task can be used for the full automatic generation of the Traction Force or Performance Diagrams.

• **Cruising:** The main goal of this task is the calculation of fuel consumption and emissions on distance based tracks. E.g. the track between two cities can be defined (with speed limit, altitude, etc.) and the overall fuel consumption can be calculated.

• **Brake / Coast / Thrust:** This task serves for the determination of the braking performance of the vehicle.

5. Drive Train Design and Comparison of Diesel Renault Clio with Hybrid Renault Clio based on AVL Cruise Software

5.1 Abstract

This part proposes to find out how to increase fuel saving abilities, decreasing the green-house effect caused by the extensive usage of the petroleum products and improving the dynamic performance of the conventional vehicles. To succeed these aims, a diesel-hybrid version of the conventional diesel vehicle is designed and simulated on AVL Cruise software. While designing the vehicle, Renault Clio II's technical data is used. The simulation results include engine operating map, fuel consumption calculation over the typical city car drive cycle of Turkey, engine torque and velocity values over time, maximum velocity calculation and acceleration time calculations. Based on these simulating results provided by AVL Cruise software, a comparison analysis is performed with the conventional diesel Renault Clio and Diesel-Hybrid Renault Clio in terms of their fuel consumption values, engine operating regions and dynamic performances. The simulation results show that the engine operates in a more efficient condition in the hybrid electric Renault Clio than that in the diesel Renault Clio. Thanks to the hybrid electric drive train system, both fuel economy and traction performance of the car increased in a considerable step.

5.2 Introduction

Cars have been around for more than 100 years. They have changed a lot in that time. Today's cars are faster and more reliable than those of long ago. They are also safer and more comfortable. One thing has not changed: the way most cars work. Most cars of the past ran on fuel made from oil. That's still true today. Usually the fuel is gasoline (often called "gas" for short). Sometimes it is diesel fuel **[70]**.

Oil is a very good source of energy, but using it has problems. One problem is that oil is not a renewable resource. Once it's used, it's gone. If people keep on using it, eventually the world will run out of oil. Meanwhile, as oil gets less plentiful, fuels made from it will probably get more and more costly over time.

Another problem is that using fuels made from oil releases certain gases into the air. Some of these gases can be bad for people's health. Many scientists say that some of the gases are changing Earth's climate. These are serious problems because the world has a huge number of vehicles, and every year more are produced. In 2007, for example, more than 50 million

cars were made. If you include trucks and buses, the number of new vehicles made that year gets even bigger. One way to deal with these problems is to use less oil. This is where hybrid cars come in. They get their power from electricity as well as from gasoline (or diesel). As a result, they use less gas.

Both come from oil. In recent years, air pollution, as one of the most important environmental problems, has become increasingly serious with the flourishing of automobile industry. To protect the environment and enhance the air quality of big cities, many governments make numerous regulations to limit the emission and fuel consumption of vehicles, most of which make the traditional vehicle design and manufacture harder and harder. Electric vehicles (EVs) and hybrid electric vehicles (HEVs) are the most potential solutions of this problem. Meanwhile, people pay more and more attentions at EVs and HEVs because of the increasing shortage of global oil supplies and the skyrocketing oil price.

All of these above appeal to research and design of EVs and HEVs in many institutes and companies.

Any vehicle that has two sources of power can be called a hybrid. A moped is a hybrid. It has an engine, but you can also make it go by pedaling. When people talk about hybrid cars, they usually mean a car that has both a gasoline engine and an electric motor. A hybrid car gets power from both a gasoline engine and an electric motor. The engine and motor can work together in different ways. In some hybrids there are times when only one of them operates. The HEVs are the most feasible solutions to meet the demands of both the environment and the consumers, for they have considerable reductions of fuel consumption and have equivalent performances of traction. There is a popular opinion among the automobile manufacturers that city cars are especially suitable for hybrid drive train system. There are two major advantages of city cars. The first one is that city cars, unlike other vehicles, have predictable routes with frequent starts and stops that of great convenience for setting control strategies of drive train. Another advantage is although they have smaller space for batteries and electrical motor, they could give expected dynamic performance even if it is used less powerful engines **[71]**.

A great lot of hybrid electric vehicles(HEV) have been in service in many countries, such as UK, US, France and Turkey. Due to the impulse of government and call of market, automobile companies in Turkey show great interests in research and manufacture of HEVs. The purpose of this paper is to develop a set of hybrid electric propulsive system on the base of a diesel Renault Clio with an internal combustion engine(ICE).

Main tasks include system configuration design, control strategy design, modeling and simulation, and comparing with the results of simulation and tests on road and chassis dynamometer.

5.3 Configuration of the Hybrid Renault Clio on AVL Cruise Software

There are two basic ways the engine and motor can work together. They are called parallel and series. In a parallel hybrid, the engine and motor both supply power that drives the wheels. In a series hybrid, the gasoline engine is used to generate electricity; the electric motor drives the wheels. Series and parallel hybrids are different in the arrangement of components of the drive train. In the series pattern, the ICE charges energy storage elements via an electric generator while energy storage elements feed an electric motor that propels the vehicle. In the parallel pattern, an electric motor on the support of a group of energy storage element cells forms an independent propelling line that parallel the ICE drive train. These two drive lines join with a torque coupler and, technically speaking, can propel the vehicle independently. The synthesis pattern is an integration of the series and parallel. For the object in this program, a city car, the parallel configuration is more suitable and practical. For one thing, in the parallel configuration, the ICE can propel the car independently in case the electric pattern is unavailable. For another thing, it is simpler and more convenient for engineers to build a parallel hybrid electric system on the base of a conventional car.

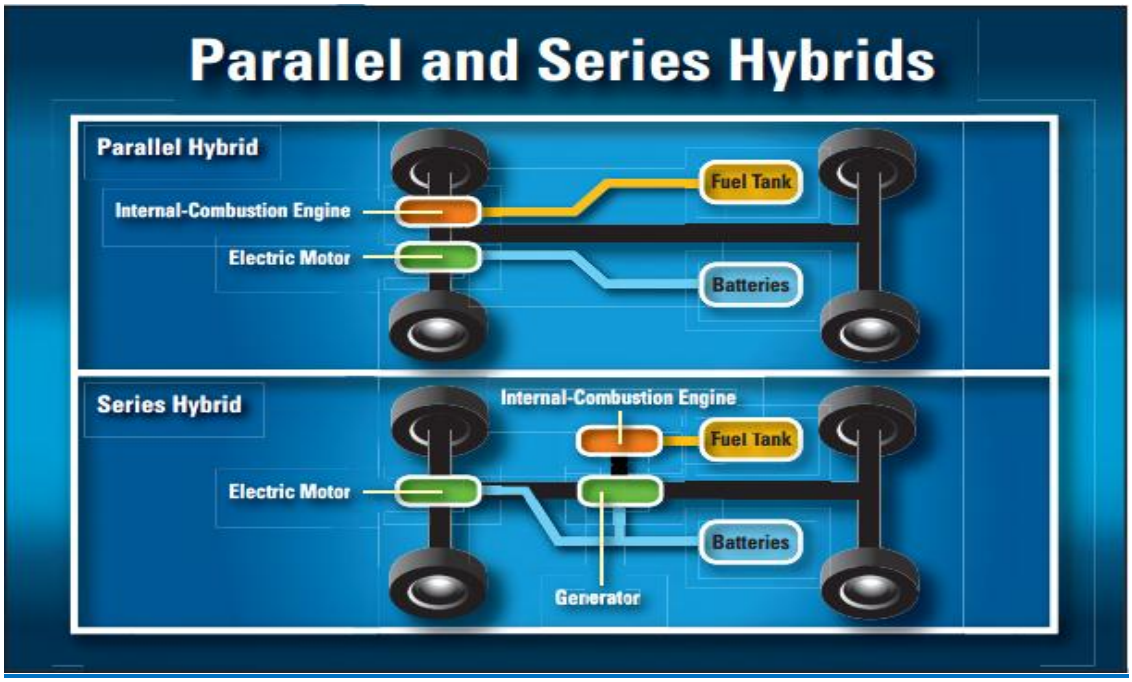

Figure 5.1: Parallel and Series Hybrid Vehicle Configuration

As shown in *figure 5.1*, the green modules are conventional modules and the red modules are new modules which are set for electric propulsion system. This PHEV has two separated drivelines and each can drive the car independently. The first driveline is just the same as the traditional drive pattern that has an engine, a clutch and a transmission system. Another driveline is composed of an energy storage element and an electric machine. Super capacitor is chosen as the energy storage element for its expeditiously peaking power supply ability. In fact, the peak power capacity of the energy storage is more important than its energy capacity for a city car because the frequent stop-and-go. These two drivelines are connected with a torque coupler. The basic parameters of the hybrid car and conventional car are given in **table 5.1**.

Parameters	Hybrid Renault Clio	Diesel Renault Clio
Curb Weight	1480,0 kg	1080,0 kg
Gross Weight	1970,0 kg	1570,0 kg
Frontal Area	1,89 m^2	1,89 m^2
Drag Coefficient	0,35	0,35
Dynamic Rolling Radius	439 mm	439 mm
Final Drive Transmission Ratio	3.905	3.905
Engine Displacement	1390,0 cm^3	1461,0 cm^3
Engine Max. Power	100 KW	127,5 KW
Engine Max. Speed	6000 [1/min]	6000 [1/min]
Wheel Base	2650 mm	2650 mm

Table 5.1: Values used in modelling on AVL Software

5.4 Conventional Renault Clio Modeling on AVL Cruise Software

Because the PHEV is built on the base of a conventional benchmarking car, the configuration model of conventional car is developed in AVL/Cruise in order to compare the fuel consumption and vehicle performance of PHEV with the conventional car. AVL/Cruise is a comprehensive tool of vehicle simulation for calculating and optimizing of fuel consumption, emissions and vehicle performance. It is designed for modeling any kind of vehicle drive train configuration (including EVs, HEVs and fuel cell vehicles). AVL CRUISE is also used for tasks like; Evaluation of new vehicle concepts such as hybrid powertrain systems, analysis of standard and new gear box layouts like DCT and AMT, Analysis of torsional vibrations of elastic drivelines (under dynamic load), drive quality assessment of transient events such as gear shifting and launching, vehicle thermal management.

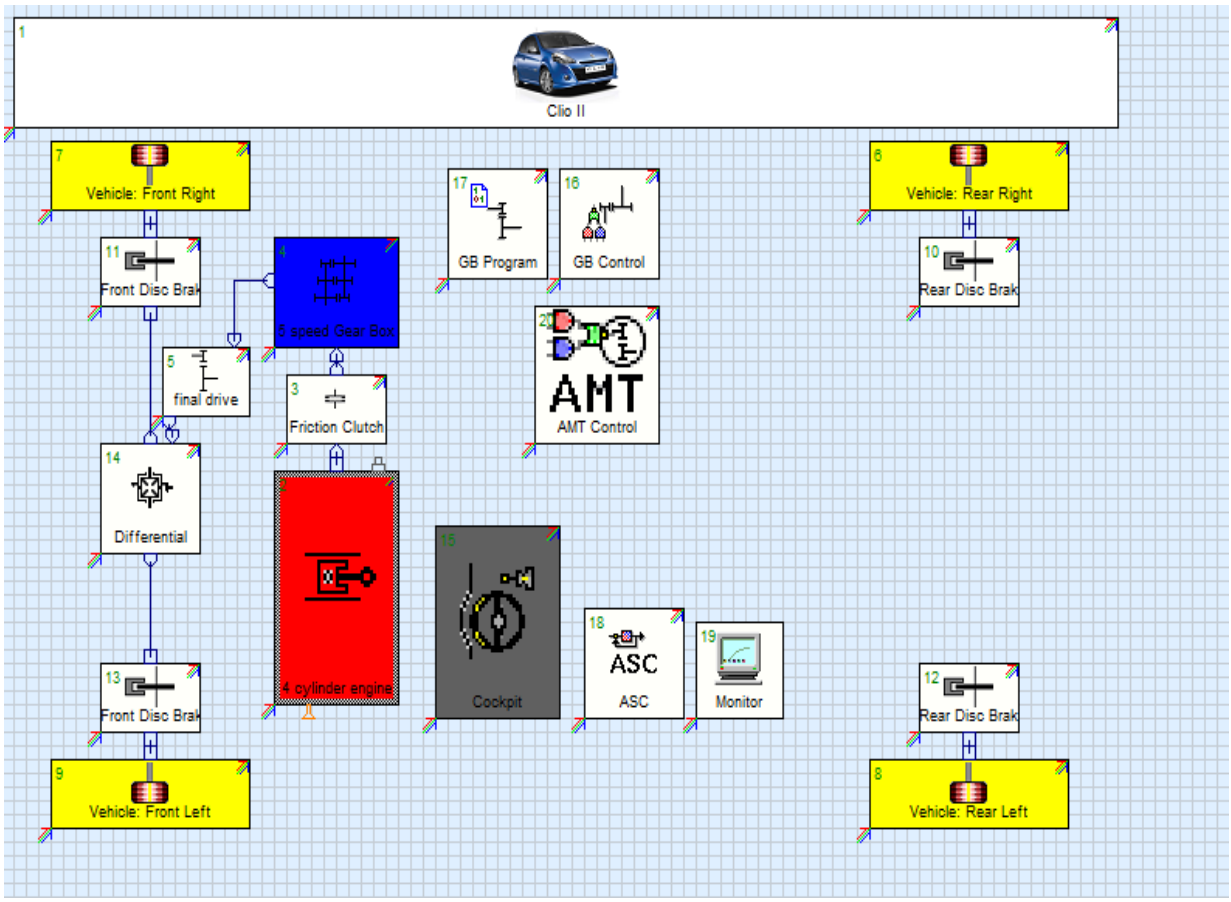

Figure 5.2: Conventional Diesel Renault Clio II Modelling

As shown in **Figure5.2**, the conventional Renault Clio2 model includes all components which are related to propulsion performance. The ICE is a four cylinder engine using diesel as fuel. The maximum speed is 6000 cycles per minute and peaking torque is 160 Nm. Engine torque is turned into a friction clutch and then enters the manual five speed gear box. The final drive is built as a single ratio gear. The torque output of final drive enters the differential and changes directions to wheels. These components are connected with mechanical connections. The Clio II component is the basic component of the model. The general data of the model such as the nominal dimensions and the weights are defined in this component. The cockpit component links the driver and the vehicle. It serves as a central controller to define the data and information of the driver and deliver drive commands to other components. The ASC (Anti Slip Control) component control the coefficient of friction of the wheels. The monitor component serves to show the chosen output values in the form of text while the calculation of the model is running.

5.5 Hybrid Renault Clio Modeling on AVL Cruise Software

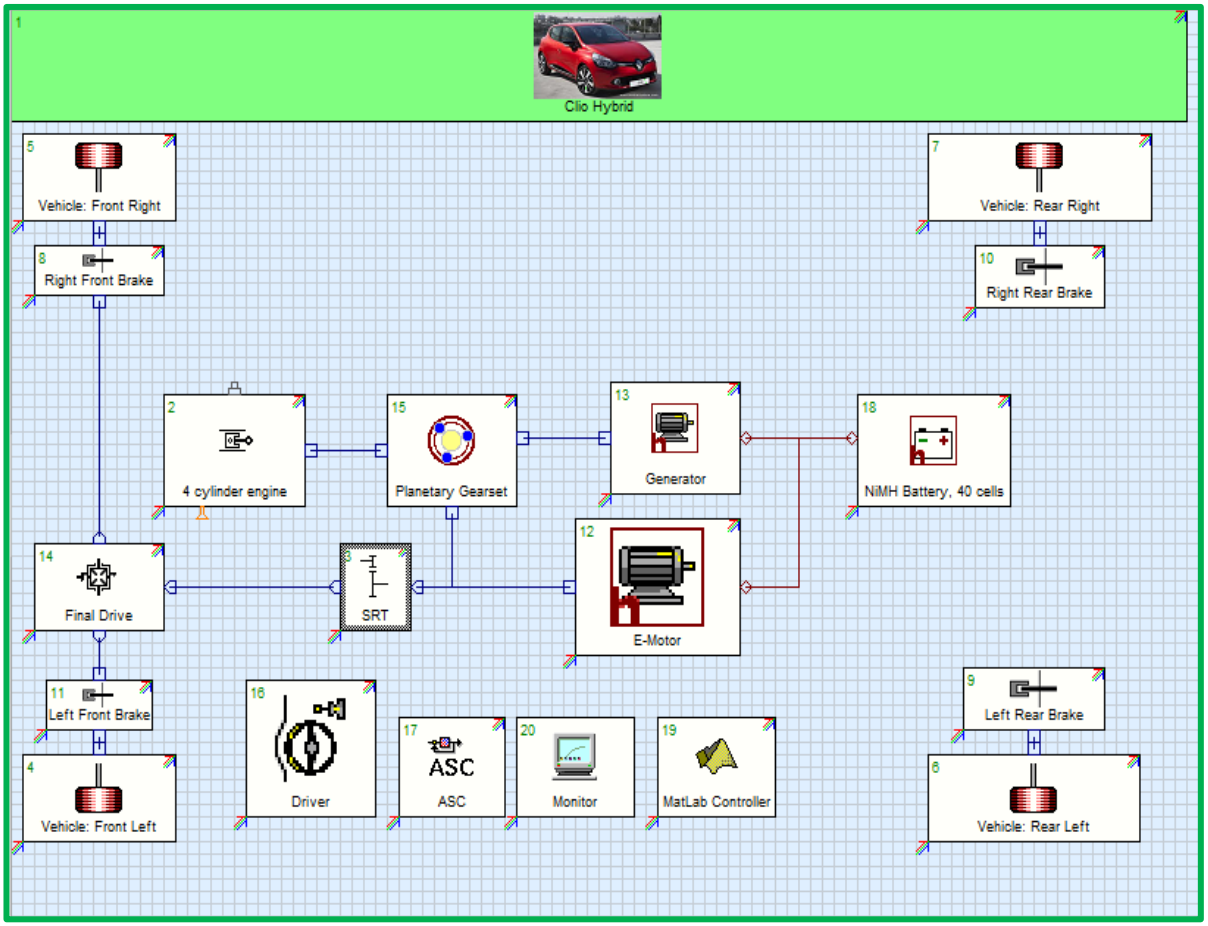

Figure 5.3: Parallel Hybrid Renault Clio II Modelling

The hybrid Renault Clio is manufactured by adds a set of electric system on the base of the conventional diesel Renault Clio. Since the electric propulsion system can help to enhance the dynamic performance of the vehicle, the displacement of the engine can be decreased in order to get a better fuel consumption data. The hybrid system includes a NiMH battery pack that includes 40 cells, an electric machine, a central controller and a final drive. **Figure 5.3** shows the hybrid Renault Clio model. The NiMH battery component is a chain of forty cells to support the required voltage of the electric machine (e-motor and generator). The electric machine that is composed of e-motor and generator charges the NiMH battery pack while braking or decelerating. The SRT is a pear of single ratio gears. The matlab.dll component is an interface of MATLAB/SIMULINK to integrate cockpit and mechanical elements, such as engine and electric machine.

5.6 Central Controller

The control strategy is built in MATLAB/SIMULINK and embedded in the AVL/CRUISE model as an executable .DLL file via an interface component. The PHEV drive train has five operating modes which are depending on the operation of the ICE and the electric machine. Which of these operating modes is used in real depends on the power demand, which is depended by the driver through the accelerate pedal or brake pedal, the SOC of the NiMH battery and vehicle velocity. The central controller receives the real-time signals from the driver, which in the simulation model is cockpit component, and other individual component, then commands the operation of each component according to the preset control logic. A significant parameter of mode choosing is the torque of engine. The red line in **Figure 5.4** is the expected engine operating points. Operating near this line will get a better fuel consumption result. Four basic operating modes are set for the purpose of fuel consumption reduction. And the fifth operating mode is switch off while both engine and electric machine are stopped.

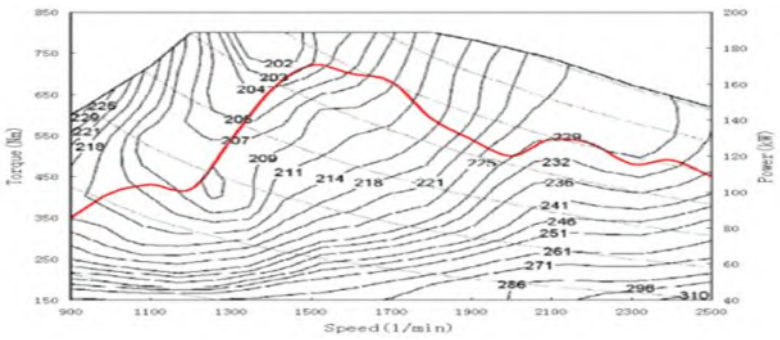

Figure 5.4: Expected Engine Operating Points

The traditional drive mode is engine-alone traction mode. In this mode, the vehicle is propelled by the engine alone. This mode is used in three possible conditions. The first condition is that the desired torque of the vehicle is equal to the expected engine torque while the voltage of the battery pack is higher than the minimum discharge voltage. The second condition is that the desired torque of the vehicle is higher than the expected engine torque while the voltage of the battery pack is lower than the minimum discharge voltage. The third condition is that the desired torque of the vehicle is lower than the expected engine torque while the voltage of the battery pack is higher than the maximum charge voltage.

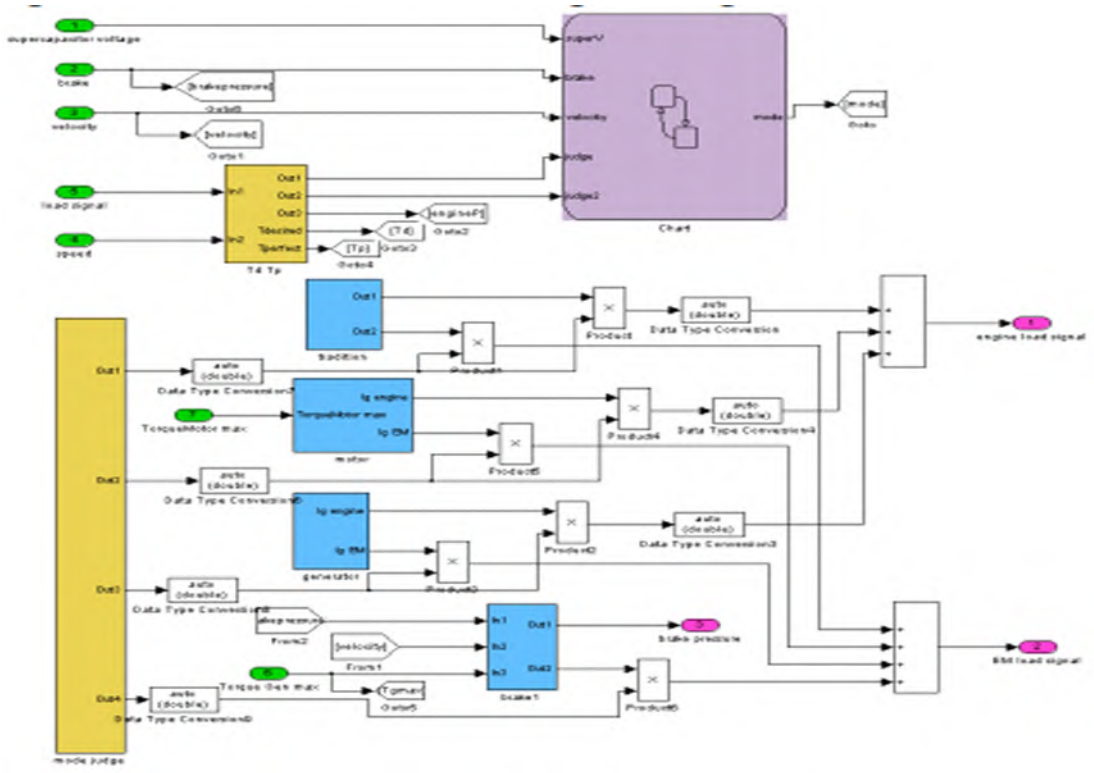

Figure 5.5: Control Strategy in Matlab/Simulink

The hybrid drive mode is set for the situation that both the engine and the electric machine deliver traction power to the drive train. This mode is used when the desired torque of the vehicle is higher than the expected engine torque and the voltage of the NiMH battery pack is higher than the minimum discharge voltage. The generator mode is NiMH battery pack charge mode. In this mode, the electric machine operates as a generator and is driven by the engine to charge the battery pack. This mode is used while the desired torque of the vehicle is lower than the

expected engine torque and the voltage of the battery pack is lower than the maximum charge voltage. The regenerative braking mode is set for the situation that the vehicle is breaking. In this mode, the engine is shut down and the electric machine works as a generator and produces a braking torque to the drive train. Part of the kinetic energy of the vehicle mass is converted into electric energy and stored in the NiMH battery pack. The control strategy built in MATLAB/SIMULINK is shown in **figure 5.5.** The controller uses a STATEFLOW chart to determine modes in which the vehicle is through real time input signals from AVL/CRUISE. The input signals include SOC(state of charge) of the NiMH battery pack, brake pressure from the cockpit, velocity of the vehicle, accelerator pedal signal of the driver and the speed of the engine. The controller demands components in AVL/CRUISE model through output signals. The output signals include load signal of engine, load signal of electric machine and brake pressures of four mechanical brakes.

5.7 Results

Based on the simulation results; data are obtained and compared to each other. **The Urban Driving Cycle** ECE-15 (or just UDC) is used as driving cycle. The cycle has been designed to represent typical driving conditions of busy European cities, and is characterized by low engine load, low exhaust gas temperature, and a maximum speed of 50 km/h. The cycle ends on 195 s after a theoretical distance of 1017 meters, then it repeats four consecutive times.

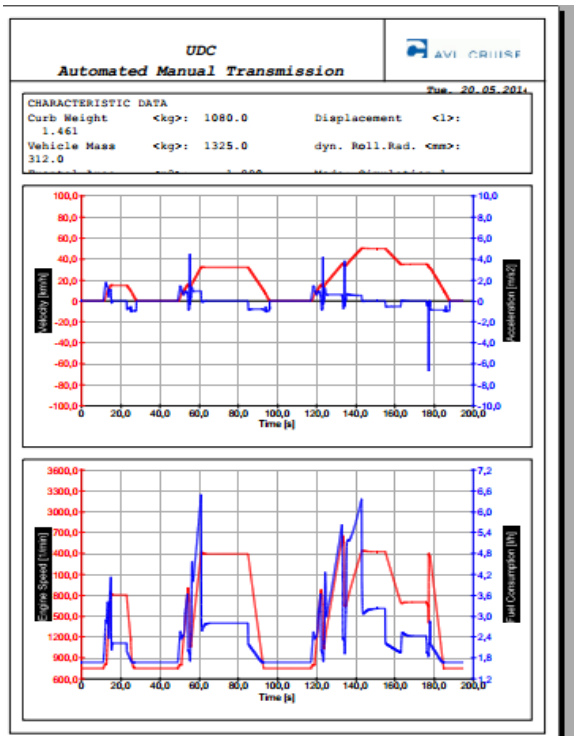

The typical cycle run of city car in Turkey is used to evaluate the fuel economy characteristics of the HEV and compare it with the conventional Renault Clio. The total distance of this cycle run is 1400 meters. The maximum acceleration is 4.2 m/s2. The average velocity is 36 km/h.

Total time is 1314 seconds amount which in as long as 200 seconds the vehicle is stopped for 3 times and the engine is at idle speed. The cycle run of diesel Clio is shown in figure (left one).

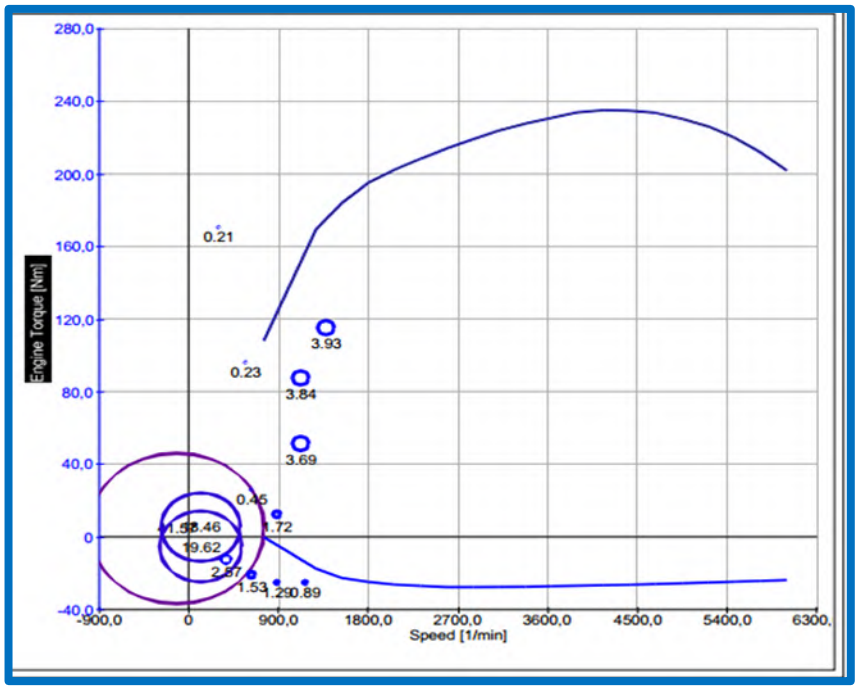

Figure 5.6: Statistical percentage of engine operating region for Hybrid Renault Clio

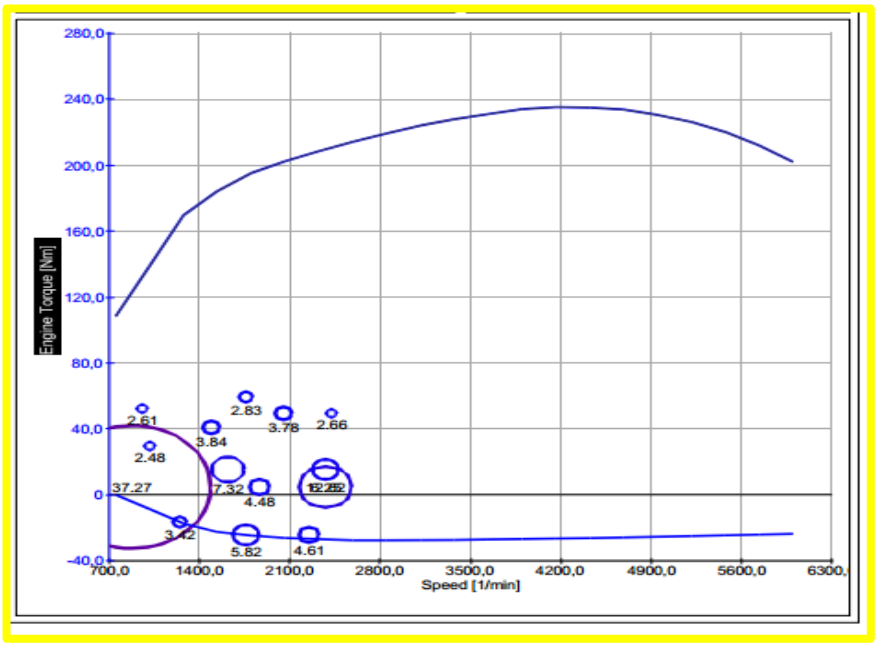

Figure 5.7: Statistical percentage of engine operating region for Diesel Renault Clio

Figure 5.6-7 show the statistical percentage of engine operating region for hybrid and conventional Renault Clio respectively. Comparing these figures shows that the engine operates in a higher efficiency region for the hybrid Renault Clio, and operates at low efficiency region for the conventional car in most time.

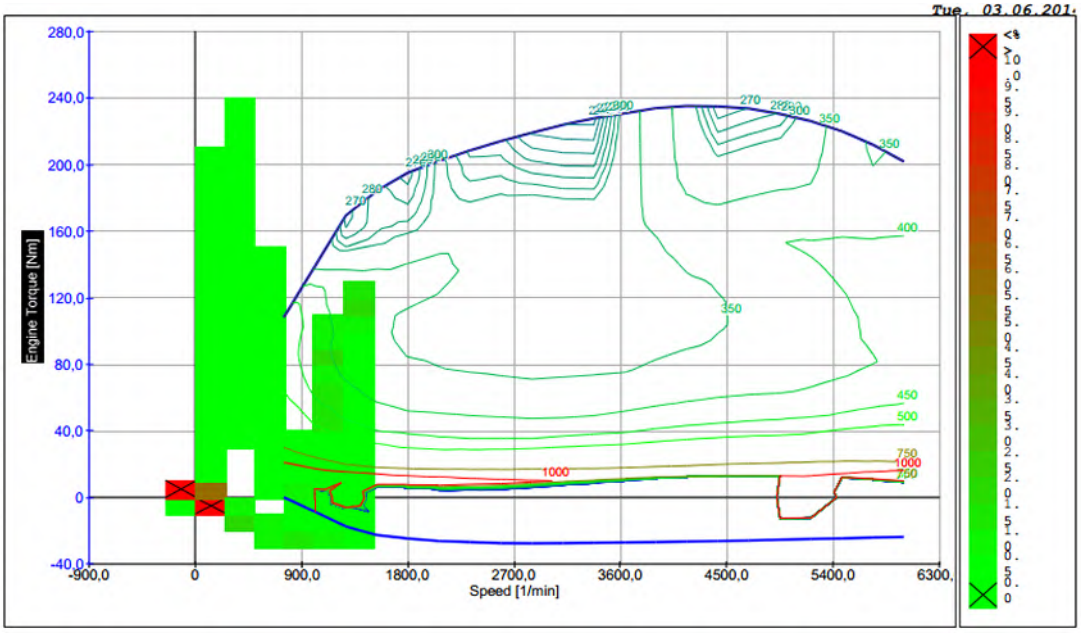

Figure 5.8: Driving Time Distribution in consumption map for Hybrid Clio

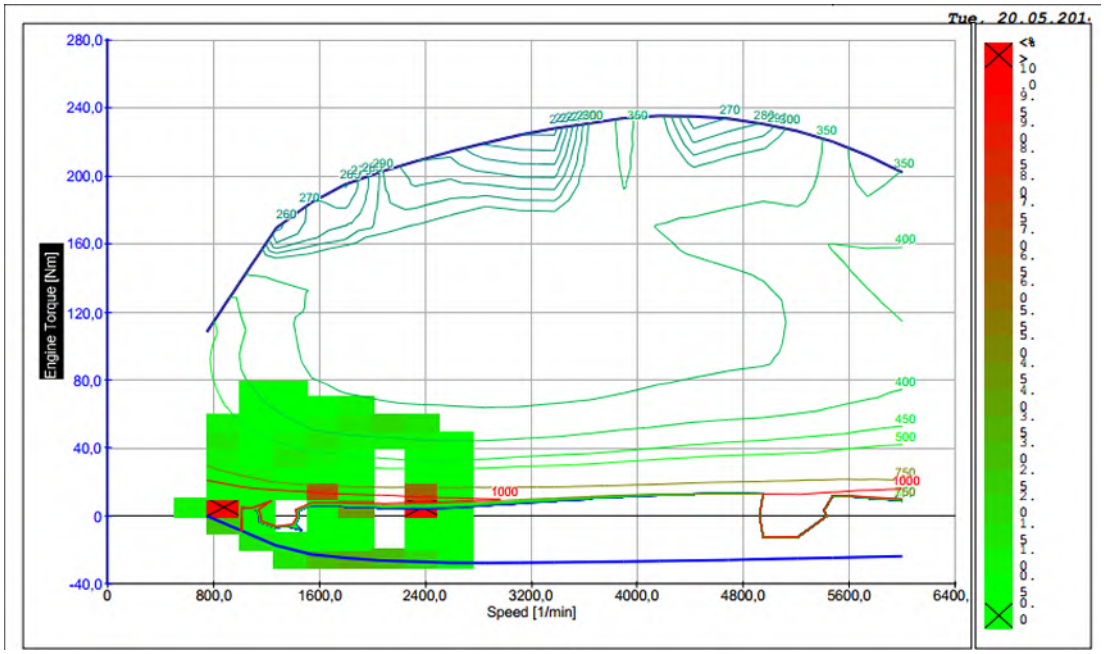

Figure 5.9: Driving Time Distribution in consumption map for Diesel Clio

Figure 5.8 and 5.9 show driving time distribution in consumption map for hybrid and conventional vehicles.

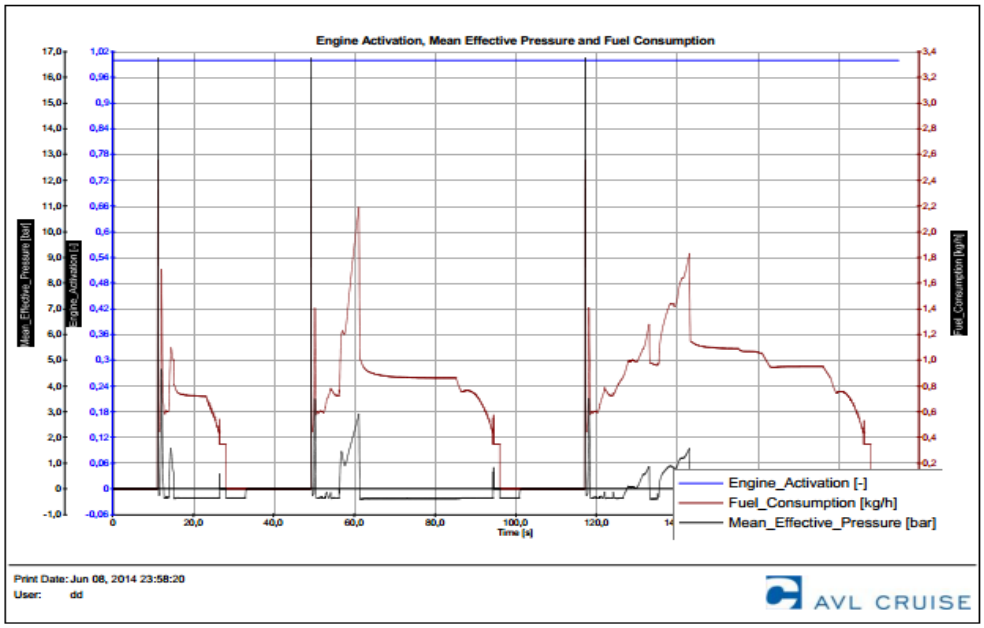

Figure 5.10: Fuel Consumption (kg/h) for Hybrid Clio

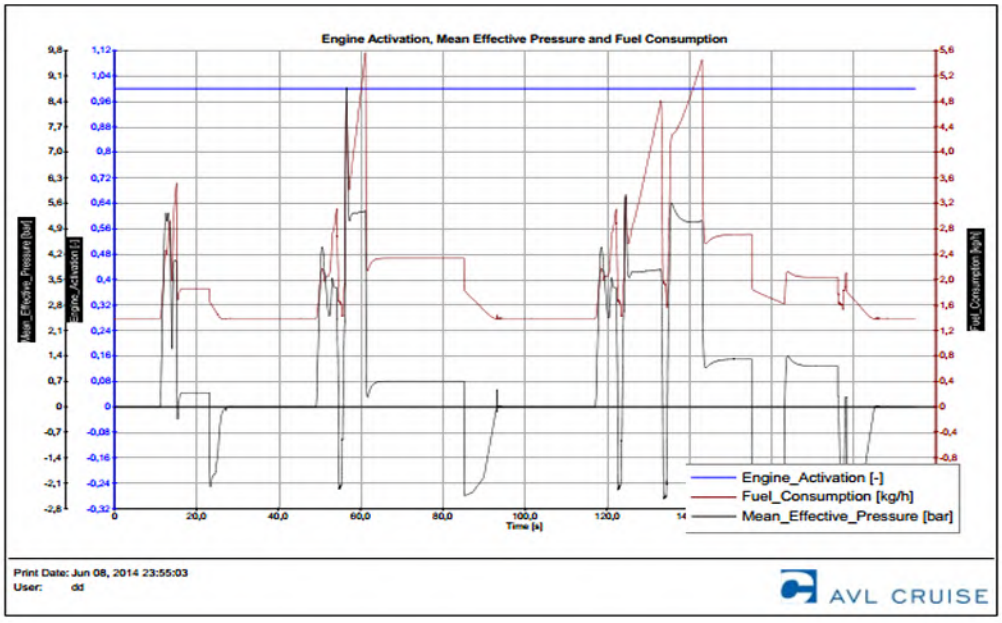

Figure 5.11: Fuel Consumption (kg/h) for Diesel Clio

Figure-5.10 and **5.11** show consumption values for hybrid and conventional car. Fuel Consumption in Hybrid is 2, 3 kg/h where 5, 6 kg/l in diesel Renault Clio.

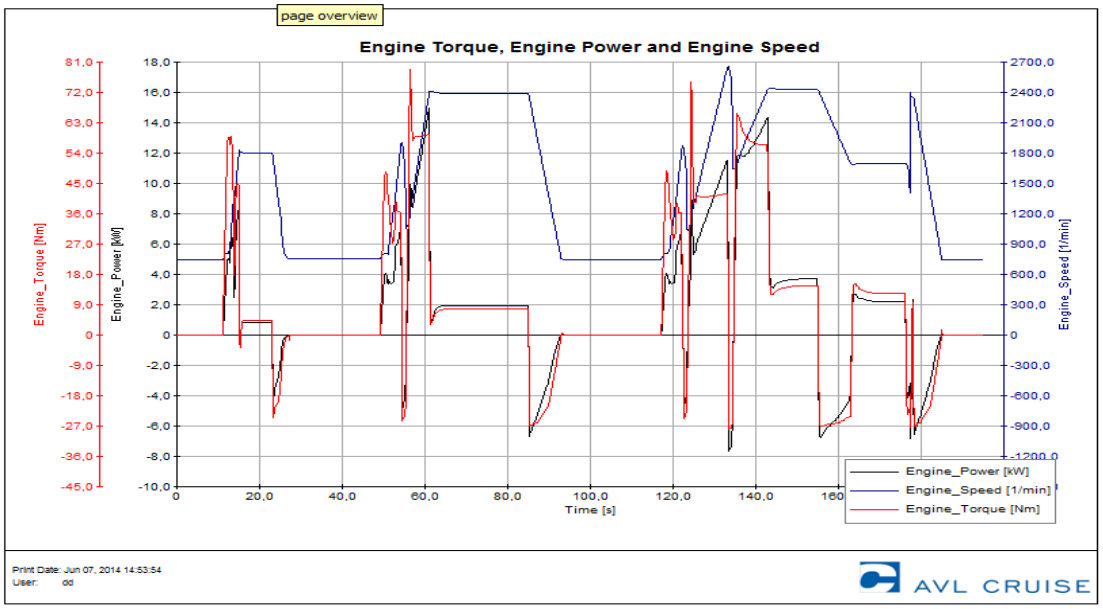

Figure 5.12: Engine Speed and Engine Torque Graph for Diesel Renault Clio

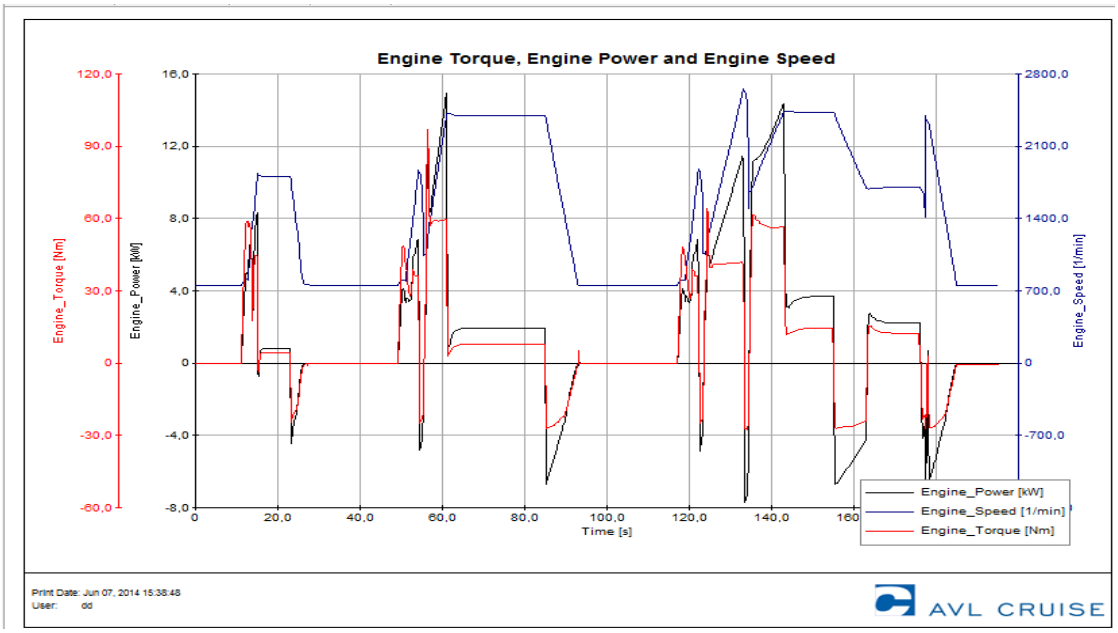

Figure 5.13: Engine Speed and Engine Torque Graph for Hybrid Renault Clio

Figure 5.12 present engine speed and torque of the diesel Renault in the drive cycle while **figure 5.13** shows the same outputs of the hybrid Renault Clio. Because the engine speed is in direct proportion to the velocity determined by the drive cycle, the engine speeds of these two cars have same curves. For the hybrid car, the engine torque is lower and it leads to less fuel consumption.

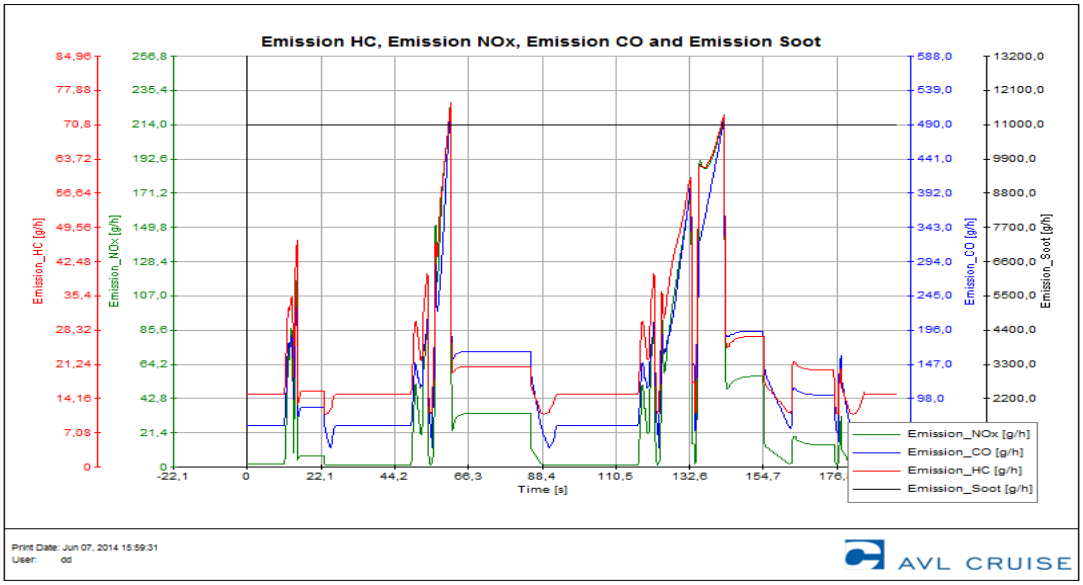

Figure 5.14: HC, NOx and CO emissions for Diesel Renault Clio

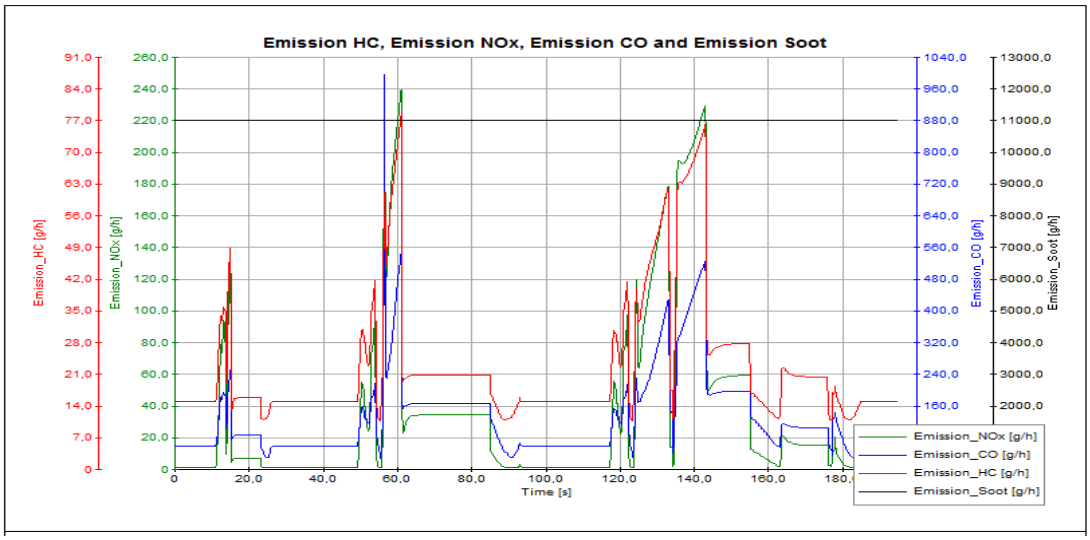

Figure 5.15: HC, NOx and CO emissions for Hybrid Renault Clio

Average Emissions	Diesel Clio (g/h)	Hybrid Clio (g/h)
NOx	30	15
HC	18	16
CO	80	55

Table 5.2: HC, NOx and CO emissions for Hybrid Renault Clio

5.8 Conclusion

The main task of this paper is to design an electric hybrid drive system and compare it with the conventional one. Compared to the conventional Renault Clio, Simulation and test results show that the fuel consumption of the hybrid car is decreased. There are several reasons why a hybrid usually uses less gasoline than a similar car with a traditional engine. It doesn't have to use fuel for idling, since the engine can just shut off when the car is stopped. Also, since the electric motor helps power the car, the engine doesn't need to be as big and heavy as in a traditional car. Smaller gasoline engines tend to be more efficient than large ones, and they burn less fuel. More savings come if the electric motor can drive the car at low speeds all by itself. Gasoline engines are not very efficient at low speeds.

The NOx, CO and HC emissions values of conventional Renault Clio are higher than hybrid Renault Clio due to having bigger ICE inside. It's really important to reduce these emissions in order to have a cleaner and safer environment. Carbon monoxide can cause health problems. Other gases called nitrogen oxides can lead to smog, which can also be harmful to people's health. Substances called hydrocarbons are another potential cause of smog.

The dynamic performance of the Diesel Renault Clio is improved apparently. The hybrid vehicle shows to be a good alternative for conventional vehicles to decrease fuel consumption. However, it is not enough for the work. By optimizing the parameters of the drive line and employing suitable control strategies, the fuel economy and dynamic performance will be better.

6.Drive Train Design and Comparison of Electrical Renault Clio with Range Extender Renault Clio based on AVL Cruise Software

6.1 Abstract

This case aims at the parametric drive train design, modelling and performance simulation of an electric Renault Clio and compare this car with range extender Renault Clio in terms of ; distance taken and fuel consumption. Limited range is one of the most important problems that electrical vehicles face to. To solve this problem, a 3 cylinder motor is used to extend the range of the vehicle. As a result, the simulation results shows that, the distance taken by the electrical vehicle increased apparently.

6.2 Introduction

Range extender is an auxiliary power unit built-in or externally attached to all-electric (BEV) or plug-in hybrid electric vehicle (PHEV) to increase its all-electric range (AER). The most commonly used range extenders are internal combustion engines that drive an electric generator which in turn supplies the battery and electric motor with electricity. The range extender can also be powered by a fuel-cell or other energy sources. The range autonomy is one of the main barriers for the commercial success of electric vehicles, and extending the vehicle's range when the battery is depleted helps alleviate range anxiety concerns **[72]**.

The extender's advantages are to allow a reduction in battery size and cost and in the related weight. Also, the car can maintain its customary travel range without having to stop for lengthy recharging. It dispels "runtime angst," a phenomenon not to be underestimated when introducing electric mobility.

We are in the decade of the hybrid electric vehicle despite the fact that most off road and underwater vehicles are pure electric. That includes most forklifts, golf cars and mobility vehicles for the disabled plus Autonomous Underwater Vehicles (AUVs) and personal submarines. Indeed, most electric aircraft are pure electric as well. The reason is that these are mainly small as are electric two-wheelers, which are also almost all pure electric. Small vehicles rarely need to travel long distances. In addition, these pure electric

vehicles are often used where a conventional engine is banned as on lakes and indoors or where it is impracticable as with underwater vehicles. By contrast, half the electric vehicle market value lies in larger road vehicles, notably cars, and here the legal restrictions are weaker or non-existent and range anxiety compels most people to buy hybrids if they go electric at all. About eight million hybrid cars will be made in 2023, each with a range extender, the additional power source that distinguishes them from pure electric cars. Add to that significant money spent on the same devices in buses, military vehicles, boats and so on and a major new market emerges. This unique report is about range extenders for all these purposes - their evolving technology and market size. Whereas today's range extenders usually consist of little more than off the shelf internal combustion engines, these are rapidly being replaced by second generation range extenders consisting of piston engines designed from scratch for fairly constant load in series hybrids. There are some wild cards like Wankel engines and rotary combustion engines or free piston engines both with integral electricity generation. However, a more radical departure is the third generation micro turbines and fuel cells that work at constant load. The report compares all these. It forecasts the lower power needed over the years given assistance from fast charging and energy harvesting innovations ahead. Every aspect of the new range extenders is covered.

Range extenders sit in a complex and rapidly evolving power environment but they are usually designed to operate at near constant load and torque for optimal efficiency and life. Range extender power may therefore be on demand at all times or most of the time, whereas the battery also experiences fast charging which is on demand when stationary and now energy harvesting power that is intermittent. Energy harvesting includes photovoltaic and regenerative braking on land, the propeller going backwards in regenerative soaring and landing of aircraft, and also regenerative mooring of a boat in a tide stream. The power electronics to interface all this becomes more complex **[73]**.

The key about combining a petrol engine/generator and battery pack is that it can deliver the performance of a big internal combustion engine along with very low emissions of both CO2 and pollutants.

6.3. Electrical and Range-Extender Renault Clio Modelling

An Electric car is powered by an Electric Motor rather than a Gasoline Engine. The Electric Motor gets its power from a controller. The Controller is powered from an array of rechargeable batteries. Range extender electrical device is a kind of hybrid device using its engine to charge electrical battery in order to provide taking more distance. A 3cylinder 1L engine is used as range extender. The vehicle is picked as Renault Clio again.

Parameters	Electric Renault Clio	Range Extender Renault Clio
Curb Weight	1195,0 kg	1320,0 kg
Gross Weight	1620,0 kg	1750,0 kg
Frontal Area	1,89 m^2	1,89 m^2
Electric Motor Output (Kw)	76,99	76,99
Electric Motor- Max. Torque (Nm)	240	240
Capacity of NiMH Battery kWh	15.5	15.5
Range (km)	80	130
ICE Engine (Range Extender)	-	4 Cylinder, 1000 m3 engine
Top Speed (km/h)	132,6	126
Charge time of high-voltage battery in h at 16 A	6-8 Hours	6-8 Hours

Table 6.1: Values used in Modelling

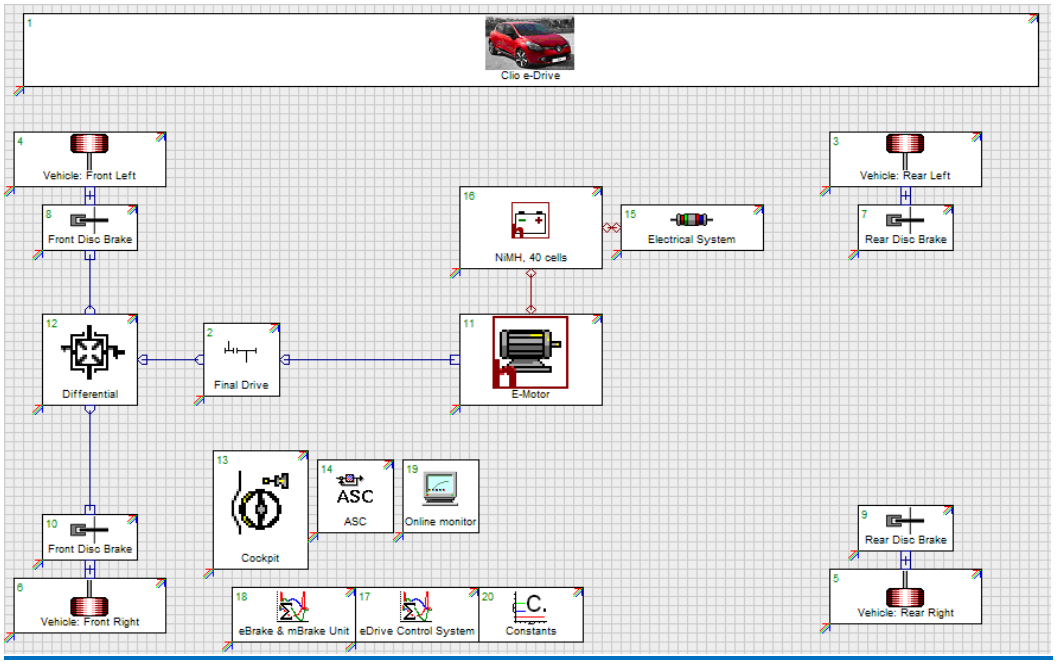

Figure 6.1: Electric Clio Modelling on AVL Cruise Software

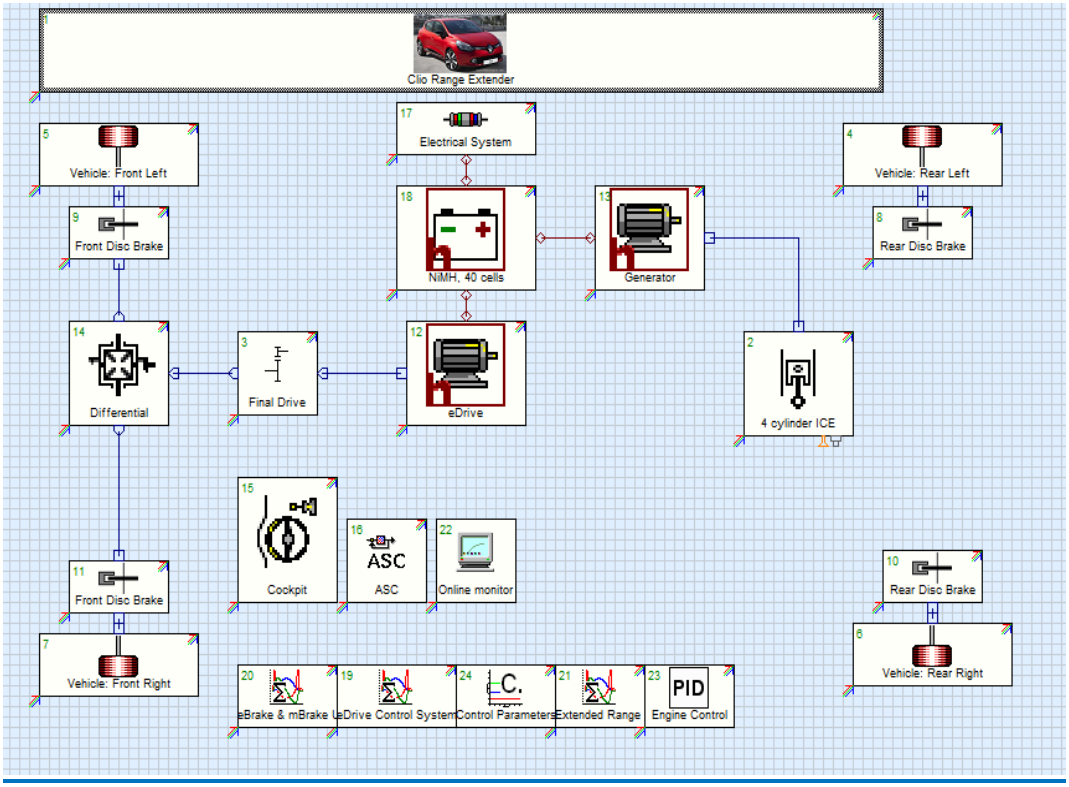

Figure 6.2: Range Extender Modelling on AVL Cruise Software

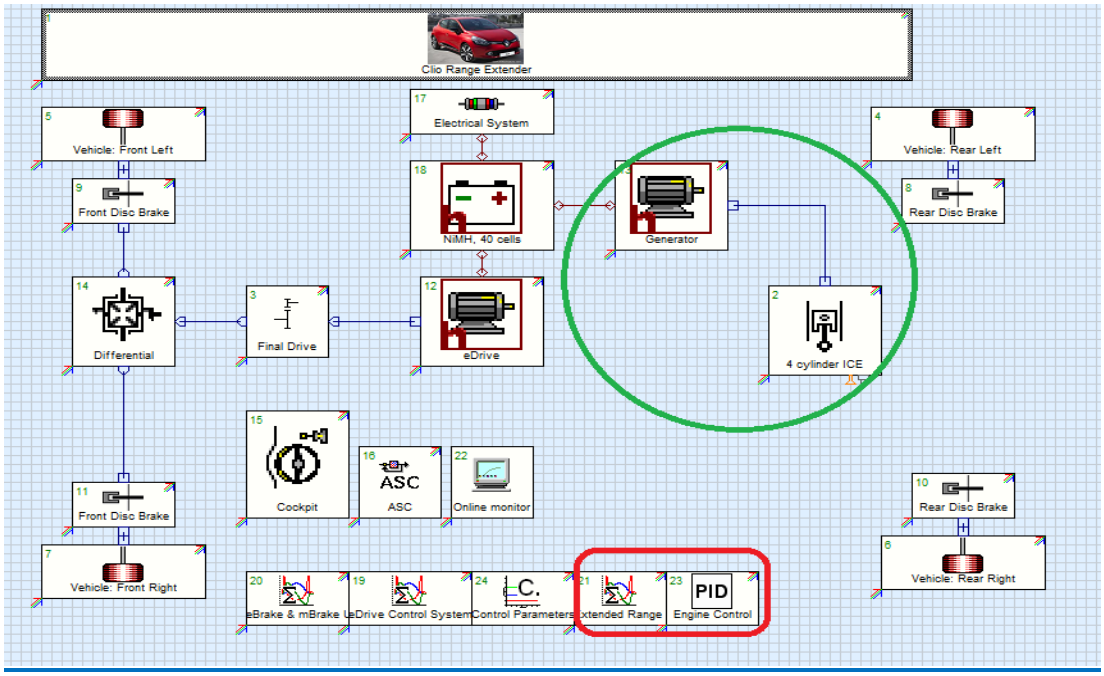

Figure 6.3: Range Extender Modelling

The Range Extender is a small internal-combustion engine with a generator that supplies energy for electric propulsion when the battery is empty. A generator and a 4 cylinder 1L ICE is added to electrical Renault Clio base. Moreover, the control unit of the range extender engine and PID control unit is also added. Then, simulations are performed in order to investigate the distance the vehicles take.

6.4. Comparison Results

The simulation results taken from AVL Cruise software is based on NEDC and FTP75 driving cycles. NEDC cycles results is used in simulating.

The NEDC is supposed to represent the typical usage of a car in Europe. It consists of four repeated **ECE-15** urban driving cycles (**UDC**) and one Extra-Urban driving cycle (**EUDC**).

The range extender electrical Renault Clio and Pure electrical Renault Clio is compared in 3 aspects;

- Acceleration, Velocity and Distance Values
- Electrical and Fuel Consumption
- Electrical Motor Torque, Speed and Mechanical Power

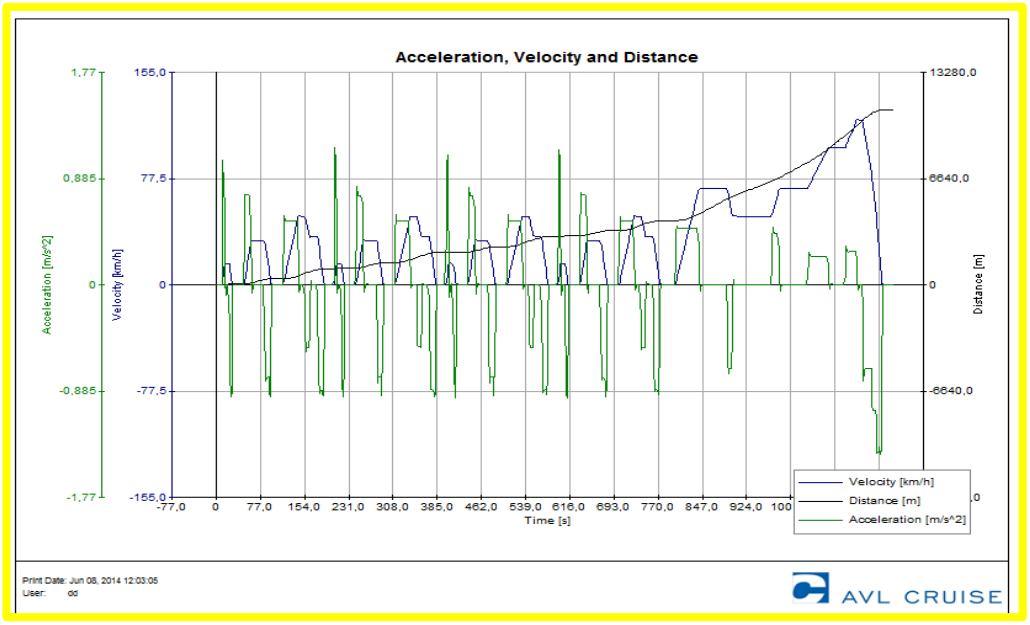

Figure 6.4: Velocity, Acceleration and Distance graphs for Electrical Renault Clio

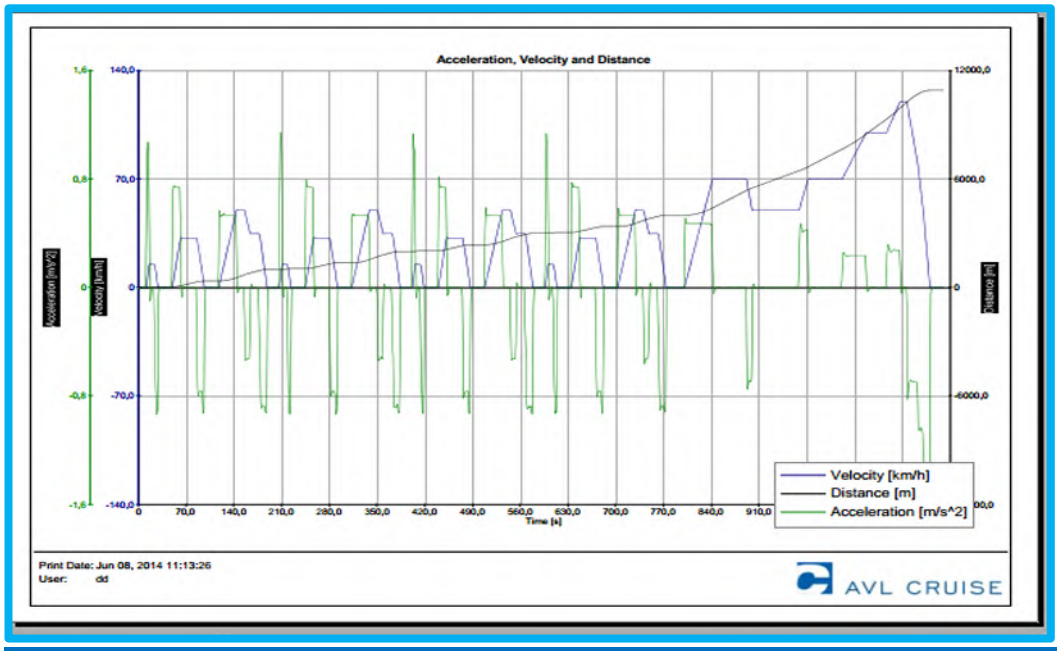

Figure 6.5: Velocity, Acceleration and Distance graphs for Range Extender Clio

- **Velocity** is slightly slower in Range Extender Clio because, a petrol engine adds 120kg to the Clio's heft
- **Distance** taken by Range extender Clio is about 60 km more than electrical Clio. It's the most important feature of Range extender.

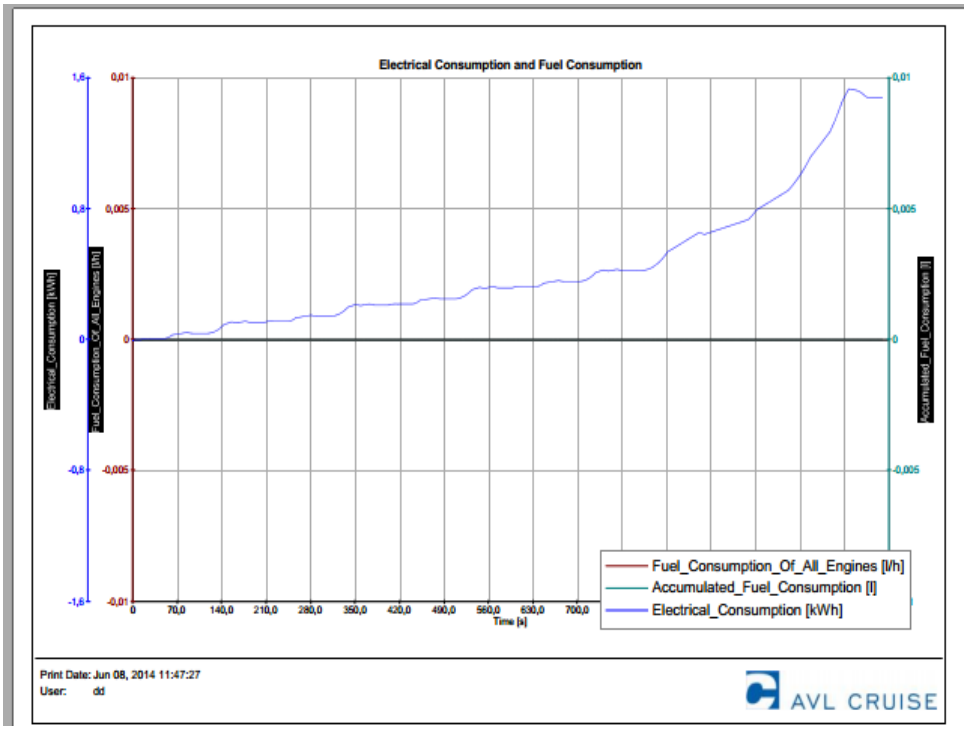

Figure 6.6: Electrical Consumption of Electiric Clio

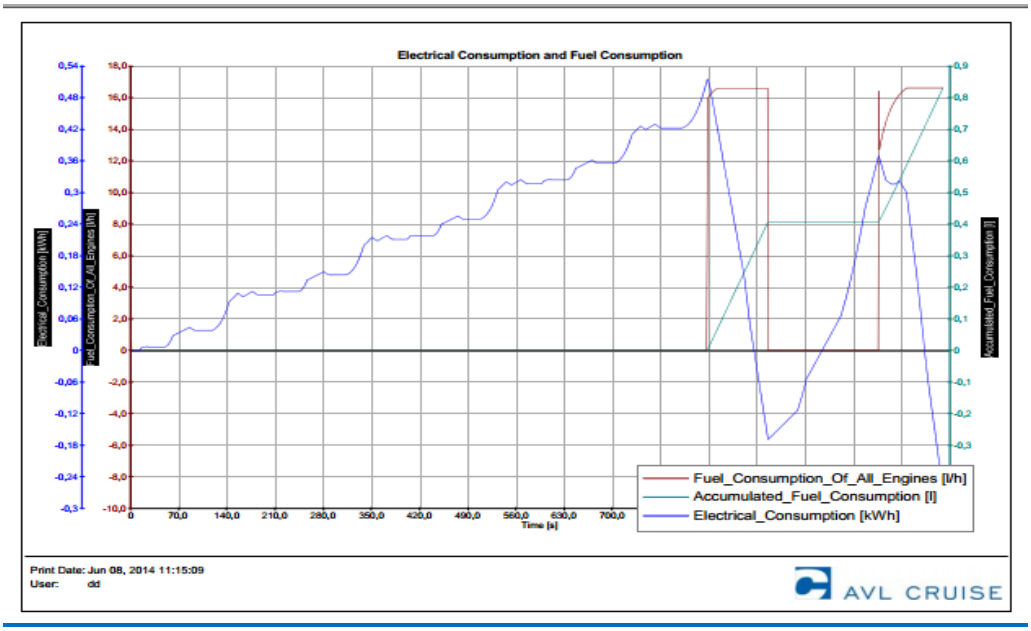

Figure 6.7: Electrical and Fuel Consumption of Range-Extender Clio

In **Figure 6.6 and 6.7** the fuel and electrical consumption of the vehicles is seen. The consumption is too little in electrical car. On the other hand, the range extender car consumes electrical energy as well as fuel.

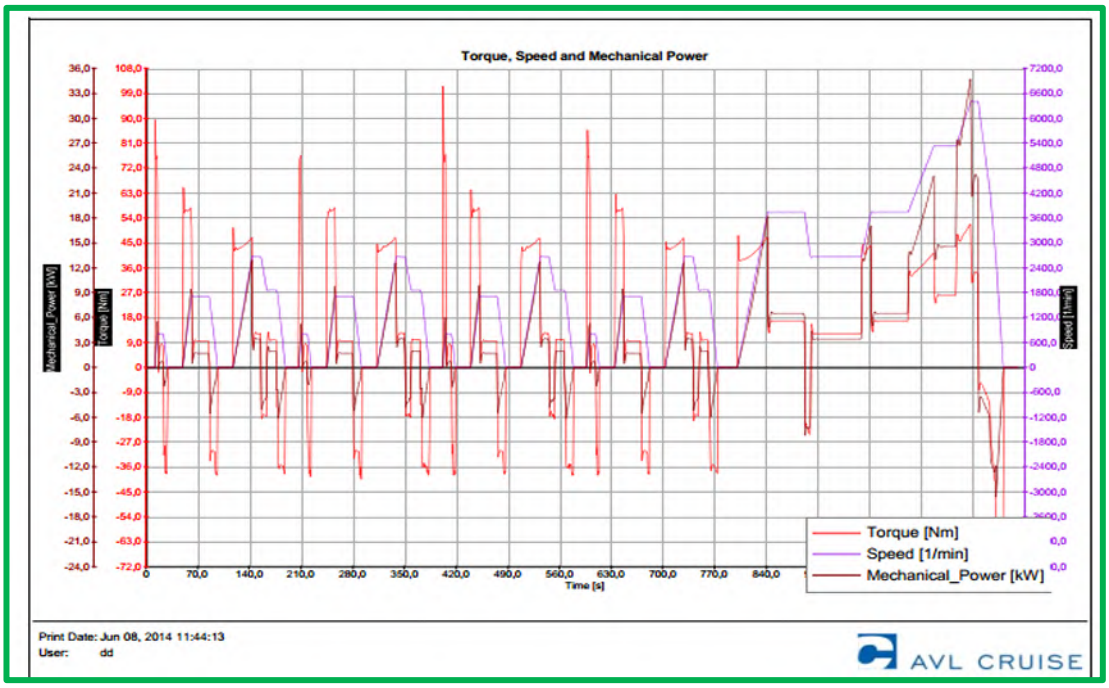

Figure 6.8: Electrical Motor Torque, Speed and Mechanical Power

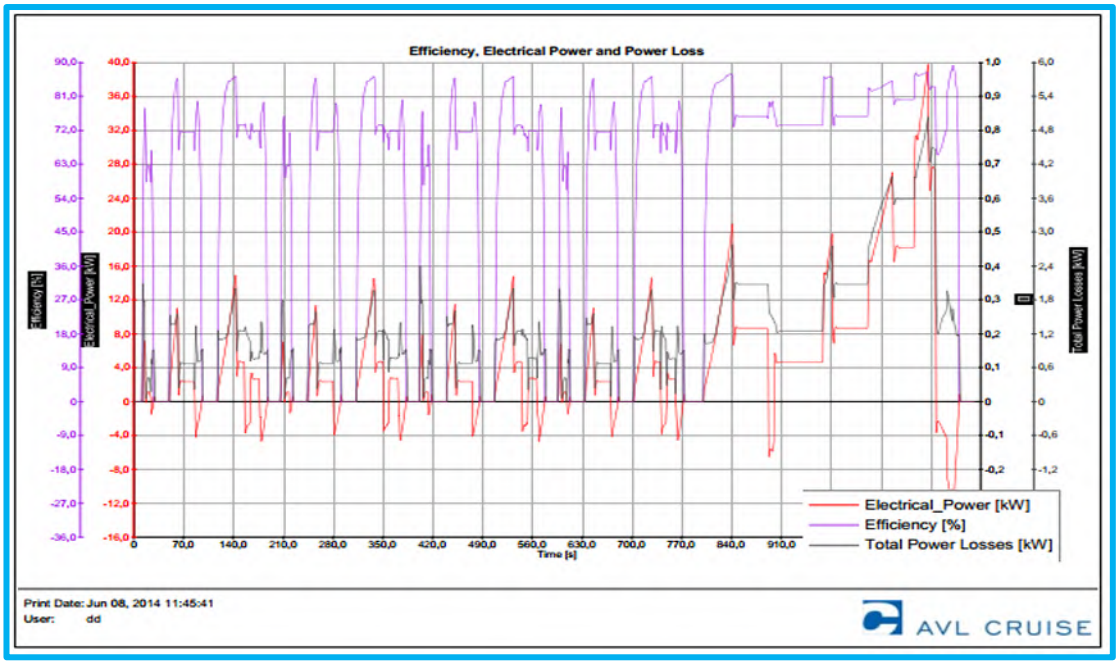

Figure 6.9: Electrical Power, Total Power Lost and efficiency

The electrical power, power lost, efficiency and also dynamic performances of the engines are same due to choosing the same electrical motor for both vehicles.

6.5. Conclusion

Although the electrical output, torque, mechanical power and electrical power values are same in Electric Clio and Range extender Clio, the most important difference between two vehicles lies in their ranges.

Due to the fact that Range extender supplies energy for electric propulsion when the battery is empty, it extends the range of the vehicle. This is too important for the electrical cars because the most important problem that is reported in electrical vehicles is their limited ranges. By using a 4 cylinder 1 L ICE, as it can be checked from the simulation results, the range extended Renault Clio take 60 km more distance than electrical one. By using Wankel engine or fuel cell battery packs as range extender engine, the distance taken by the vehicle can be extended much more. Moreover, the fuel consumption of the internal combustion engine is not high due to using only for the purpose of charging the battery.

References

[1] Electric Vehicles –Modelling and Simulations By Seref Soylu,2011

[2] California Air Resources Board Office Of Strategic Planning, Air-Pollution Transportation Linkage, 1989

[3] Wakefield, E.H., *History of Electric Automobile,* Society of Automotive Engineers, Warrendale, 1994

[4] Electric and Hybrid Vehicles Design Fundamentals, statement by *Iqbal Husain*

[5] K. Muta, M. Yamazaki, and J. Tokieda, BDevelopment of new-generation hybrid system THS IIVDrastic improvement of power performance and fuel economy, March 8–11, 2004, SAE Paper

[6] T. Horie, BDevelopment aims of the new CIVIC hybrid and achieved performance, San Diego, CA, Feb. 12, 2006.

[7] Development of the Motor Car and Bicycle", Travel Smart Teacher Resource Kit (Government of Australia), 2003, retrieved 2009-04-24

[8] Timeline: Life & Death of the Electric Car, NOW on PBS, Public Broadcasting Service, 9 June 2006, retrieved 2009-04-24

[9] Bellis, M. (2006), "The Early Years", The History of Electric Vehicles, retrieved 6 July 2006

[10] Wakefield, Ernest H. (1994), History of the Electric Automobile, Society of Automotive Engineers, pp. 2–3,ISBN 1-56091-299-5

[11] Cub Scout Car Show, January 2008, retrieved 2009-04-12

[12] Hybrid cars are so last century, 18 April 2006, retrieved 14 July 2009

[13] "Rearview Mirror". *Ward's AutoWorld*. 1 April 2000. Retrieved 13 July 2013.

[14] Russell, Roger. "Sonotone History: Tubes, Hi-Fi Electronics, Tape heads and Nicad Batteries". Sonotone Corporation History. Retrieved 13 July 2013.

[15] Goodstein, Judith (2004). "Godfather of the Hybrid".*Engineering & Science* (California Institute of Technology). LXVII (3). Archived from the original on 7 January 2011. Retrieved 13 July 2013.

[16] Carr, Richard (1 July 1966). "In search of the town car".*Design* (Council of Industrial Design) (211): 29–37.

[17] Westbrook, Michael Hereward (2001). *The Electric Car*. Institute of Engineering & Technology. ISBN 0-85296-013-1.

[18] "GM's long road back to electric cars". *CNN*. 7 April 2009. Retrieved 13 July 2013.

[19] Sperling, Daniel and Deborah Gordon (2009), Two billion cars: driving toward sustainability, Oxford University Press, New York, pp. 24 and 189–191, ISBN 978-0-19-537664-7

[20] Who Killed the Electric Car? Directed by Chris Paine, Distributed by Sony Pictures Classics

[21] "Gen II GM EV1 electric car". Kingoftheroad.net. Retrieved 2010-10-20.
[22] 05/26/2008 (2008-05-26). "20 Truths About the GM EV1 Electric Car". GreenCar.com. Retrieved 2009-07-22.

[23] Danny King (20 June 2011). "Neighborhood Electric Vehicle Sales To Climb". Edmunds.com Auto Observer. Retrieved 2012-02-05.

[24] "GE Capital to Finance Commercial Purchases of Global Electric Motorcars (GEM®)". Yahoo! Finance. 2013-05-02. Retrieved 2013-05-03.

[25] Saranow, Jennifer (27 July 2006), "The Electric Car Gets Some Muscle", *Pittsburgh Post-Gazette*, retrieved 2009-04-24

[26] Dave Hurst and Clint Wheelock (2011). "Executive Summary: Neighborhood Electric Vehicles – Low Speed Electric Vehicles for Consumer and Fleet Markets". Pike Research. Retrieved 2012-02-05.
[27] Historien bak Buddy (in Norwegian)

[28] *We have begun regular production of the Tesla Roadster*, Tesla Motors, 2008-03-17, retrieved 2008-03-20

[29] Danny King (11 January 2012). "Tesla continues Roadster sales with tweaks in Europe, Asia and Australia". Autoblog Green. Retrieved 2012-01-13.

[30] "Tesla Motors Moving Quickly to Commercialization of an Electric Car". GreenCar Magazine. 9 July 2009. Retrieved 2009-08-01.

[31] Chris Woodyard (3 August 2011). "Tesla boasts about electric car deliveries, plans for sedan". *USA Today*. Retrieved 2011-10-04.

[32] Josie Garthwaite (6 May 2011). "Tesla Prepares for a Gap as Roadster Winds Down". *The New York Times*. Retrieved 2011-05-07.

[33] http://www.popsci.com/cars/article/2011-06/farewell-roadster-tesla-will-stop-taking-orders-its-iconic-ev-two-months

[34] http://autos.yahoo.com/news/tesla-roadster-reaches-the-end-of-the-line.html

[35] Nikki Gordon-Bloomfield (12 January 2012). "Tesla Updates Roadster For 2012. There's Just One Catch...". Green Car Reports. Retrieved 2012-01-16.

[36] Mark Tisshaw (26 October 2011). "Tesla plans all-new Roadster". *Autocar*. Retrieved 2011-10-29.[37] "Mitsubishi Motors Begins Production of i-MiEV; Targeting 1,400 Units in Fiscal 2009". Green Car Congress. 5 June 2009. Retrieved 2010-04-04.

[37] "Mitsubishi Motors Begins Production of i-MiEV; Targeting 1,400 Units in Fiscal 2009". Green Car Congress. 5 June 2009. Retrieved 2010-04-04.

[38] Kageyama, Yuri (2010-03-31). "Japanese Start Buying Affordable Electric Cars". *The Seattle Times*. Associated Press. Retrieved 2010-04-24.

[39] Chang-Ran Kim (30 March 2010). "Mitsubishi Motors lowers price of electric i-MiEV". Reuters. Retrieved 2010-04-25.

[40] "Mitsubishi Begins Sales of i-MiEV to Individuals in Hong Kong; First Individual Sales Outside of Japan". Green Car Congress. 20 May 2010. Retrieved 2010-05-21.

[41] "Mitsubishi Motors to Begin Shipping i-MiEV to Australia in July; 2nd Market Outside Japan". Green Car Congress. 2 June 2010. Retrieved 2010-06-02.

[42] "The i-MiEV goes on sale in 15 European countries; near-term plan to boost that to 19". GreenCarCongress. 14 January 2011.

[43] Bengt Halvorson (4 October 2011). "2012 Mitsubishi i: First Drive, U.S.-Spec MiEV". Green Car Reports. Retrieved 2011-10-04.

[44] "Mitsubishi To Launch Its Electric Car First in Costa Rica". InsideCostaRica. 27 December 2010. Retrieved 2011-01-12.

[45] Alejandro Marimán Ibarra (4 May 2011). "Mitsubishi i-MIEV: Lanzado oficialmente en Chile" (in Spanish). Yahoo Chile. Retrieved 2011-07-21.

[46] Chris Woodyard (8 December 2011). "Mitsubishi delivers its first 'i' electric car". *USA Today*. Retrieved 2011-12-10.

[47] "Mitsubishi Motors Begins Production of i-MiEV; Targeting 1,400 Units in Fiscal 2009". Green Car Congress. 5 June 2009. Retrieved 2010-04-04.[48]

[48] Kageyama, Yuri (2010-03-31). "Japanese Start Buying Affordable Electric Cars". *The Seattle Times*. Associated Press. Retrieved 2010-04-24.

[49] Chang-Ran Kim (30 March 2010). "Mitsubishi Motors lowers price of electric i-MiEV". Reuters. Retrieved 2010-04-25.

[50] UC Irvine Press Release (2013-03-21). "UC Irvine's car-sharing program charges ahead". University of California, Irvine. Retrieved 2013-03-28.

[51] Reuters (2013-05-01). "Electric Car Maker Files for Bankruptcy Protection". *The New York Times*. Retrieved 2013-05-01.

[52] Alan Ohnsman (2013-05-08). "Tesla Posts First Quarterly Profit on Model S Deliveries". *Bloomberg L.P.*Retrieved 2013-05-08. *During Q1 2013 a total of 4,900 Model S cars were delivered in North America (mostly in the U.S. and a few units delivered in Canada). Volt and Leaf sales correspond to the U.S. and Canada combined*

[53] Domenick Yoney (2013-02-20). "Tesla delivered 2,650 Model S EVs last year, Musk confident of profit in Q1 and beyond". Autoblog Green. Retrieved 2013-03-10. *Around 2,650 Model S cars were delivered in the U.S. during 2012*.

[54] Gao et al., 2007; Mapelli et al., 2010; Schaltz, 2010

[55] Electrical Vehicle Design and Modeling, Electric Vehicles - Modelling and Simulations, Dr. Seref Soylu (Ed.), ISBN: 978-953-307-477-1, InTech

[56] Modeling the Electric Vehicle By Matthew Duescher

[57] Casanellas, F. (1994). Losses in pwm inverters using igbts, *IEE Proceedings - Electric Power Applications* 141(5): 235 – 239.

[58] Chan, C. C., Bouscayrol, A. & Chen, K. (2010). Electric, hybrid, and fuel-cell vehicles: Architectures and modeling, *IEEE Transactions on Vehicular Technology* 59(2): 589 – 598.

[59] Ehsani, M., Gao, Y., Gay, S. E. & Emadi, A. (2005). *Modern Electric, Hybrid Electric, and Fuel Cell Vehicles - Fundamentals, Theory, and Design*, first edn, CRC Press LLC.

[60] Emadi, A. (2005). *Handbook of Automotive Power Electronics and Motor Drives*, first edn, Taylor & Francis. Gao, D. W., Mi, C. & Emadi, A. (2007). Modeling and simulation of electric and hybrid vehicles, *Proceedings of the IEEE* 95(4): 729 – 745.

[61] Jensen, K. K., Mortensen, K. A., Jessen, K., Frandsen, T., Runolfsson, G. & Thorsdottir, T. (2009). Design of spmsm drive system for renault kangoo, *Aalborg University* .

[62] Lukic, S. & Emadi, A. (2002). Performance analysis of automotive power systems: effects of power electronic intensive loads and electrically-assisted propulsion systems, *Proc. of IEEE Vehicular Technology Conference (VTC)* 3: 1835 – 1839.

[63] Mapelli, F. L., Tarsitano, D. & Mauri, M. (2010). Plug-in hybrid electric vehicle: Modeling, prototype realization, and inverter losses reduction analysis, *IEEE Transactions on Industrial Electronics* 57(2): 598 – 607.

[64] Mohan, N., Underland, T. M. & Robbins, W. P. (2003). *Power electronics*, third edn, JohnWiley. Saft (2010). Saftbatteries. URL: *http://www.saftbatteries.com*

[65] Schaltz, E. (2010). *Design of a Fuel Cell Hybrid Electric Vehicle Drive System*, Department of Energy Technology, Aalborg University. UQM (2010). Uqm technologies. URL: *http://www.uqm.com*

[66] Rand, D.A.J., Woods, R., and Dell, R.M., *Batteries for Electric Vehicles,* John Wiley & Sons, New York, 1998.

.

[67] Dhameja, S., *Electric Vehicle Battery Systems,* Newnes (Elsevier Science), Burlington, MA, 2002

[68]Dell, R.M. and Rand, D.A.J., *Understanding Batteries,* Royal Society of Chemistry, United Kingdom, 2001.

[69] www.avl.com

[70] Liang Chu, Qingnian Wang, Minghui Liu and Jun Li, Parametric Design of Parallel Hybrid Power-train for Transit Bus, 2004 SAE World Congress, March 8-11,2004, pp:2

[71] Farhad Sangtarash, Vahid Esfahanian, Hassan Nehzati, Samaneh Haddadi, Meisam Amiri Bavanpour and Babak Haghpanah, Effect of Different Regenerative Braking Strategies on Braking Performance and Fuel Economy in a Hybrid Electric Bus Employing CRUISE Vehicle Simulation, 2008 World Congress, April 14-17, 2008, pp:830-831

[72] Mehrdad Ehsani, Yimin Gao, Ali Emadi, Modern Electric, Hybrid Electric, and Fuel Cell Vehicles Fundamentals, Theory, and Design, Power Electronics and Applications Series, CRC Press, 2010, pp:283-295

[73] Experimental Investigation of the Wankel Engine for Extending the Range of Electric Vehicles By SCOTT JULIAN VARNHAGEN